

1 MOS Model 11, level 1101

1.1 Introduction

MOS Model 11 (MM11) is a compact MOSFET model, intended for digital, analogue and RF circuit simulation in modern and future CMOS technologies. MM11 is the successor of MOS Model 9, it was especially developed to give not only an accurate description of currents and charges and their first-order derivatives (i.e., transconductance, conductance, capacitances), but also of the higher-order derivatives, resulting in an accurate description of electrical distortion behaviour. The latter is especially important for analog and RF circuit design. The model furthermore gives an accurate description of the noise behaviour of MOSFETs.

MOS Model 11 is a surface-potential-based model, using an explicit approximation for surface potential, resulting in an accurate description in all operation regions (i.e., accumulation region, weak, moderate and strong inversion region). Additionally, in order for the model to be valid for modern and future MOS devices, several important physical effects have been included in the model: mobility reduction, bias-dependent series-resistance, velocity saturation, drain-induced barrier lowering, static feedback, channel length modulation, self-heating, weak-avalanche (or impact ionization), gate current due to tunnelling, gate-induced drain leakage, poly-depletion, quantum-mechanical effects on charges and bias-dependent overlap capacitances.

MOS Model 11, Level 1101, is an updated version of Level 1100. It uses the same basic equations as Level 1100, but uses different geometry scaling rules. It includes two types of geometrical scaling rules: physical rules and binning rules. Moreover, in Level 1101 the temperature scaling has been implemented on the local or "miniset" level instead of the global or "maxiset" level as was the case for Level 1100. Self-heating has been included in the description.

Structural Elements of MOS Model 11

The structure of MOS Model 11 is the same as the structure of MOS Model 9. The model is separable into a number of relatively independent parts, namely:

- **Model embedding**

It is convenient to use one single model for both n - and p -channel devices. For this reason, any p -channel device and its bias conditions are mapped onto those of an equivalent n -channel transistor. This mapping comprises a number of sign changes. Also, the model describes a symmetrical device, i.e. the source and drain nodes can be interchanged without changing the electrical properties. The assignment of source and drain to the channel nodes is based on the voltages of these nodes: for an n -channel transistor the node at the highest potential is called drain. In a circuit simulator the nodes are denoted by their network numbers, based on the

circuit configuration. Again, a transformation is necessary involving a number of sign changes, including the directional noise-current sources.

- **Preprocessing**

The complete set of all the parameters, as they occur in the equations for the various electrical quantities, is denoted as the set of actual parameters, usually called the "miniset". In MM11, Level 1101, the temperature scaling parameters are included in the "miniset". Each of these actual parameters can be determined by purely electrical measurements. Since most of these parameters scale with geometry the process as a whole is characterized by an enlarged set of parameters, which is denoted as the set of scaling parameters, usually called the "maxiset". This set of parameters contains most of the actual parameters for an infinitely long and broad device and a large set of sensitivity coefficients. From this, the actual parameters for an arbitrary transistor are obtained by applying a set of transformation rules. The transformation rules describe the dependencies of the actual parameters on the length, width, and temperature. This procedure is called preprocessing, as it is normally done only once, prior to the actual electrical simulation.

In MM11, Level 1101, parameter binning has been facilitated by adding a second, separate set of geometry scaling rules. Consequently, besides the *physical* geometrical scaling rules there is also a set of *binning* geometrical scaling rules. The physical geometry scaling rules of Level 1101 have been developed to give a good description over the whole geometry range of CMOS technologies. For processes under development, however, it is sometimes useful to have more flexible scaling relations. In this case one could opt for a binning strategy, where the accuracy with geometry is mostly determined by the number of bins used. The physical scaling rules of Level 1101 are not straightforwardly applicable to binning strategies, since they may result in discontinuities in parameter values at the bin boundaries. Consequently, special geometrical binning scaling relations have been developed, which guarantee continuity in the model parameters at the bin boundaries. It should be noted that using the source code of the Modelkit on the Philips' website (which can be found at http://www.semiconductors.philips.com/Philips_Models)

1. the physical geometry scaling rules can be selected by using Level11010, while
2. the binning geometry scaling rules can be selected by using Level 11011.

- **Clipping**

For very uncommon geometries or temperatures, the preprocessing rules may generate parameters that are outside a physically realistic range or that may create difficulties in the numerical evaluation of the model, for example division by zero. In order to prevent this, all parameters are limited to a pre-specified range directly after the preprocessing. This procedure is called clipping.

- **Current equations**

These are all expressions needed to obtain the DC nodal currents as a function of the bias conditions. They are segmentable in equations for the channel current, the gate tunnelling current and the avalanche current.

- **Charge equations**

These are all the equations that are used to calculate both the intrinsic and extrinsic charge quantities, which are assigned to the nodes.

- **Noise equations**

The total noise output of a transistor consists of a thermal- and a flicker noise part, which create fluctuations in the channel current. Owing to the capacitive coupling between gate and channel region, current fluctuations in the gate current are induced as well, which is referred to as induced gate noise.

1.2 Physics

In this section some physical background on the current, charge and noise description of MOS Model 1101 will be given. For the full details of the physical background of the drain-source channel current equations the reader is referred to [5], [6], [8]-[10]. The gate current, charge and noise equations have been newly developed and their physical background will be discussed in a future report. All equations referred to are to be found in section 1.5

Comments on Current Equations

Conventional MOS models such as MOS Model 9 and BSIM4 are threshold-voltage-based models, which make use of approximate expressions of the drain-source channel current I_{DS} in the weak-inversion region (i.e. subthreshold) and in the strong-inversion region (i.e. well above threshold). These approximate equations are tied together using a mathematical smoothing function, resulting in neither a physical nor an accurate description of I_{DS} in the moderate inversion region (i.e. around threshold). With the constant downscaling of supply voltage the moderate inversion region becomes more and more important, and an accurate description of this region is thus essential.

A more accurate type of model is the surface-potential-based model, where the channel current I_{DS} is split up in a drift (I_{drift}) and a diffusion (I_{diff}) component, which are a function of the gate bias V_{GB} and the surface potential at the source (ψ_{s_0}) and the drain (ψ_{s_L}) side. In this way I_{DS} can be accurately described using one equation for all operating regions (i.e. weak, moderate and strong-inversion). MOS Model 1101 is a surface-potential-based model.

Surface Potential

The surface potential ψ_s is defined as the electrostatic potential at the gate oxide/ substrate interface with respect to the neutral bulk (due to the band bending, see Figure 7a). For an n-MOS transistor with uniform doping concentration it can be calculated from the following implicit relation:

$$\left(\frac{V_{GB} - V_{FB} - \psi_p - \psi_s}{k_0}\right)^2 = \psi_s + \phi_T \cdot \left[\exp\left(-\frac{\psi_s}{\phi_T}\right) - 1\right] \\ + \phi_T \cdot \exp\left(-\frac{\phi_B + V}{(1 + m_0) \cdot \phi_T}\right) \cdot \left[\exp\left(\frac{\psi_s}{(1 + m_0) \cdot \phi_T}\right) - 1\right]$$

where V is the quasi-Fermi potential, which ranges from V_{SB} at the source side to V_{DB} at the drain side. The parameter m_0 has been added to model the non-ideal subthreshold behaviour of short-channel transistors¹, and ψ_p is the potential drop in the polysilicon gate material due to the poly-depletion effect. The latter is given by²:

$$\psi_p = \begin{cases} 0 & V_{GB} \leq V_{FB} \\ \left(\sqrt{V_{GB} - V_{FB} - \psi_s + \frac{k_p^2}{4} - \frac{k_p}{2}}\right)^2 & V_{GB} > V_{FB} \end{cases}$$

In Figure 7b the surface potential is shown as a function of gate bias for a typical n-type MOS device. The surface potential ψ_s is implicitly related to the gate bias V_{GB} and the quasi-Fermi potential V , and cannot be calculated analytically. It can only be calculated using an iterative solution, which in general is computation-time consuming. In MOS Model 1101 an explicit approximation of the surface potential is used, which has partly been treated in [6]. In the inversion region ($V_{GB} > V_{FB}$) the surface potential is approximated by $\psi_{s_{inv}}$ given by eqs. (1.34)-(1.36) and (1.43)-(1.48), where variable Δacc is used to describe the influence of majority carriers. In the accumulation region ($V_{GB} < V_{FB}$) the surface potential is approximated by $\psi_{s_{acc}}$ given by eqs. (1.49)-(1.51). The total surface potential ψ_s is simply given by

$$\psi_{s_{inv}} + \psi_{s_{acc}}.$$

1. Parameter $m_0 = 0$ for the ideal long-channel case.

2. For $V_{GB} < V_{FB}$ an accumulation layer is formed in both the substrate silicon and the gate polysilicon, in this case ψ_p is slightly negative and weakly dependent on V_{GB} . This effect has been neglected.

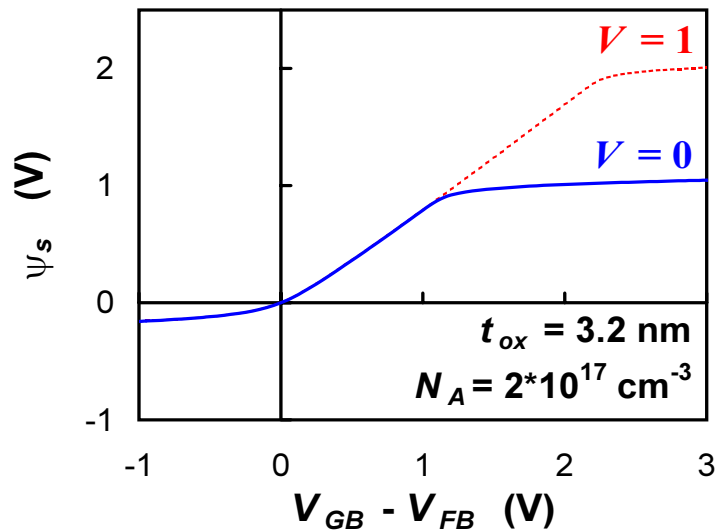
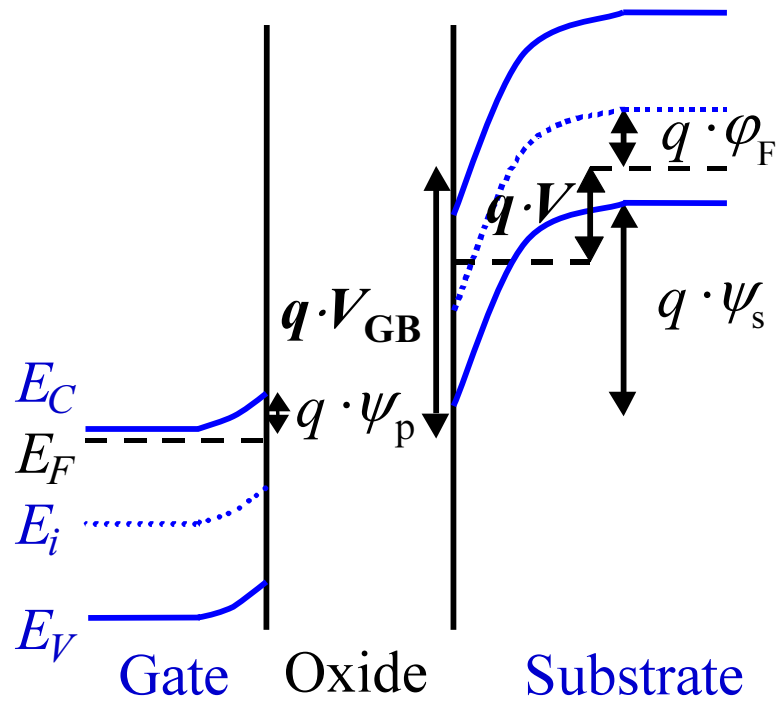


Figure 1: Upper figure: The energy band diagram of an n-type MOS transistor in inversion $V_{GB} > V_{FB}$, where ψ_s is the surface potential, ψ_p is the potential drop in the gate due to the poly-depletion effect, V is the quasi-Fermi potential and ϕ_F is the intrinsic Fermi-potential ($\phi_B = 2 \cdot \phi_F$). Lower figure: The surface potential as a function of gate bias for different values of quasi-Fermi potential V ($m_0 = 0$).

A surface-potential-based model automatically incorporates the pinch-off condition at the drain side, and as a result it gives a description of both the linear (or ohmic) region and the saturation region for the ideal long-channel case. In this case the saturation voltage V_{DSAT} (i.e. the drain-source voltage above which saturation occurs) corresponds to eq. (1.37). For short-channel devices, however, no real pinch-off occurs and the saturation voltage is affected by velocity saturation and series-resistance. In this case the saturation voltage V_{DSAT} is calculated using eqs. (1.37)-(1.41). The transition from linear to saturation region is no longer automatically described by the surface-potential-based model. This has been solved in the same way as in [12] by introducing an effective drain-source bias V_{DS_x} which changes smoothly from V_{DS} in the linear region to V_{DSAT} in the saturation region, see eq. (1.42).

A surface-potential-based model makes no use of threshold voltage V_T . Circuit designers, however, are used to think in terms of threshold voltage, and as a consequence it would be useful to have a description of V_T in the framework of a surface-potential-model. It has been found that an accurate expression of threshold voltage is simply given by:

$$V_T = V_{FB} + \left(1 + \frac{k_0^2}{k_p^2}\right) \cdot (V_{SB} + \phi_B + 2 \cdot \phi_T) - V_{SB} + k_0 \cdot \sqrt{V_{SB} + \phi_B + 2 \cdot \phi_T}$$

The threshold voltage and other important parameters for circuit design are part of the operating point output as given in Section 1.7.

Channel Current

Neglecting the influence of gate and bulk current, the channel current can be written as: $I_{DS} = I_{drift} + I_{diff}$ where ideally the drift component I_{drift} can be approximated by (for $V_{GB} > V_{FB}$):

$$I_{drift} = \beta \cdot \left(\frac{2 \cdot \left[V_{GB} - V_{FB} - \frac{\Psi_{s_L} + \Psi_{s_0}}{2} \right]}{1 + \sqrt{1 + \frac{4}{k_p^2} \cdot \left[V_{GB} - V_{FB} - \frac{\Psi_{s_L} + \Psi_{s_0}}{2} \right]}} - k_0 \cdot \sqrt{\frac{\Psi_{s_L} + \Psi_{s_0}}{2}} \right) \cdot (\Psi_{s_L} - \Psi_{s_0})$$

and the diffusion component I_{diff} can be approximated by (for $V_{GB} > V_{FB}$):

$$I_{diff} = \beta \cdot \phi_T \cdot (Q_{inv_L} - Q_{inv_0}) \cdot \frac{t_{ox}}{\epsilon_{ox}}$$

In the latter equation Q_{inv_0} and Q_{inv_L} denote the inversion-layer charge density at the source and drain side, respectively, which are given by eqs. (1.71)-(1.73) (where $Q_{inv} = -\epsilon_{ox}/t_{ox} \cdot V_{inv}$).

In the non-ideal case the channel current is affected by several physical effects, such as drain-induced barrier lowering, static feedback, mobility reduction, series-resistance, velocity saturation, channel length modulation and self-heating, which have to be taken into account in the channel current expression:

- In threshold-voltage-based models drain-induced barrier lowering and static feedback are traditionally implemented as a decrease in threshold voltage with drain bias. Here these effects have been implemented as an increase in effective gate bias ΔV_G given by eqs. (1.29)-(1.33). An effective drain-source voltage $V_{DS_{eff}}$ has been used to preserve non-singular behaviour in the higher-order derivatives of I_{DS} at $V_{DS} = 0$ V.
- The effects of mobility reduction and series-resistance on channel current have been described in [9], and have consequently been implemented using eqs. (1.64) and (1.68), respectively.
- The effect of velocity saturation has been modelled along the same lines as was done in [10] with the exception of the electrical field distribution. In [10] the influence of the electron velocity saturation expression

$$v = \frac{\mu \cdot E_{\parallel}}{\sqrt{1 + (\mu/v_{sat} \cdot E_{\parallel})^2}}$$

was approximated assuming that the lateral electric field E_{\parallel} in the denominator is constant and equal to $(\psi_{s_L} - \psi_{s_0})/L$. Here we assume that E_{\parallel} (in the denominator) increases linearly along the channel (from 0 at the source to $2 \cdot (\psi_{s_L} - \psi_{s_0})/L$ at the drain), and obtain a more accurate expression for velocity saturation, which has been implemented using eq. (1.66).

- The effect of channel length modulation and self-heating on channel current have been described in [10], and have consequently been implemented using eqs. (1.67) and (1.69), respectively.

All the above effects can be incorporated into the channel current expression using eq. (1.70) and eq. (1.76).

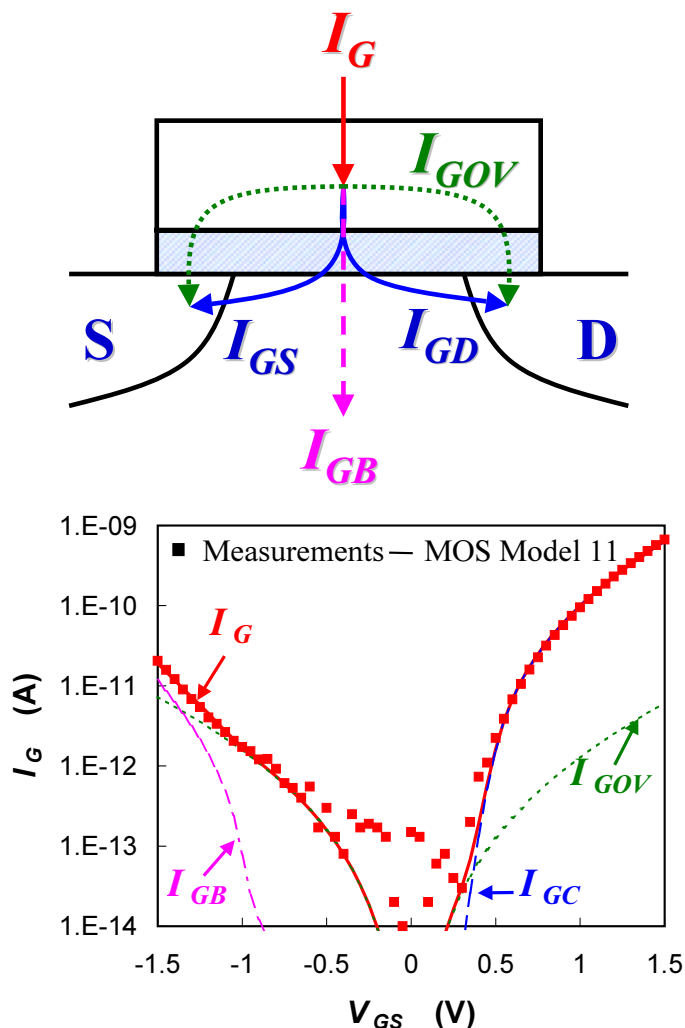


Figure 2: Upper figure: The different gate current components in a MOS transistor. One can distinguish the intrinsic components, i.e. the gate-to-channel current $I_{GC}(= I_{GS}+I_{GD})$ and the gate-to-bulk current I_{GB} , and the extrinsic, i.e. the gate/source and gate/drain overlap components $I_{G_{ov}}$. Lower figure: Measured and modelled gate current as a function of gate bias V_{GS} at $V_{DS} = V_{SB} = 0$ V, the different gate current components are also shown. NMOS-transistor, $W/L = 10/0.6\mu\text{m}$ and $t_{ox} = 2$ nm.

Weak-Avalanche Current

At high drain bias, owing to the weak-avalanche effect (or impact ionization), a current I_{avl} will flow between drain and bulk¹. The description of the weak-avalanche current has been taken from MOS Model 9 [7], and is given by eq. (1.77). With the down-scaling of supply voltage for modern CMOS technologies, weak-avalanche becomes less and less important.

Gate Tunnelling Current

With CMOS technology scaling the gate oxide thickness is reduced and, due to the direct-tunnelling of carriers through the oxide, the gate current is no longer negligible, and has to be taken into account. Several gate current components can be distinguished, three components (I_{GS} , I_{GD} and I_{GB}) due to the intrinsic MOS channel, and two components (I_{Gov_0} and I_{Gov_L}) due to gate/source and gate/drain overlap region, see Figure 7(a).

For an n-type MOS transistor operating in inversion, the intrinsic gate current density J_G consists of electrons tunnelling from the inversion layer to the gate, the so-called conductance band tunnelling, which in general can be written as [13] (for $V_{GB} > V_{FB}$):

$$J_G \propto -V_{ox} \cdot Q_{inv} \cdot P_{tun}\{V_{ox}; \chi_B; B\}$$

where V_{ox} is the oxide voltage given by $V_{ox} = V_{GB} - V_{FB} - \psi_p - \psi_s$. The carrier tunnelling probability P_{tun} is a function of the oxide voltage V_{ox} , the oxide energy barrier χ_B as observed by the inversion-layer carriers, and a parameter B . This probability is given by eq. (1.78), where both direct-tunnelling for $V_{ox} < \chi_B$ and Fowler-Nordheim tunnelling for $V_{ox} > \chi_B$ have been taken into account.

Owing to quantum-mechanical energy quantization in the potential well at the SiO₂-surface, the electrons in the inversion layer are not situated at the bottom of the conduction band, but in the lowest energy subband which lies $\Delta\chi_B$ above the conduction band. Assuming that only the lowest energy subband is occupied by electrons, the value of $\Delta\chi_B$ can be given by eq. (1.95) [14]. As a result the oxide barrier $\chi_{B_{eff}}$ has to be lowered by an amount of $\Delta\chi_B$, see eq. (1.96).

1. In reality part of the generated avalanche current will also flow from drain to source [5], this has been neglected

In inversion the total intrinsic gate current consists of electrons tunnelling from inversion layer to gate, the so-called gate-to-channel current I_{GC} . These electrons are supplied by both source (I_{GS}) and drain (I_{GD}). The gate-to-channel current I_{GC} can be calculated from:

$$I_{GC} = W \cdot \int_0^L J_G \cdot dx$$

where x is the coordinate along the channel. Using a first-order perturbation approximation, i.e. assuming the gate current is small enough so that it does not change the distribution of surface potential along the channel, I_{GC} can be calculated by eqs. (1.95)-(1.105). In the same way the partitioning of I_{GC} into I_{GS} and I_{GD} can be calculated using:

$$I_{GS} = W \cdot \int_0^L \left(1 - \frac{x}{L}\right) \cdot J_G \cdot dx$$

$$I_{GD} = W \cdot \int_0^L \frac{x}{L} \cdot J_G \cdot dx$$

which results in expressions for I_{GS} and I_{GD} as given by eqs. (1.106)-(1.108). The gate-to-channel current I_{GC} can be seen in Figure 7(b) as a function of gate bias for a typical n-MOS transistor at $V_{DS} = 0$ (i.e. $I_{GS} = I_{GD} = 1/2 \cdot I_{GC}$).

For an n-type MOS transistor operating in accumulation, an accumulation layer of holes is formed in the p-type substrate and an accumulation layer of electrons is formed in the n⁺-type polysilicon gate. Since the oxide energy barrier for electrons χ_{B_N} is considerably lower than that for holes χ_{B_p} , the gate current will mainly consist of electrons tunnelling from the gate to the bulk silicon, where they are swept to the bulk terminal. In this case the (intrinsic) gate current density J_G can be written as [13] (for $V_{GB} < V_{FB}$):

$$J_G \propto -V_{ox} \cdot Q_{acc} \cdot P_{tun}\{-V_{ox}; \chi_B; B\}$$

where Q_{acc} is the accumulation charge density in the gate given by $\epsilon_{ox}/t_{ox} \cdot V_{ox}$. In order to limit calculation time the quantum-mechanical oxide barrier lowering in this case is neglected, and the resulting expression for I_{GB} is given by eqs. (1.93)-(1.94). The gate-to-

bulk current I_{GB} can be seen in Figure 7(b) as a function of gate bias for a typical n-MOS transistor at $V_{DS} = 0$.

Apart from the intrinsic components I_{GC} and I_{GB} , considerable gate current can be generated in the gate/source- and gate/drain-overlap regions. Concentrating on the gate/source¹-overlap region, in order to calculate the overlap gate current, the overlap region is treated as an n^+ -gate/oxide/ n^+ -bulk MOS capacitance where the source acts as bulk. Although the impurity doping concentration in the n^+ -source extension region is non-uniform in both lateral and transversal direction, it is assumed that an effective flat-band voltage V_{FBov} and body-factor k_{ov} can be defined for this structure. Furthermore assuming that only accumulation and depletion occur in the n^+ -source region², a surface potential $\psi_{s_{ov}}$ can be calculated using:

$$\left(\frac{V_{GS} - V_{FBov} - \psi_{p_{ov}} - \psi_{s_{ov}}}{k_{ov}} \right)^2 = -\psi_{s_{ov}} + \phi_T \cdot \left[\exp\left(\frac{\psi_{s_{ov}}}{\phi_T} \right) - 1 \right]$$

where the potential drop in the polysilicon gate material due to the poly-depletion effect $\psi_{p_{ov}}$ is given by:

$$\psi_{p_{ov}} = \begin{cases} 0 & V_{GS} \leq V_{GBov} \\ \left(\sqrt{V_{GS} - V_{FBov} - \psi_{s_{ov}} + \frac{k_p^2}{4} - \frac{k_p}{2}} \right)^2 & V_{GS} > V_{FBov} \end{cases}$$

Again, the surface potential $\psi_{p_{ov}}$ can be explicitly approximated, this is done by using eqs. (1.79)-(1.85).

For $V_{GS} > V_{FBov}$ a negatively charged accumulation layer is formed in the overlapped n^+ -source extension and a positively charged depletion layer is formed in the overlapping gate. In this case the overlap gate current will mostly consist of electrons tunnelling from the source accumulation layer to the gate, it is given by:

$$I_{G_{ov}} \propto -V_{ov} \cdot Q_{ov} \cdot P_{tun}\{V_{ov}; \chi_B; B\}$$

1. In the following derivation, the same can be done for the gate/drain-overlap region by replacing the source by the drain.

2. Since the source extension has a very high doping concentration, an inversion layer in the gate/source overlap will only be formed at very negative gate-source bias values. This effect has been neglected.

where V_{ov} is the oxide voltage for the gate/source-overlap ($= V_{GS} - V_{FBov} - \Psi_{p_{ov}} - \Psi_{s_{ov}}$), given by eqs. (1.86)-(1.92), and Q_{ov} is the total charge density in the n^+ -source region ($= \epsilon_{ox}/t_{ox} \cdot V_{ov}$). For $V_{GS} < V_{FBov}$ the situation is reversed, a positively charged depletion layer is formed in the overlapped n^+ -source extension and a negatively charged accumulation layer is formed in the overlapping gate. In this case the overlap gate current will mostly consist of electrons tunnelling from the gate accumulation layer to the source, it is given by:

$$I_{G_{ov}} \propto V_{ov} \cdot Q_{ov} \cdot P_{tun}\{-V_{ov}; \chi_B; B\}$$

The overlap gate current components can now be given by eqs. (1.89)-(1.92). In Figure 7(b) the gate overlap current $I_{G_{ov}}$ is shown as a function of gate bias for a typical n-MOS transistor at $V_{DS} = 0$ (i.e. $I_{G_{ovL}} = I_{G_{ov0}}$). For n-type and p-type MOS transistors the gate current behaviour is different due to the type of carriers that constitute the different gate current components¹. The difference is summarized in Table 1.

1. It is assumed here that the gate current is only determined by conductance band tunnelling. For high values of gate bias (i.e. $q \cdot V_{ox} > E_g$) electrons in the bulk valence band may also tunnel through the oxide to the gate conduction band. This mechanism is referred to as valence band tunnelling, and it has not been taken into account in MOS Model 1101.

Table 1: The type of carriers that contribute to the gate tunnelling current in the various operation regions for the intrinsic MOSFET, the gate/drain- and gate/source-overlap regions. The type of carriers determine the value of oxide energy barrier χ_B that has to be used (χ_{B_N} for electrons, χ_{B_P} for holes). In the last row the direction of gate current is indicated.

Type	Intrinsic MOSFET		Overlap Regions
	Accumulation	Inversion	
NMOS	electrons	electrons	electrons
PMOS	electrons	holes	holes
	I_{GB}	I_{GS}/I_{GD}	I_{GS}/I_{GD}

Comments on Charge Equations

In a typical MOS structure we can distinguish intrinsic and extrinsic charges. The latter are due to the gate/source and gate/drain overlap regions. The drain/source junctions also contribute to the capacitance behaviour of a MOSFET, but this is not taken into account in MOS Model 1101; it is described by a separate junction diode model.

Intrinsic Charges

In the intrinsic MOS transistor charges can be attributed to the four terminals. The bulk charge Q_B , which is determined by either the depletion charge (for $V_{GB} > V_{FB}$) or the accumulation charge (for $V_{GB} < V_{FB}$), can be calculated from:

$$Q_B = W \cdot \int_0^L (Q_{tot} - Q_{inv}) \cdot dx$$

where Q_{tot} is the total charge density in the silicon bulk ($Q_{tot} = -\epsilon_{ox}/t_{ox} \cdot V_{ox}$). The total inversion-layer charge Q_{inv} is split up in a source Q_S and a drain Q_D charge, they can be calculated using the Ward-Dutton charge partitioning scheme [15]:

$$Q_S = W \cdot \int_0^L \left(1 - \frac{x}{L}\right) \cdot Q_{inv} \cdot dx$$

$$Q_D = W \cdot \int_0^L \frac{x}{L} \cdot Q_{inv} \cdot dx$$

Since charge neutrality holds for the complete transistor, the gate charge is simply given by:

$$Q_G = -Q_S - Q_D - Q_B$$

The above equations have been solved, and the charges are given by eqs. (1.115)-(1.121). In these equations $C_{ox_{eff}}$ is the effective oxide capacitance, which is smaller than the ideal oxide capacitance C_{ox} due to quantum-mechanical effects: Quantum-mechanically, the inversion/accumulation charge concentration is not maximum at the Si-SiO₂-interface (as it would be in the classical case), but reaches a maximum at a distance Δz from the interface [14]. This quantum-mechanical effect can be taken into account by an effective oxide thickness $t_{ox} + \epsilon_{ox}/\epsilon_{si} \cdot \Delta z$, where Δz is dependent on the effective electric field E_{eff} [14], [16] ($E_{eff} = -\epsilon_{ox}/\epsilon_{si} \cdot V_{eff}/t_{ox}$). The effective oxide thickness results in an effective oxide capacitance $C_{ox_{eff}}$, see eq. (1.113).

It should be noted that the above charge model is quasi-static. A phase-shift between drain channel current and gate voltage is not taken into account. This implies that for a few applications at high frequencies approaching the cut-off frequency, errors have to be expected due to non-quasi-static effects. Nevertheless non-quasi-effects can be taken into account using a segmentation model as described in [17].

Extrinsic Charges

The gate/source- and gate/drain-overlap regions act as bias-dependent capacitances. In order to take this bias-dependence into account the overlap regions are treated as an n⁺-gate/oxide/n⁺-bulk MOS capacitance along the same lines as was done for the overlap gate current, see the section: *Comments on Current Equations*. The charge in the overlap regions can simply be given by eqs. (1.113)-(1.114). The quantum-mechanical effect on oxide thickness has been neglected here in order to reduce calculation time.

Comments on Noise Equations

In a MOS transistor generally three different types of noise can be observed: $1/f$ noise, thermal noise and induced gate noise. The gate tunnel current and the bulk avalanche current will also exhibit noisy behaviour (due to shot noise), however this has been neglected in MOS Model 1101.

$1/f$ -Noise

At low frequencies flicker (or $1/f$) noise becomes dominant in MOSFETs. In the past this type of noise has been interpreted either in terms of trapping and detrapping of charge carri-

ers in the gate oxide or in terms of mobility fluctuations. Over the past years, a general model for $1/f$ -noise which combines both of the above physical origins [2], [3], has found wide acceptance in the field of MOS modelling. The model assumes that the carrier number in the channel fluctuates due to trapping/detrapping in the gate oxide, and that these number fluctuations also affect the carrier mobility resulting in (correlated) mobility fluctuations.

The same model is part of MOS Model 9 [4], and has been used to calculate the $1/f$ -noise for MOS Model 1101. The calculations have been performed in such a way that the resulting expression for spectral density is valid for all operation regions (i.e. both in subthreshold and above threshold), it is given by eqs. (1.126)-(1.129).

Thermal Noise

Since the MOSFET channel can be considered as a non linear resistor, the channel current is subject to thermal noise. Let thermal noise current sources be parallel connected to each infinitesimal short element of the channel, it can be shown that the noise spectral density, which is defined by [21]:

$$\langle \Delta i_{th}^2 \rangle = \int_0^{\infty} s_{th}(f) df$$

is given by a generalized Nyquist relation:

$$S_{th} = \frac{N_T}{L^2} \cdot \int_0^L g(x) dx$$

where N_T is equal to $4 \cdot k_B \cdot T$ and $g(x)$ is the local specific channel conductance:

$$g(x) = -\mu(x) \cdot W \cdot Q_{inv}(x)$$

Here the mobility $\mu(x)$ is position dependent mainly due to the effect of velocity saturation. Elaborating the latter integral via a transform of the x variable into the quasi-Fermi potential $V(x)$, we obtain the spectral density given by eqs. (1.123)-(1.125). Again continuity of the noise model is assured along all modes of operation. The above thermal noise model has been found to accurately describe experimental results for various CMOS technologies without having to invoke carrier heating effects [23].

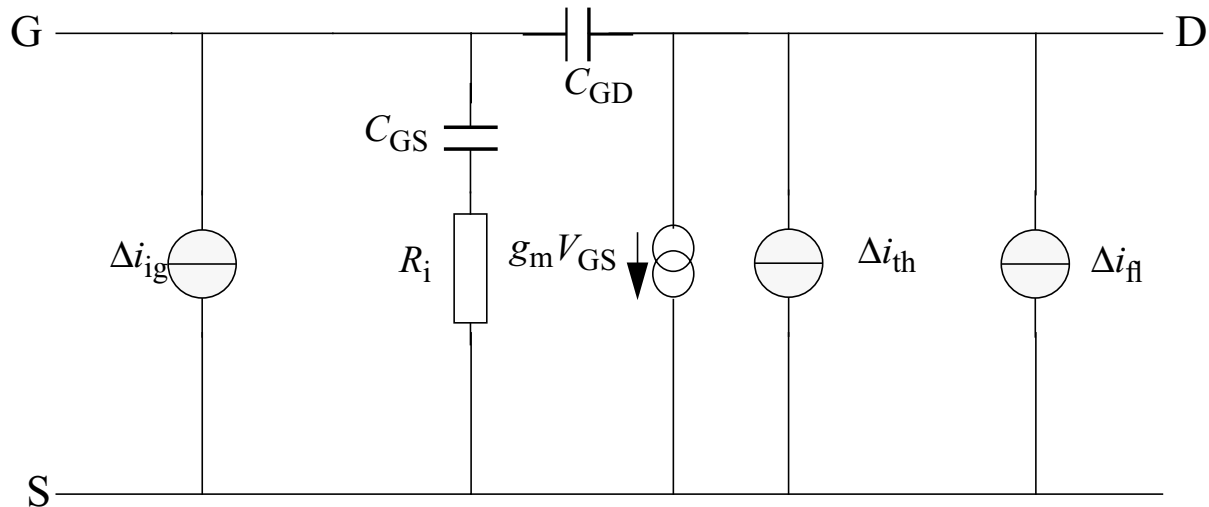


Figure 3: Noise current sources in the electrical scheme of the MOS transistor

Induced Gate Noise

Owing to capacitive coupling between gate and channel, the fluctuating channel current induces noise in the gate terminal at high frequencies. Unfortunately the calculation of this component from first principles is too complicated to provide a result applicable to circuit simulation. It is more practical to derive the desired result from an equivalent circuit presentation given in Figure 3. Owing to the mentioned capacitive coupling, a part of the channel is present as a resistance in series with the gate input capacitance. In saturation this resistance is approximately equal to:

$$R_i = \frac{1}{3 \cdot g_m}$$

It can be easily shown that the latter resistance produces an input noise current with a spectral density given by eq. (1.130). In addition, since Δi_{th} and Δi_{ig} have the same physical source, both spectral densities are correlated. This is expressed by eqs. (1.131) and (1.132). The induced gate noise S_{ig} is a so-called non-quasi static (NQS) effect. Since the use of the channel current noise description in an NQS segmentation model [17] would automatically result in a correct description of induced gate noise, S_{ig} can be made equal to zero by using parameter GATENOISE, see eq. (1.130).

1.3 Symbols, parameters and constants

The symbolic representation and the recommended programming names of the quantities listed in the following sections, have been chosen in such a way to express their purpose and relations to other quantities and to preclude ambiguity and inconsistency.

1.3.1 Glossary of used symbols

All parameters which refer to the reference transistor and/or the reference temperature have a symbol with the subscript R and a programming name ending with R. All characters 0 (zero) in subscripts of parameters are represented by the capital letter O in the programming name, because often they are distinguishable with great difficulty! Scaling parameters are indicated by *S* with a subscript where the variables on which the parameter depends, precede a semicolon whereas the parameter succeeds it, e.g. $S_{T;\theta_{sr}}$

List of numerical constants

Constant	Prog. Name	Value
<i>A</i>	LN_MINDOUBLE	-800

List of circuit simulator variables

Symbol	Prog. Name	Units	Description
<i>L</i>	L	m	Drawn channel length in the lay-out of the actual transistor
<i>W</i>	W	m	Drawn channel width in the lay-out of the actual transistor
T_A	TA	°C	Ambient circuit temperature
<i>f</i>	F	s ⁻¹	Operation frequency

External Electrical Variables

The definitions of the external electrical variables are illustrated in Figure 4.

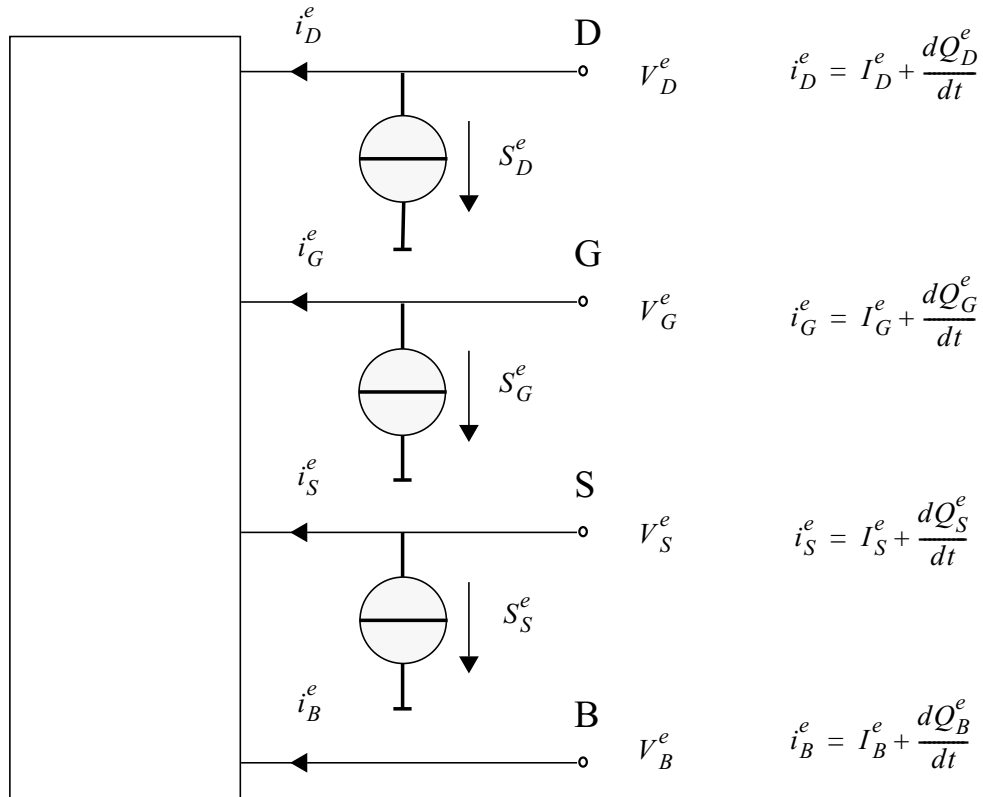


Figure 4: Definition of the external electrical quantities and variables

Variable	Prog. Name	Units	Description
V_D^e	VDE	V	Potential applied to the drain node
V_G^e	VGE	V	Potential applied to the gate node
V_S^e	VSE	V	Potential applied to the source node
V_B^e	VBE	V	Potential applied to the bulk node
I_D^e	IDE	A	DC current into the drain
I_G^e	IGE	A	DC current into the gate
I_S^e	ISE	A	DC current into the source
I_B^e	IBE	A	DC current into the bulk
Q_D^e	QDE	C	Charge in the device attributed to the drain node
Q_G^e	QGE	C	Charge in the device attributed to the gate node
Q_S^e	QSE	C	Charge in the device attributed to the source node
Q_B^e	QBE	C	Charge in the device attributed to the bulk node
S_D^e	SDE	A ² s	Spectral density of the noise current into the drain
S_G^e	SGE	A ² s	Spectral density of the noise current into the gate
S_S^e	SSE	A ² s	Spectral density of the noise current into the source

Variable	Prog. Name	Units	Description
S_{DG}^e	SDGE	A ² s	Cross spectral density between the drain and the gate noise currents
S_{GS}^e	SGSE	A ² s	Cross spectral density between the gate and the source noise currents
S_{SD}^e	SSDE	A ² s	Cross spectral density between the source and the drain noise currents

Internal Electrical Variables

Variable	Progr. Name	Units	Description
V_{DS}	VDS	V	Drain-to-source voltage applied to the equivalent n-MOST
V_{GS}	VGS	V	Gate-to-source voltage applied to the equivalent n-MOST
V_{SB}	VS	V	Source-to-bulk voltage applied to the equivalent n-MOST
I_{DS}	IDS	A	DC current through the channel flowing from drain to source
I_{AVL}	IAVL	A	DC current flowing from drain to bulk due to the weak-avalanche effect
I_{GS}	IGS	A	DC current flowing from gate to source due to the direct tunnelling effect
I_{GD}	IGD	A	DC current flowing from gate to drain due to the direct tunnelling effect
I_{GB}	IGB	A	DC current flowing from gate to bulk due to the direct tunnelling effect
Q_D	QD	C	Charge in the equivalent n-MOST attributed to the drain node
Q_G	QG	C	Charge in the equivalent n-MOST attributed to the gate node
Q_S	QS	C	Charge in the equivalent n-MOST attributed to the source node
Q_B	QB	C	Charge in the equivalent n-MOST attributed to the bulk node
Q_{ov0}	QOVO	C	Extrinsic charge in the equivalent n-MOST attributed to the gate-source overlap
Q_{ovL}	QOVL	C	Extrinsic charge in the equivalent n-MOST attributed to the gate-drain overlap
S_{th}	STH	A ² s	Spectral density of the thermal-noise current of the channel

S_{fl}	SFL	A^2_s	Spectral density of the flicker-noise current of the channel
S_{ig}	SIG	A^2_s	Spectral density of the noise current induced in the gate
S_{igth}	SIGTH	A^2_s	Cross spectral density of the noise current induced in the gate and the thermal-noise current of the channel

1.3.2 Parameters and clipping: physical geometrical scaling rules

These parameters correspond to the geometrical model (MN, MP, MOS11010).

Symbol	Progr. Name	Units	Description
-	LEVEL	-	Must be 11010
-	PARAMCHK	-	Level of clip warning info *)
ΔL_{PS}	LVAR	m	Difference between the actual and the programmed poly-silicon gate length
$\Delta L_{\text{overlap}}$	LAP	m	Effective channel length reduction per side due to the lateral diffusion of the source/drain dopant ions
ΔW_{OD}	WVAR	m	Difference between the actual and the programmed field-oxide opening
ΔW_{narrow}	WOT	m	Effective reduction of the channel width per side due to the lateral diffusion of the channel-stop dopant ions
T_R	TR	°C	Reference temperature
V_{FB}	VFB	V	Flat-band voltage at the reference temperature
$S_{T;V_{FB}}$	STVFB	VK ⁻¹	Coefficient of the temperature dependence of V_{FB}
k_{0R}	KOR	V ^{1/2}	Body-effect factor for an infinite square transistor
$S_{L;k_0}$	SLKO	-	Coefficient of the length dependence of k_0
$S_{L2;k_0}$	SL2KO	-	Second coefficient of the length dependence of k_0
$S_{L3;k_0}$	SL3KO	-	Third coefficient of the length dependence of k_0
	SL3KOEXP	-	Exponent belonging to the third coefficient of the length dependence of k_0
$S_{W;k_0}$	SWKO	-	Coefficient of the width dependence of k_0

Symbol	Progr. Name	Units	Description
$1/k_p$	KPINV	$V^{-1/2}$	Inverse of body-effect factor of the poly-silicon gate
ϕ_{BR}	PHIBR	V	Surface potential at the onset of strong inversion at the reference temperature
$S_{T;\phi_B}$	STPHIB	VK^{-1}	Coefficient of the temperature dependence of ϕ_B
$S_{L;\phi_B}$	SLPHIB	-	Coefficient of the length dependence of ϕ_B
$S_{L2;\phi_B}$	SL2PHIB	-	Second coefficient of the length dependence of ϕ_B
$S_{W;\phi_B}$	SWPHIB	-	Coefficient of the width dependence of ϕ_B
β_{sq}	BETSQ	AV^{-2}	Gain factor for an infinite square transistor at the reference temperature
$\eta_{\beta R}$	ETABETR	-	Exponent of the temperature dependence of the gain factor of an infinite square transistor
$S_{L;\eta_\beta}$	SLETABET	-	Coefficient of the length dependence of $\eta_{\beta R}$
$f_{\beta,1}$	FBET1	-	Relative mobility decrease due to first lateral profile
$L_{P,1}$	LP1	m	Characteristic length of first lateral profile
$f_{\beta,2}$	FBET2	-	Relative mobility decrease due to second lateral profile
$L_{P,2}$	LP2	m	Characteristic length of second lateral profile
θ_{srR}	THESRR	V^{-1}	Coefficient of the mobility reduction due to surface roughness scattering for an infinite square transistor at the reference temperature
η_{sr}	ETASR	-	Exponent of the temperature dependence of θ_{sr}
$S_{W;\theta_{sr}}$	SWTHESR	-	Coefficient of the width dependence of θ_{sr}

Symbol	Progr. Name	Units	Description
θ_{phR}	THEPHR	V ⁻¹	Coefficient of the mobility reduction due to phonon scattering for an infinite square transistor at the reference temperature
η_{ph}	ETAPH	-	Exponent of the temperature dependence of θ_{ph} for the reference transistor
$S_{W;\theta_{ph}}$	SWTHEPH	-	Coefficient of the width dependence of θ_{ph}
η_{mobR}	ETAMOBR	-	Effective field parameter for dependence on depletion/ inversion charge for an infinite square transistor
$S_{T;\eta_{mob}}$	STETAMOB	K ⁻¹	Coefficient of the temperature dependence of η_{mob}
$S_{W;\eta_{mob}}$	SWETAMOB	-	Coefficient of the width dependence of η_{mob}
ν	NU	-	Exponent of the field dependence of the mobility model at the reference temperature
ν_{EXP}	NUEXP	-	Exponent of the temperature dependence of parameter ν
θ_{RR}	THERR	V ⁻¹	Coefficient of the series resistance per unit length for an infinitely wide transistor at the reference temperature
η_R	ETAR	-	Exponent of the temperature dependence of θ_R
$S_{W;\theta_R}$	SWTHER	-	Coefficient of the width dependence of θ_R
θ_{R1}	THER1	V	Numerator of the gate voltage dependent part of series resistance
θ_{R2}	THER2	V	Denominator of the gate voltage dependent part of series resistance
θ_{satR}	THESATR	V ⁻¹	Velocity saturation parameter due to optical/acoustic phonon scattering for an infinite square transistor at the reference temperature

Symbol	Progr. Name	Units	Description
η_{sat}	ETASAT	-	Exponent of the temperature dependence of θ_{sat}
$S_{L;\theta_{sat}}$	SLTHESAT	-	Coefficient of the length dependence of θ_{sat}
θ_{satEXP}	THESATEXP	-	Exponent of the length dependence of θ_{sat}
$S_{W;\theta_{sat}}$	SWTHESAT	-	Coefficient of the width dependence of θ_{sat}
θ_{Thr}	THETHR	V^{-3}	Coefficient of self-heating per unit length for an infinitely wide transistor at the reference temperature
θ_{ThEXP}	THETHEXP	-	Exponent of the length dependence of θ_{Th}
$S_{W;\theta_{Th}}$	SWTHETH	-	Coefficient of the width dependence of θ_{Th}
σ_{dibl0}	SDIBLO	$V^{-1/2}$	Drain-induced barrier-lowering parameter per unit length
$\sigma_{diblEXP}$	SDIBLEXP	-	Exponent of the length dependence of σ_{dibl}
m_{00}	MOO	-	Parameter for short-channel subthreshold slope
m_{0R}	MOR	-	Parameter for short-channel subthreshold slope per unit length
m_{0EXP}	MOEXP	-	Exponent of the length dependence of m_0
σ_{sfR}	SSFR	$V^{-1/2}$	Static feedback parameter for an infinite square transistor
$S_{L;\sigma_{sf}}$	SLSSF	-	Coefficient of the length dependence of σ_{sf}
$S_{W;\sigma_{sf}}$	SWSSF	-	Coefficient of the width dependence of σ_{sf}
α_R	ALPR	-	Factor of the channel length modulation for an infinite square transistor
$S_{L;\alpha}$	SLALP	-	Coefficient of the length dependence of α
α_{EXP}	ALPEXP	-	Exponent of the length dependence of α
$S_{W;\alpha}$	SWALP	-	Coefficient of the width dependence of α

Symbol	Progr. Name	Units	Description
V_P	VP	V	Characteristic voltage of the channel length modulation
L_{min}	LMIN	m	Minimum effective channel length in technology, used for calculation of smoothing factor m
a_{1R}	A1R	-	Factor of the weak-avalanche current for an infinite square transistor at the reference temperature
$S_{T;a_1}$	STA1	K ⁻¹	Coefficient of the temperature dependence of a_1
$S_{L;a_1}$	SLA1	-	Coefficient of the length dependence of a_1
$S_{W;a_1}$	SWA1	-	Coefficient of the width dependence of a_1
a_{2R}	A2R	V	Exponent of the weak-avalanche current for an infinite square transistor
$S_{L;a_2}$	SLA2	-	Coefficient of the length dependence of a_2
$S_{W;a_2}$	SWA2	-	Coefficient of the width dependence of a_2
a_{3R}	A3R	-	Factor of the drain-source voltage above which weak-avalanche occurs, for an infinite square transistor
$S_{L;a_3}$	SLA3	-	Coefficient of the length dependence of a_3
$S_{W;a_3}$	SWA3	-	Coefficient of the width dependence of a_3
I_{GINVR}	IGINVR	AV ⁻²	Gain factor for intrinsic gate tunnelling current in inversion for a channel area of $1\mu m^2$
B_{inv}	BINV	V	Probability factor for intrinsic gate tunnelling current in inversion
I_{GACCR}	IGACCR	AV ⁻²	Gain factor for intrinsic gate tunnelling current in accumulation for a channel area of $1\mu m^2$

Symbol	Progr. Name	Units	Description
B_{acc}	BACC	V	Probability factor for intrinsic gate tunneling current in accumulation
V_{FBov}	VFBOV	V	Flat-band voltage for the source/drain overlap extensions
k_{ov}	KOV	$V^{1/2}$	Body-effect factor for the source/drain overlap extensions
I_{GOVR}	IGOVR	AV^{-2}	Gain factor for source/drain overlap gate tunnelling current for a channel width of $1\mu m$
	AGIDLR	AV^{-3}	Gain factor for gate-induced drain leakage current for a channel width of $1\mu m$
	BGIDL	V	Probability factor for gate-induced drain leakage current at the reference temperature
	STBGIDL	VK^{-1}	Coefficient of the temperature dependence of BGIDL
	CGIDL	-	Factor for the lateral field dependence of the gate-induced drain leakage current
t_{ox}	TOX	m	Thickness of the gate-oxide layer.
C_{ol}	COL	F	Gate overlap capacitance for a channel width of $1\mu m$
-	GATENOISE	-	Flag for in/exclusion of induced gate thermal noise
N_T	NT	J	Coefficient of the thermal noise at the reference temperature
N_{FAR}	NFAR	$V^{-1}m^{-4}$	First coefficient of the flicker noise for a channel area of $1\mu m^2$
N_{FBR}	NFBR	$V^{-1}m^{-2}$	Second coefficient of the flicker noise for a channel area of $1\mu m^2$
N_{FCR}	NFCR	V^{-1}	Third coefficient of the flicker noise for a channel area of $1\mu m^2$

Symbol	Progr. Name	Units	Description
ΔT_A	DTA	K	Temperature offset of the device with respect to T_A

The additional parameters for the model including self-heating (see section 1.6 on page 125) are listed in the table below.

Symbol	Progr. Name	Units	Description
R_{Th}	RTH	°C/W	Thermal resistance
C_{Th}	CTH	J/°C	Thermal capacitance
A_{TH}	ATH	-	Temperature coefficient of the thermal resistance

The L , W and $MULT$ parameters are listed in the table below.

Symbol	Progr. Name	Units	Description
L	L	m	Drawn channel length in the lay-out of the actual transistor
W	W	m	Drawn channel width in the lay-out of the actual transistor
N_{MULT}	MULT	-	Number of devices in parallel
-	PRINT-SCALED	-	Flag to add scaled parameters to the OP output

Remark: The parameters L , W , and DTA are used to calculate the electrical parameters of the actual transistor, as specified in the section on parameter preprocessing.

*) See Appendix D for the definition of PARAMCHK.

Default and clipping values (physical geometrical model)

The default values and clipping values as used for the parameters of the physical geometrical MOS model, level 1101 (n-channel) are listed below.

Parameter	Units	Default	Clip low	Clip high
<i>LEVEL</i>	-	11010	-	-
<i>PARAMCHK</i>	-	0	-	-
<i>LVAR</i>	m	0.000	-	-
<i>LAP</i>	m	4.0×10^{-8}	-	-
<i>WVAR</i>	m	0.000	-	-
<i>WOT</i>	m	0.000	-	-
<i>TR</i>	°C	21.0	-273.0	-
<i>VFB</i>	V	-1.050	-	-
<i>STVFB</i>	VK ⁻¹	0.5×10^{-3}	-	-
<i>KOR</i>	V ^{1/2}	0.500	-	-
<i>SLKO</i>	-	0.000	-	-
<i>SL2KO</i>	-	0.000	-	-
<i>SL3KO</i>	-	0.000	-	-
<i>SL3KOEXP</i>	-	1.000	-	-
<i>SWKO</i>	-	0.000	-	-
<i>KPINV</i>	V ^{-1/2}	0.000	-	-
<i>PHIBR</i>	V	0.950	-	-
<i>STPHIB</i>	VK ⁻¹	-8.5×10^{-4}	-	-
<i>SLPHIB</i>	-	0.000	-	-
<i>SL2PHIB</i>	-	0.000	-	-
<i>SWPHIB</i>	-	0.000	-	-
<i>BETSQ</i>	AV ⁻²	3.709×10^{-4}	-	-
<i>ETABETR</i>	-	1.300	-	-

Parameter	Units	Default	Clip low	Clip high
<i>SLETABET</i>	-	0.000	-	-
<i>FBET1</i>	-	0.000	-	-
<i>LP1</i>	m	0.8×10^{-6}	1.0×10^{-10}	-
<i>FBET2</i>	-	0.000	-	-
<i>LP2</i>	m	0.8×10^{-6}	1.0×10^{-10}	-
<i>THESRR</i>	V ⁻¹	0.400	-	-
<i>ETASR</i>	-	0.650	-	-
<i>SWTHESR</i>	-	0.000	-	-
<i>THEPHR</i>	V ⁻¹	1.29×10^{-2}	-	-
<i>ETAPH</i>	-	1.350	-	-
<i>SWTHEPH</i>	-	0.000	-	-
<i>ETAMOBR</i>	-	1.40	-	-
<i>STETAMOB</i>	K ⁻¹	0.000	-	-
<i>SWETAMOB</i>	-	0.000	-	-
<i>NU</i>	-	2.000	1.000	100
<i>NUEXP</i>	-	5.250	-	-
<i>THERR</i>	V ⁻¹	0.155	1.0×10^{-10}	-
<i>ETAR</i>	-	0.950	-	-
<i>SWTHER</i>	-	0.000	-	-
<i>THER1</i>	V	0.000	-	-
<i>THER2</i>	V	1.000	-	-
<i>THESATR</i>	V ⁻¹	0.500	-	-
<i>ETASAT</i>	-	1.040	-	-
<i>SLTHESAT</i>	-	1.000	-	-
<i>THESATEXP</i>	-	1.000	0.000	-
<i>SWTHESAT</i>	-	0.000	-	-

Parameter	Units	Default	Clip low	Clip high
<i>THETHR</i>	V ³	1.0 × 10 ⁻³	-	-
<i>THETHEXP</i>	-	1.000	0.000	-
<i>SWTHETH</i>	-	0.000	-	-
<i>SDIBLO</i>	V ^{-1/2}	1.0 × 10 ⁻⁴	-	-
<i>SDIBLEXP</i>	-	1.350	-	-
<i>MOO</i>	-	0.000	-	-
<i>MOR</i>	-	0.000	-	-
<i>MOEXP</i>	-	1.340	-	-
<i>SSFR</i>	V ^{-1/2}	6.25 × 10 ⁻³	-	-
<i>SLSSF</i>	-	1.000	-	-
<i>SWSSF</i>	-	0.000	-	-
<i>ALPR</i>	-	1.0 × 10 ⁻²	-	-
<i>SLALP</i>	-	1.000	-	-
<i>ALPEXP</i>	-	1.000	0.000	-
<i>SWALP</i>	-	0.000	-	-
<i>VP</i>	V	5.0 × 10 ⁻²	-	-
<i>LMIN</i>	m	1.5 × 10 ⁻⁷	1.0 × 10 ⁻¹⁰	2.5 × 10 ⁻⁶
<i>AIR</i>	-	6.000	-	-
<i>STAI</i>	K ⁻¹	0.000	-	-
<i>SLA1</i>	-	0.000	-	-
<i>SWA1</i>	-	0.000	-	-
<i>A2R</i>	V	38.00	-	-
<i>SLA2</i>	-	0.000	-	-
<i>SWA2</i>	-	0.000	-	-
<i>A3R</i>	-	1.000	-	-
<i>SLA3</i>	-	0.000	-	-

Parameter	Units	Default	Clip low	Clip high
<i>SWA3</i>	-	0.000	-	-
<i>IGINVR</i>	AV ⁻²	0.000	0.000	-
<i>BINV</i>	V	48.00	0.000	-
<i>IGACCR</i>	AV ⁻²	0.000	0.000	-
<i>BACC</i>	V	48.00	0.000	-
<i>VFBOV</i>	V	0.000	-	-
<i>KOV</i>	V ^{1/2}	2.500	1.0 × 10 ⁻¹²	-
<i>IGOVR</i>	AV ⁻²	0.000	0.000	-
<i>AGIDLR</i>	AV ⁻³	0.000	0.000	-
<i>BGIDL</i>	V	41.00	0.000	-
<i>STBGIDL</i>	VK ⁻¹	-3.638X10 ⁻⁴	-	-
<i>CGIDL</i>	-	0.000	0.000	-
<i>TOX</i>	m	3.2 × 10 ⁻⁹	1.0 × 10 ⁻¹²	-
<i>COL</i>	F	3.2 × 10 ⁻¹⁶	-	-
<i>GATENOISE</i>	-	0.000	0.000	1.000
<i>NT</i>	J	1.624 × 10 ⁻²⁰	0.000	-
<i>NFAR</i>	V ⁻¹ m ⁻⁴	1.573 × 10 ²³	-	-
<i>NFBR</i>	V ⁻¹ m ⁻²	4.752 × 10 ⁹	-	-
<i>NFCR</i>	V ⁻¹	0.000	-	-
<i>DTA</i>	K	0.000	-	-

The additional values and clipping values of the additional parameters for the (**n-channel**) model including self-heating (see section 1.6 on page 125) are listed in the table below.

Parameter	Units	Default	Clip low	Clip high
<i>RTH</i>	°C/W	300.0	0.000	-

Parameter	Units	Default	Clip low	Clip high
<i>CTH</i>	J°C	3.0×10^{-9}	0.000	-
<i>ATH</i>	-	0.0	-	-

The *L*, *W* and *MULT* parameters are listed in the table below.

Parameter	Units	Default	Clip low	Clip high
<i>L</i>	m	2.000×10^{-6}	-	-
<i>W</i>	m	1.000×10^{-5}	-	-
<i>MULT</i>	-	1.000	0.000	-
<i>PRINT-SCALED</i>	-	0	-	-

Remark: The parameters *L*, *W*, and *DTA* are used to calculate the electrical parameters of the actual transistor, as specified in the section on parameter preprocessing.

The default values and clipping values as used for the parameters of the physical geometrical MOS model, level 1101 (p-channel) are listed below.

Parameter	Units	Default	Clip low	Clip high
<i>LEVEL</i>	-	11010	-	-
<i>PARAMCHK</i>	-	0	-	-
<i>LVAR</i>	m	0.000	-	-
<i>LAP</i>	m	4.0×10^{-8}	-	-
<i>WVAR</i>	m	0.000	-	-
<i>WOT</i>	m	0.000	-	-
<i>TR</i>	°C	21.0	-273.0	-
<i>VFB</i>	V	-1.050	-	-
<i>STVFB</i>	VK ⁻¹	0.5×10^{-3}	-	-
<i>KOR</i>	V ^{1/2}	0.500	-	-
<i>SLKO</i>	-	0.000	-	-
<i>SL2KO</i>	-	0.000	-	-
<i>SL3KO</i>	-	0.000	-	-
<i>SL3KOEXP</i>	-	1.000	-	-
<i>SWKO</i>	-	0.000	-	-
<i>KPINV</i>	V ^{-1/2}	0.000	-	-
<i>PHIBR</i>	V	0.950	-	-
<i>STPHIB</i>	VK ⁻¹	-8.5×10^{-4}	-	-
<i>SLPHIB</i>	-	0.000	-	-
<i>SL2PHIB</i>	-	0.000	-	-
<i>SWPHIB</i>	-	0.000	-	-
<i>BETSQ</i>	AV ⁻²	1.150×10^{-4}	-	-
<i>ETABETR</i>	-	0.500	-	-
<i>SLETABET</i>	-	0.000	-	-

Parameter	Units	Default	Clip low	Clip high
<i>FBET1</i>	-	0.000	-	-
<i>LP1</i>	m	0.8×10^{-6}	1.0×10^{-10}	-
<i>FBET2</i>	-	0.000	-	-
<i>LP2</i>	m	0.8×10^{-6}	1.0×10^{-10}	-
<i>THESRR</i>	V ⁻¹	0.730	-	-
<i>ETASR</i>	-	0500	-	-
<i>SWTHESR</i>	-	0.000	-	-
<i>THEPHR</i>	V ⁻¹	1.0×10^{-3}	-	-
<i>ETAPH</i>	-	3.750	-	-
<i>SWTHEPH</i>	-	0.000	-	-
<i>ETAMOBR</i>	-	3.000	-	-
<i>STETAMOB</i>	K ⁻¹	0.000	-	-
<i>SWETAMOB</i>	-	0.000	-	-
<i>NU</i>	-	2.000	1.000	100
<i>NUEXP</i>	-	3.230	-	-
<i>THERR</i>	V ⁻¹	0.080	1.0×10^{-10}	-
<i>ETAR</i>	-	0.400	-	-
<i>SWTHER</i>	-	0.000	-	-
<i>THER1</i>	V	0.000	-	-
<i>THER2</i>	V	1.000	-	-
<i>THESATR</i>	V ⁻¹	0.200	-	-
<i>ETASAT</i>	-	0.860	-	-
<i>SLTHESAT</i>	-	1.000	-	-
<i>THESATEXP</i>	-	1.000	0.000	-
<i>SWTHESAT</i>	-	0.000	-	-
<i>THETHR</i>	V ⁻³	0.5×10^{-3}	-	-

Parameter	Units	Default	Clip low	Clip high
<i>THETHEXP</i>	-	1.000	0.000	-
<i>SWTHETH</i>	-	0.000	-	-
<i>SDIBLO</i>	V ^{-1/2}	1.0 × 10 ⁻⁴	-	-
<i>SDIBLEXP</i>	-	1.350	-	-
<i>MOO</i>	-	0.000	-	-
<i>MOR</i>	-	0.000	-	-
<i>MOEXP</i>	-	1.340	-	-
<i>SSSFR</i>	V ^{-1/2}	6.25 × 10 ⁻³	-	-
<i>SLSSF</i>	-	1.000	-	-
<i>SWSSF</i>	-	0.000	-	-
<i>ALPR</i>	-	1.0 × 10 ⁻²	-	-
<i>SLALP</i>	-	1.000	-	-
<i>ALPEXP</i>	-	1.000	0.000	-
<i>SWALP</i>	-	0.000	-	-
<i>VP</i>	V	5.0 × 10 ⁻²	-	-
<i>LMIN</i>	m	1.5 × 10 ⁻⁷	1.0 × 10 ⁻¹⁰	2.5 × 10 ⁻⁶
<i>AIR</i>	-	6.000	-	-
<i>STA1</i>	K ⁻¹	0.000	-	-
<i>SLA1</i>	-	0.000	-	-
<i>SWA1</i>	-	0.000	-	-
<i>A2R</i>	V	38.00	-	-
<i>SLA2</i>	-	0.000	-	-
<i>SWA2</i>	-	0.000	-	-
<i>A3R</i>	-	1.000	-	-
<i>SLA3</i>	-	0.000	-	-
<i>SWA3</i>	-	0.000	-	-

Parameter	Units	Default	Clip low	Clip high
<i>IGINVR</i>	AV ⁻²	0.000	0.000	-
<i>BINV</i>	V	87.50	0.000	-
<i>IGACCR</i>	AV ⁻²	0.000	0.000	-
<i>BACC</i>	V	48.00	0.000	-
<i>VFBOV</i>	V	0.000	-	-
<i>KOV</i>	V ^{1/2}	2.500	1.0 × 10 ⁻¹²	-
<i>IGOVR</i>	AV ⁻²	0.000	0.000	-
<i>AGIDLR</i>	AV ⁻³	0.000	0.000	-
<i>BGIDL</i>	V	41.00	0.000	-
<i>STBGIDL</i>	VK ⁻¹	-3.638X10 ⁻⁴	-	-
<i>CGIDL</i>	-	0.000	0.000	-
<i>TOX</i>	m	3.2 × 10 ⁻⁹	1.0 × 10 ⁻¹²	-
<i>COL</i>	F	3.2 × 10 ⁻¹⁶	-	-
<i>GATENOISE</i>	-	0.000	0.000	1.000
<i>NT</i>	J	1.656 × 10 ⁻²⁰	0.000	-
<i>NFAR</i>	V ⁻¹ m ⁻⁴	3.825 × 10 ²⁴	-	-
<i>NFBR</i>	V ⁻¹ m ⁻²	1.015 × 10 ⁹	-	-
<i>NFCR</i>	V ⁻¹	7.300 × 10 ⁻⁸	-	-
<i>DTA</i>	K	0.000	-	-

The additional values and clipping values of the additional parameters for the (**p-channel**) model including self-heating (see section 1.6 on page 125) are listed in the table below.

Parameter	Units	Default	Clip low	Clip high
<i>RTH</i>	°C/W	300.0	0.000	-
<i>CTH</i>	J/°C	3.0×10 ⁻⁹	0.000	-

Parameter	Units	Default	Clip low	Clip high
<i>ATH</i>	-	0.0	-	-

The *L*, *W* and *MULT* parameters are listed in the table below.

Parameter	Units	Default	Clip low	Clip high
<i>L</i>	m	2.000×10^{-6}	-	-
<i>W</i>	m	1.000×10^{-5}	-	-
<i>MULT</i>	-	1.000	0.000	-
<i>PRINT-SCALED</i>	-	0	-	-

Remark: The parameters *L*, *W*, and *DTA* are used to calculate the electrical parameters of the actual transistor, as specified in the section on parameter preprocessing.

1.3.3 Parameters and clipping: binning geometrical scaling rules

These parameters correspond to the geometrical model (MN, MP, MOS11011) for binning geometrical scaling in the model.

Note that for each bin ($W_{min}, W_{max}, L_{min}, L_{max}$) there is a separate parameter set, which is valid for (W, L) values with $W_{min} \leq W \leq W_{max}$ and $L_{min} \leq L \leq L_{max}$.

Symbol	Progr. Name	Units	Description
-	LEVEL	-	Must be 11011
-	PARAMCHK	-	Level of clip warning info
ΔL_{PS}	LVAR	m	Difference between the actual and the programmed poly-silicon gate length
$\Delta L_{overlap}$	LAP	m	Effective channel length reduction per side due to the lateral diffusion of the source/drain dopant ions
ΔW_{OD}	WVAR	m	Difference between the actual and the programmed field-oxide opening
ΔW_{narrow}	WOT	m	Effective reduction of the channel width per side due to the lateral diffusion of the channel-stop dopant ions
T_R	TR	°C	Reference temperature
V_{FB}	VFB	V	Flat-band voltage for all the transistors in the bin at the reference temperature
$P_{0;k_0}$	POKO	$V^{1/2}$	Coefficient for the geometry independent part of k_0
$P_{L;k_0}$	PLKO	$V^{1/2}$	Coefficient for the length dependence of k_0
$P_{W;k_0}$	PWKO	$V^{1/2}$	Coefficient for the width dependence of k_0
$P_{LW;k_0}$	PLWKO	$V^{1/2}$	Coefficient for the length times width dependence of k_0
$1/k_P$	KPINV	$V^{-1/2}$	Inverse of the body-effect factor of the poly-silicon gate

Symbol	Progr. Name	Units	Description
$P_{0;\phi_B}$	POPHIB	V	Coefficient for the geometry independent part of ϕ_B
$P_{L;\phi_B}$	PLPHIB	V	Coefficient for the length dependence of ϕ_B
$P_{W;\phi_B}$	PWPHIB	V	Coefficient for the width dependence of ϕ_B
$P_{LW;\phi_B}$	PLWPHIB	V	Coefficient for the length times width dependence of ϕ_B
$P_{0;\beta}$	POBET	AV^{-2}	Coefficient for the geometry independent part of β
$P_{L;\beta}$	PLBET	AV^{-2}	Coefficient for the length dependence of β
$P_{W;\beta}$	PWBET	AV^{-2}	Coefficient for the width dependence of β
$P_{LW;\beta}$	PLWBET	AV^{-2}	Coefficient for the width over length dependence of β
$P_{0;\theta_{sr}}$	POTHE SR	V^{-1}	Coefficient for the geometry independent part of θ_{sr}
$P_{L;\theta_{sr}}$	PLTHE SR	V^{-1}	Coefficient for the length dependence of θ_{sr}
$P_{W;\theta_{sr}}$	PWTHE SR	V^{-1}	Coefficient for the width dependence of θ_{sr}
$P_{LW;\theta_{sr}}$	PLWTHE SR	V^{-1}	Coefficient for the length times width dependence of θ_{sr}
$P_{0;\theta_{ph}}$	POTHE PH	V^{-1}	Coefficient for the geometry independent part of θ_{ph}
$P_{L;\theta_{ph}}$	PLTHE PH	V^{-1}	Coefficient for the length dependence of θ_{ph}

Symbol	Progr. Name	Units	Description
$P_{W;\theta_{ph}}$	PWTHEPH	V^{-1}	Coefficient for the width dependence of θ_{ph}
$P_{LW;\theta_{ph}}$	PLWTHEPH	V^{-1}	Coefficient for the length times width dependence of θ_{ph}
$P_{0;\eta_{mob}}$	POETAMOB	-	Coefficient for the geometry independent part of η_{mob}
$P_{L;\eta_{mob}}$	PLETAMOB	-	Coefficient for the length dependence of η_{mob}
$P_{W;\eta_{mob}}$	PWETAMOB	-	Coefficient for the width dependence of η_{mob}
$P_{LW;\eta_{mob}}$	PLWETAMOB	-	Coefficient for the length times width dependence of η_{mob}
$P_{0;\theta_R}$	POTHER	V^{-1}	Coefficient for the geometry independent part of θ_R
$P_{L;\theta_R}$	PLTHER	V^{-1}	Coefficient for the length dependence of θ_R
$P_{W;\theta_R}$	PWTHER	V^{-1}	Coefficient for the width dependence of θ_R
$P_{LW;\theta_R}$	PLWTHER	V^{-1}	Coefficient for the length times width dependence of θ_R
θ_{R1}	THER1	V	Numerator of the gate voltage dependent part of series resistance for all the transistors in the bin
θ_{R2}	THER2	V	Denominator of the gate voltage dependent part of series resistance for all the transistors in the bin
$P_{0;\theta_{sat}}$	POTHSAT	V^{-1}	Coefficient for the geometry independent part of θ_{sat}
$P_{L;\theta_{sat}}$	PLTHESAT	V^{-1}	Coefficient for the length dependence of θ_{sat}

Symbol	Progr. Name	Units	Description
$P_{W;\theta_{sat}}$	PWTHESAT	V^{-1}	Coefficient for the width dependence of θ_{sat}
$P_{LW;\theta_{sat}}$	PLWTHESAT	V^{-1}	Coefficient for the length times width dependence of θ_{sat}
$P_{0;\theta_{Th}}$	POTHETH	V^{-3}	Coefficient for the geometry independent part of θ_{Th}
$P_{L;\theta_{Th}}$	PLTHETH	V^{-3}	Coefficient for the length dependence of θ_{Th}
$P_{W;\theta_{Th}}$	PWTHETH	V^{-3}	Coefficient for the width dependence of θ_{Th}
$P_{LW;\theta_{Th}}$	PLWTHETH	V^{-3}	Coefficient for the length times width dependence of θ_{Th}
$P_{0;\sigma_{dibl}}$	POSDIBL	$V^{-1/2}$	Coefficient for the geometry independent part of σ_{dibl}
$P_{L;\sigma_{dibl}}$	PLSDIBL	$V^{-1/2}$	Coefficient for the length dependence of σ_{dibl}
$P_{W;\sigma_{dibl}}$	PWSDIBL	$V^{-1/2}$	Coefficient for the width dependence of σ_{dibl}
$P_{LW;\sigma_{dibl}}$	PLWSDIBL	$V^{-1/2}$	Coefficient for the length times width dependence of σ_{dibl}
$P_{0;m_0}$	POMO	-	Coefficient for the geometry independent part of m_0
$P_{L;m_0}$	PLMO	-	Coefficient for the length dependence of m_0
$P_{W;m_0}$	PWMO	-	Coefficient for the width dependence of m_0
$P_{LW;m_0}$	PLWMO	-	Coefficient for the length times width dependence of m_0

Symbol	Progr. Name	Units	Description
$P_{0;\sigma_{sf}}$	POSSF	$V^{-1/2}$	Coefficient for the geometry independent part of σ_{sf}
$P_{L;\sigma_{sf}}$	PLSSF	$V^{-1/2}$	Coefficient for the length dependence of σ_{sf}
$P_{W;\sigma_{sf}}$	PWSSF	$V^{-1/2}$	Coefficient for the width dependence of σ_{sf}
$P_{LW;\sigma_{sf}}$	PLWSSF	$V^{-1/2}$	Coefficient for the length times width dependence of σ_{sf}
$P_{0;\alpha}$	POALP	-	Coefficient for the geometry independent part of α
$P_{L;\alpha}$	PLALP	-	Coefficient for the length dependence of α
$P_{W;\alpha}$	PWALP	-	Coefficient for the width dependence of α
$P_{LW;\alpha}$	PLWALP	-	Coefficient for the length times width dependence of α
V_P	VP	V	Characteristic voltage of the channel length modulation
$P_{0;m}$	POMEXP	-	Coefficient for the geometry independent part of $1/m$
$P_{L;m}$	PLMEXP	-	Coefficient for the length dependence of $1/m$
$P_{W;m}$	PWMEXP	-	Coefficient for the width dependence of $1/m$
$P_{LW;m}$	PLWMEXP	-	Coefficient for the length times width dependence of $1/m$
$P_{0;a_1}$	POA1	-	Coefficient for the geometry independent part of a_1
$P_{L;a_1}$	PLA1	-	Coefficient for the length dependence of a_1

Symbol	Progr. Name	Units	Description
$P_{W;a_1}$	PWA1	-	Coefficient for the width dependence of a_1
$P_{LW;a_1}$	PLWA1	-	Coefficient for the length times width dependence of a_1
$P_{0;a_2}$	POA2	V	Coefficient for the geometry independent part of a_2
$P_{L;a_2}$	PLA2	V	Coefficient for the length dependence of a_2
$P_{W;a_2}$	PWA2	V	Coefficient for the width dependence of a_2
$P_{LW;a_2}$	PLWA2	V	Coefficient for the length times width dependence of a_2
$P_{0;a_3}$	POA3	-	Coefficient for the geometry independent part of a_3
$P_{L;a_3}$	PLA3	-	Coefficient for the length dependence of a_3
$P_{W;a_3}$	PWA3	-	Coefficient for the width dependence of a_3
$P_{LW;a_3}$	PLWA3	-	Coefficient for the length times width dependence of a_3
$P_{0;I_{GINV}}$	POIGINV	AV^{-2}	Coefficient for the geometry independent part of I_{GINV}
$P_{L;I_{GINV}}$	PLIGINV	AV^{-2}	Coefficient for the length dependence of I_{GINV}
$P_{W;I_{GINV}}$	PWIGINV	AV^{-2}	Coefficient for the width dependence of I_{GINV}
$P_{LW;I_{GINV}}$	PLWIGINV	AV^{-2}	Coefficient for the length times width dependence of I_{GINV}

Symbol	Progr. Name	Units	Description
$P_{0;B_{inv}}$	POBINV	V	Coefficient for the geometry independent part of B_{inv}
$P_{L;B_{inv}}$	PLBINV	V	Coefficient for the length dependence of B_{inv}
$P_{W;B_{inv}}$	PWBINV	V	Coefficient for the width dependence of B_{inv}
$P_{LW;B_{inv}}$	PLWBINV	V	Coefficient for the length times width dependence of B_{inv}
$P_{0;I_{GACC}}$	POIGACC	AV^{-2}	Coefficient for the geometry independent part of I_{GACC}
$P_{L;I_{GACC}}$	PLIGACC	AV^{-2}	Coefficient for the length dependence of I_{GACC}
$P_{W;I_{GACC}}$	PWIGACC	AV^{-2}	Coefficient for the width dependence of I_{GACC}
$P_{LW;I_{GACC}}$	PLWIGACC	AV^{-2}	Coefficient for the length times width dependence of I_{GACC}
$P_{0;B_{acc}}$	POBACC	V	Coefficient for the geometry independent part of B_{acc}
$P_{L;B_{acc}}$	PLBACC	V	Coefficient for the length dependence of B_{acc}
$P_{W;B_{acc}}$	PWBACC	V	Coefficient for the width dependence of B_{acc}
$P_{LW;B_{acc}}$	PLWBACC	V	Coefficient for the length times width dependence of B_{acc}
V_{FBov}	VFBOV	V	Flat-band voltage for the source/drain overlap extensions
k_{ov}	KOV	$V^{1/2}$	Bodu-effect factor for the source/drain overlap extensions

Symbol	Progr. Name	Units	Description
$P_{0;I_{GOV}}$	POIGOV	AV ⁻²	Coefficient for the geometry independent part of I_{GOV}
$P_{L;I_{GOV}}$	PLIGOV	AV ⁻²	Coefficient for the length dependence of I_{GOV}
$P_{W;I_{GOV}}$	PWIGOV	AV ⁻²	Coefficient for the width dependence of I_{GOV}
$P_{LW;I_{GOV}}$	PLWIGOV	AV ⁻²	Coefficient for the length times width dependence of I_{GOV}
$P_{0;A_{GIDL}}$	POAGIDL	AV ⁻³	Coefficient for the geometry independent part of A_{GIDL}
$P_{L;A_{GIDL}}$	PLAGIDL	AV ⁻³	Coefficient for the length dependence of A_{GIDL}
$P_{W;A_{GIDL}}$	PWAGIDL	AV ⁻³	Coefficient for the width dependence of A_{GIDL}
$P_{LW;A_{GIDL}}$	PLWAGIDL	AV ⁻³	Coefficient for the width over length dependence of A_{GIDL}
$P_{0;B_{GIDL}}$	POBGIDL	V	Coefficient for the geometry independent part of B_{GIDL}
$P_{L;B_{GIDL}}$	PLBGIDL	V	Coefficient for the length dependence of B_{GIDL}
$P_{W;B_{GIDL}}$	PWBGIDL	V	Coefficient for the width dependence of B_{GIDL}
$P_{LW;B_{GIDL}}$	PLWBGIDL	V	Coefficient for the length times width dependence of B_{GIDL}
$P_{0;C_{GIDL}}$	POCGIDL	-	Coefficient for the geometry independent part of C_{GIDL}
$P_{L;C_{GIDL}}$	PLCGIDL	-	Coefficient for the length dependence of C_{GIDL}

Symbol	Progr. Name	Units	Description
$P_{W;C_{GIDL}}$	PWCGIDL	-	Coefficient for the width dependence of C_{GIDL}
$P_{LW;C_{GIDL}}$	PLWCGIDL	-	Coefficient for the length times width dependence of C_{GIDL}
t_{ox}	TOX	m	Thickness of the gate oxide layer
$P_{0;C_{ox}}$	POCOX	F	Coefficient for the geometry independent part of C_{ox}
$P_{L;C_{ox}}$	PLCOX	F	Coefficient for the length dependence of C_{ox}
$P_{W;C_{ox}}$	PWCOX	F	Coefficient for the width dependence of C_{ox}
$P_{LW;C_{ox}}$	PLWCOX	F	Coefficient for the length times width dependence of C_{ox}
$P_{0;C_{GDO}}$	POCGDO	F	Coefficient for the geometry independent part of C_{GDO}
$P_{L;C_{GDO}}$	PLCGDO	F	Coefficient for the length dependence of C_{GDO}
$P_{W;C_{GDO}}$	PWCGDO	F	Coefficient for the width dependence of C_{GDO}
$P_{LW;C_{GDO}}$	PLWCGDO	F	Coefficient for the width over length dependence of C_{GDO}
$P_{0;C_{GSO}}$	POCGSO	F	Coefficient for the geometry independent part of C_{GSO}
$P_{L;C_{GSO}}$	PLCGSO	F	Coefficient for the length dependence of C_{GSO}
$P_{W;C_{GSO}}$	PWCGSO	F	Coefficient for the width dependence of C_{GSO}
$P_{LW;C_{GSO}}$	PLWCGSO	F	Coefficient for the width over length dependence of C_{GSO}

Symbol	Progr. Name	Units	Description
-	GATENOISE		Flag for in/exclusion of induced gate thermal noise
N_T	NT	J	Coefficient of the thermal noise at the reference temperature
$P_{0;N_{FA}}$	PONFA	$V^{-1}m^{-4}$	Coefficient for the geometry independent part of N_{FA}
$P_{L;N_{FA}}$	PLNFA	$V^{-1}m^{-4}$	Coefficient for the length dependence of N_{FA}
$P_{W;N_{FA}}$	PWNFA	$V^{-1}m^{-4}$	Coefficient for the width dependence of N_{FA}
$P_{LW;N_{FA}}$	PLWNFA	$V^{-1}m^{-4}$	Coefficient for the length times width dependence of N_{FA}
$P_{0;N_{FB}}$	PONFB	$V^{-1}m^{-2}$	Coefficient for the geometry independent part of N_{FB}
$P_{L;N_{FB}}$	PLNFB	$V^{-1}m^{-2}$	Coefficient for the length dependence of N_{FB}
$P_{W;N_{FB}}$	PWNFB	$V^{-1}m^{-2}$	Coefficient for the width dependence of N_{FB}
$P_{LW;N_{FB}}$	PLWNFB	$V^{-1}m^{-2}$	Coefficient for the length times width dependence of N_{FB}
$P_{0;N_{FC}}$	PONFC	V^{-1}	Coefficient for the geometry independent part of N_{FC}
$P_{L;N_{FC}}$	PLNFC	V^{-1}	Coefficient for the length dependence of N_{FC}
$P_{W;N_{FC}}$	PWNFC	V^{-1}	Coefficient for the width dependence of N_{FC}
$P_{LW;N_{FC}}$	PLWNFC	V^{-1}	Coefficient for the length times width dependence of N_{FC}

Symbol	Progr. Name	Units	Description
$P_{0;T;V_{FB}}$	POTVFB	VK ⁻¹	Coefficient for the geometry independent part of $S_{T;V_{FB}}$
$P_{L;T;V_{FB}}$	PLTVFB	VK ⁻¹	Coefficient for the length dependence of $S_{T;V_{FB}}$
$P_{W;T;V_{FB}}$	PWTVFB	VK ⁻¹	Coefficient for the width dependence of $S_{T;V_{FB}}$
$P_{LW;T;V_{FB}}$	PLWTVFB	VK ⁻¹	Coefficient for the length times width dependence of $S_{T;V_{FB}}$
$P_{0;T;\phi_B}$	POTPHIB	VK ⁻¹	Coefficient for the geometry independent part of $S_{T;\phi_B}$
$P_{L;T;\phi_B}$	PLTPHIB	VK ⁻¹	Coefficient for the length dependence of $S_{T;\phi_B}$
$P_{W;T;\phi_B}$	PWTPHIB	VK ⁻¹	Coefficient for the width dependence of $S_{T;\phi_B}$
$P_{LW;T;\phi_B}$	PLWTPHIB	VK ⁻¹	Coefficient for the length times width dependence of $S_{T;\phi_B}$
$P_{0;T;\eta_\beta}$	POTETABET	-	Coefficient for the geometry independent part of η_β
$P_{L;T;\eta_\beta}$	PLTETABET	-	Coefficient for the length dependence of η_β
$P_{W;T;\eta_\beta}$	PWTETABET	-	Coefficient for the width dependence of η_β
$P_{LW;T;\eta_\beta}$	PLWTETABET	-	Coefficient for the length times width dependence of η_β
$P_{0;T;\eta_{sr}}$	POTETASR	-	Coefficient for the geometry independent part of η_{sr}
$P_{L;T;\eta_{sr}}$	PLTETASR	-	Coefficient for the length dependence of η_{sr}

Symbol	Progr. Name	Units	Description
$P_{W;T;\eta_{sr}}$	PWTETASR	-	Coefficient for the width dependence of η_{sr}
$P_{LW;T;\eta_{sr}}$	PLWTETASR	-	Coefficient for the length times width dependence of η_{sr}
$P_{0;T;\eta_{ph}}$	POTETAPH	-	Coefficient for the geometry independent part of η_{ph}
$P_{L;T;\eta_{ph}}$	PLTETAPH	-	Coefficient for the length dependence of η_{ph}
$P_{W;T;\eta_{ph}}$	PWTETAPH	-	Coefficient for the width dependence of η_{ph}
$P_{LW;T;\eta_{ph}}$	PLWTETAPH	-	Coefficient for the length times width dependence of η_{ph}
$P_{0;T;\eta_{mob}}$	POTETAMOB	K^{-1}	Coefficient for the geometry independent part of $S_{T;\eta_{mob}}$
$P_{L;T;\eta_{mob}}$	PLTETAMOB	K^{-1}	Coefficient for the length dependence of $S_{T;\eta_{mob}}$
$P_{W;T;\eta_{mob}}$	PWTETAMOB	K^{-1}	Coefficient for the width dependence of $S_{T;\eta_{mob}}$
$P_{LW;T;\eta_{mob}}$	PLWTETAMOB	K^{-1}	Coefficient for the length times width dependence of $S_{T;\eta_{mob}}$
ν	NU	-	Exponent of the field dependence of the mobility model at the reference temperature
$P_{0;T;\nu_{exp}}$	POTNUEXP	-	Coefficient for the geometry independent part of ν_{exp}
$P_{L;T;\nu_{exp}}$	PLTNUEXP	-	Coefficient for the length dependence of ν_{exp}
$P_{W;T;\nu_{exp}}$	PWTNUEXP	-	Coefficient for the width dependence of ν_{exp}

Symbol	Progr. Name	Units	Description
$P_{LW;T;\nu_{exp}}$	PLWTNUEXP	-	Coefficient for the length times width dependence of ν_{exp}
$P_{0;T;\eta_R}$	POTETAR	-	Coefficient for the geometry independent part of η_R
$P_{L;T;\eta_R}$	PLTETAR	-	Coefficient for the length dependence of η_R
$P_{W;T;\eta_R}$	PWTETAR	-	Coefficient for the width dependence of η_R
$P_{LW;T;\eta_R}$	PLWTETAR	-	Coefficient for the length times width dependence of η_R
$P_{0;T;\eta_{sat}}$	POTETASAT	-	Coefficient for the geometry independent part of η_{sat}
$P_{L;T;\eta_{sat}}$	PLTETASAT	-	Coefficient for the length dependence of η_{sat}
$P_{W;T;\eta_{sat}}$	PWTETASAT	-	Coefficient for the width dependence of η_{sat}
$P_{LW;T;\eta_{sat}}$	PLWTETASAT	-	Coefficient for the length times width dependence of η_{sat}
$P_{0;T;a_1}$	POTA1	K^{-1}	Coefficient for the geometry independent part of $S_{T;a_1}$
$P_{L;T;a_1}$	PLTA1	K^{-1}	Coefficient for the length dependence of $S_{T;a_1}$
$P_{W;T;a_1}$	PWTA1	K^{-1}	Coefficient for the width dependence of $S_{T;a_1}$
$P_{LW;T;a_1}$	PLWTA1	K^{-1}	Coefficient for the length times width dependence of $S_{T;a_1}$
$P_{0;T;B_{GIDL}}$	POTBGIDL	VK^{-1}	Coefficient for the geometry independent part of $S_{T;B_{GIDL}}$

Symbol	Progr. Name	Units	Description
$P_{L;T;B_{GIDL}}$	PLTBGIDL	VK^{-1}	Coefficient for the length dependence of $S_{T;B_{GIDL}}$
$P_{W;T;B_{GIDL}}$	PWTBGIDL	VK^{-1}	Coefficient for the width dependence of $S_{T;B_{GIDL}}$
$P_{LW;T;B_{GIDL}}$	PLWTBGIDL	VK^{-1}	Coefficient for the length times width dependence of $S_{T;B_{GIDL}}$
ΔT_A	DTA	K	Temperature offset of the device with respect to T_A
l_{\min}	LMIN	m	minimum length of the bin
l_{\max}	LMAX	m	maximum length of the bin
w_{\min}	WMIN	m	minimum width of the bin
w_{\max}	WMAX	m	maximum width of the bin

The additional parameters for the model including self-heating (see section 1.6 on page 125) are listed in the table below.

Symbol	Progr. Name	Units	Description
R_{TH}	RTH	$^{\circ}\text{C}/\text{W}$	Thermal resistance
C_{TH}	CTH	$\text{J}/^{\circ}\text{C}$	Thermal capacitance
A_{TH}	ATH	-	Temperature coefficient of the thermal resistance

The L , W and $MULT$ parameters are listed in the table below.

Symbol	Progr. Name	Units	Description
L	L	m	Drawn channel length in the lay-out of the actual transistor
W	W	m	Drawn channel width in the lay-out of the actual transistor
N_{MULT}	MULT	-	Number of devices in parallel

Symbol	Progr. Name	Units	Description
-	<i>PRINTSCALED</i>	0	Flag to add scaled parameters to the OP output

Remark: The parameters *L*, *W*, and *DTA* are used to calculate the electrical parameters of the actual transistor, as specified in the section on parameter preprocessing.

Default and clipping values (binning geometrical model)

The default values and clipping values for the parameters of the binning geometrical scaling rules of MOS model, level 1101 (n-channel) are listed below.

Parameter	Units	Default	Clip low	Clip high
<i>LEVEL</i>	-	11011	-	-
<i>PARAMCHK</i>	-	0	-	-
<i>LVAR</i>	m	0.000	-	-
<i>LAP</i>	m	4.0×10^{-8}	-	-
<i>WVAR</i>	m	0.000	-	-
<i>WOT</i>	m	0.000	-	-
<i>TR</i>	°C	21.0	-273.0	-
<i>VFB</i>	V	-1.050	-	-
<i>POKO</i>	V ^{1/2}	0.500	-	-
<i>PLKO</i>	V ^{1/2}	0.000	-	-
<i>PWKO</i>	V ^{1/2}	0.000	-	-
<i>PLWKO</i>	V ^{1/2}	0.000	-	-
<i>KPINV</i>	V ^{-1/2}	0.000	-	-
<i>POPHIB</i>	V	0.950	-	-
<i>PLPHIB</i>	V	0.000	-	-
<i>PWPHIB</i>	v	0.000	-	-
<i>PLWPHIB</i>	V	0.000	-	-
<i>POBET</i>	AV ⁻²	1.922×10^{-3}	-	-
<i>PLBET</i>	AV ⁻²	0.000	-	-
<i>PWBET</i>	AV ⁻²	0.000	-	-
<i>PLWBET</i>	AV ⁻²	0.000	-	-
<i>POTHSER</i>	V ⁻¹	3.562×10^{-1}	-	-

Parameter	Units	Default	Clip low	Clip high
<i>PLTHESR</i>	V ⁻¹	0.000	-	-
<i>PWTHESR</i>	V ⁻¹	0.000	-	-
<i>PLWTHESR</i>	V ⁻¹	0.000	-	-
<i>POTHEPH</i>	V ⁻¹	1.290×10^{-2}	-	-
<i>PLTHEPH</i>	V ⁻¹	0.000	-	-
<i>PWTHEPH</i>	V ⁻¹	0.000	-	-
<i>PLWTHEPH</i>	V ⁻¹	0.000	-	-
<i>POETAMOB</i>	-	1.400	-	-
<i>PLETAMOB</i>	-	0.000	-	-
<i>PWETAMOB</i>	-	0.000	-	-
<i>PLWETAMOB</i>	-	0.000	-	-
<i>POTHER</i>	V ⁻¹	8.120×10^{-2}	-	-
<i>PLTHER</i>	V ⁻¹	0.000	-	-
<i>PWTHER</i>	V ⁻¹	0.000	-	-
<i>PLWTHER</i>	V ⁻¹	0.000	-	-
<i>THER1</i>	V	0.000	-	-
<i>THER2</i>	V	1.000	-	-
<i>POTHSAT</i>	V ⁻¹	2.513×10^{-1}	-	-
<i>PLHSAT</i>	V ⁻¹	0.000	-	-
<i>PWHSAT</i>	V ⁻¹	0.000	-	-
<i>PLWHSAT</i>	V ⁻¹	0.000	-	-
<i>POTHEETH</i>	V ⁻³	1.0×10^{-5}	-	-
<i>PLHEETH</i>	V ⁻³	0.000	-	-
<i>PWHEETH</i>	V ⁻³	0.000	-	-

Parameter	Units	Default	Clip low	Clip high
<i>PLWTHETH</i>	V ⁻³	0.000	-	-
<i>POSDIBL</i>	V ^{-1/2}	8.530 ×10 ⁻⁴	-	-
<i>PLSDIBL</i>	V ^{-1/2}	0.000	-	-
<i>PWSDIBL</i>	V ^{-1/2}	0.000	-	-
<i>PLWSDIBL</i>	V ^{-1/2}	0.000	-	-
<i>POMO</i>	-	0.000	-	-
<i>PLMO</i>	-	0.000	-	-
<i>PWMO</i>	-	0.000	-	-
<i>PLWMO</i>	-	0.000	-	-
<i>POSSF</i>	V ^{-1/2}	1.200 ×10 ⁻²	-	-
<i>PLSSF</i>	V ^{-1/2}	0.000	-	-
<i>PWSSF</i>	V ^{-1/2}	0.000	-	-
<i>PLWSSF</i>	V ^{-1/2}	0.000	-	-
<i>POALP</i>	-	2.500 ×10 ⁻²	-	-
<i>PLALP</i>	-	0.000	-	-
<i>PWALP</i>	-	0.000	-	-
<i>PLWALP</i>	-	0.000	-	-
<i>VP</i>	V	5.000 ×10 ⁻²	-	-
<i>POMEXP</i>	-	0.200	-	-
<i>PLMEXP</i>	-	0.000	-	-
<i>PWMEXP</i>	-	0.000	-	-
<i>PLWMEXP</i>	-	0.000	-	-
<i>POAI</i>	-	6.022	-	-
<i>PLAI</i>	-	0.000	-	-
<i>PWAI</i>	-	0.000	-	-

Parameter	Units	Default	Clip low	Clip high
<i>PLWA1</i>	-	0.000	-	-
<i>POA2</i>	V	3.802×10^1	-	-
<i>PLA2</i>	V	0.000	-	-
<i>PWA2</i>	V	0.000	-	-
<i>PLWA2</i>	V	0.000	-	-
<i>POA3</i>	-	6.407×10^{-1}	-	-
<i>PLA3</i>	-	0.000	-	-
<i>PWA3</i>	-	0.000	-	-
<i>PLWA3</i>	-	0.000	-	-
<i>POIGINV</i>	AV^{-2}	0.000	-	-
<i>PLIGINV</i>	-	0.000	-	-
<i>PWIGINV</i>	-	0.000	-	-
<i>PLWIGINV</i>	-	0.000	-	-
<i>POBINV</i>	V	4.800×10^1	-	-
<i>PLBINV</i>	V	0.000	-	-
<i>PWBINV</i>	V	0.000	-	-
<i>PLWBINV</i>	V	0.000	-	-
<i>POIGACC</i>	AV^{-2}	0.000	-	-
<i>PLIGACC</i>	AV^{-2}	0.000	-	-
<i>PWIGACC</i>	AV^{-2}	0.000	-	-
<i>PLWIGACC</i>	AV^{-2}	0.000	-	-
<i>POBACC</i>	V	4.800×10^1	-	-
<i>PLBACC</i>	V	0.000	-	-
<i>PWBACC</i>	V	0.000	-	-
<i>PLWBACC</i>	V	0.000	-	-

Parameter	Units	Default	Clip low	Clip high
<i>VFBOV</i>	V	0.000	-	-
<i>KOV</i>	V ^{1/2}	2.500	1.0 × 10 ⁻¹²	-
<i>POIGOV</i>	AV ⁻²	0.000	-	-
<i>PLIGOV</i>	AV ⁻²	0.000	-	-
<i>PWIGOV</i>	AV ⁻²	0.000	-	-
<i>PLWIGOV</i>	AV ⁻²	0.000	-	-
<i>POAGIDL</i>	AV ⁻³	0.000	-	-
<i>PLAGIDL</i>	AV ⁻³	0.000	-	-
<i>PWAGIDL</i>	AV ⁻³	0.000	-	-
<i>PLWAGIDL</i>	AV ⁻³	0.000	-	-
<i>POBGIDL</i>	V	4.100 × 10 ⁺¹	-	-
<i>PLBGIDL</i>	V	0.000	-	-
<i>PWBGIDL</i>	V	0.000	-	-
<i>PLWBGIDL</i>	V	0.000	-	-
<i>POCGIDL</i>	-	0.000	-	-
<i>PLCGIDL</i>	-	0.000	-	-
<i>PWCGIDL</i>	-	0.000	-	-
<i>PLWCCGIDL</i>	-	0.000	-	-
<i>TOX</i>	m	3.200 × 10 ⁻⁹	1.0 × 10 ⁻¹²	-
<i>POCOX</i>	F	2.980 × 10 ⁻¹⁴	-	-
<i>PLCOX</i>	F	0.000	-	-
<i>PWCOX</i>	F	0.000	-	-
<i>PLWCOX</i>	F	0.000	-	-
<i>POCGDO</i>	F	6.392 × 10 ⁻¹⁵	-	-
<i>PLCGDO</i>	F	0.000	-	-

Parameter	Units	Default	Clip low	Clip high
<i>PWCGDO</i>	F	0.000	-	-
<i>PLWCGDO</i>	F	0.000	-	-
<i>POCGSO</i>	F	6.392×10^{-15}	-	-
<i>PLCGSO</i>	F	0.000	-	-
<i>PWCGSO</i>	F	0.000	-	-
<i>PLWCGSO</i>	F	0.000	-	-
<i>GATENOISE</i>	-	0.000	0.000	1.000
<i>NT</i>	J	1.656×10^{-20}	0.000	-
<i>PONFA</i>	$V^{-1}m^{-4}$	8.323×10^{22}	-	-
<i>PLNFA</i>	$V^{-1}m^{-4}$	0.000	-	-
<i>PWNFA</i>	$V^{-1}m^{-4}$	0.000	-	-
<i>PLWNFA</i>	$V^{-1}m^{-4}$	0.000	-	-
<i>PONFB</i>	$V^{-1}m^{-2}$	2.514×10^7	-	-
<i>PLNFB</i>	$V^{-1}m^{-2}$	0.000	-	-
<i>PWNFB</i>	$V^{-1}m^{-2}$	0.000	-	-
<i>PLWNFB</i>	$V^{-1}m^{-2}$	0.000	-	-
<i>PONFC</i>	V^{-1}	0.000	-	-
<i>PLNFC</i>	V^{-1}	0.000	-	-
<i>PWNFC</i>	V^{-1}	0.000	-	-
<i>PLWNFC</i>	V^{-1}	0.000	-	-
<i>POTVFB</i>	VK^{-1}	5.000×10^{-4}	-	-
<i>PLTVFB</i>	VK^{-1}	0.000	-	-
<i>PWTVFB</i>	VK^{-1}	0.000	-	-
<i>PLWTVFB</i>	VK^{-1}	0.000	-	-

Parameter	Units	Default	Clip low	Clip high
<i>POTPHIB</i>	VK ⁻¹	-8.500 × 10 ⁻⁴	-	-
<i>PLTPHIB</i>	VK ⁻¹	0.000	-	-
<i>PWTPHIB</i>	VK ⁻¹	0.000	-	-
<i>PLWTPHIB</i>	VK ⁻¹	0.000	-	-
<i>POTETABET</i>	-	1.300	-	-
<i>PLTETABET</i>	-	0.000	-	-
<i>PWTETABET</i>	-	0.000	-	-
<i>PLWTETABET</i>	-	0.000	-	-
<i>POTETASR</i>	-	0.650	-	-
<i>PLTETASR</i>	-	0.000	-	-
<i>PWTETASR</i>	-	0.000	-	-
<i>PLWETASR</i>	-	0.000	-	-
<i>POTETAPH</i>	-	1.350	-	-
<i>PLTETAPH</i>	-	0.000	-	-
<i>PWTETAPH</i>	-	0.000	-	-
<i>PLWETAPH</i>	-	0.000	-	-
<i>POTETAMOB</i>	K ⁻¹	0.000	-	-
<i>PLTETAMOB</i>	K ⁻¹	0.000	-	-
<i>PWTETAMOB</i>	K ⁻¹	0.000	-	-
<i>PLWTETAMOB</i>	K ⁻¹	0.000	-	-
<i>NU</i>	-	2.000	1.000	100
<i>POTNUEXP</i>	-	5.250	-	-
<i>PLTNUEXP</i>	-	0.000	-	-
<i>PWTNUEXP</i>	-	0.000	-	-
<i>PLWTNUEXP</i>	-	0.000	-	-
<i>POTETAR</i>	-	0.950	-	-

Parameter	Units	Default	Clip low	Clip high
<i>PLTETAR</i>	-	0.000	-	-
<i>PWTETAR</i>	-	0.000	-	-
<i>PLWTETAR</i>	-	0.000	-	-
<i>POTETASAT</i>	-	1.040	-	-
<i>PLTETASAT</i>	-	0.000	-	-
<i>PWTETASAT</i>	-	0.000	-	-
<i>PLWTETASAT</i>	-	0.000	-	-
<i>POTAI</i>	K ⁻¹	0.000	-	-
<i>PLTAI</i>	K ⁻¹	0.000	-	-
<i>PWTAI</i>	K ⁻¹	0.000	-	-
<i>PLWTAI</i>	K ⁻¹	0.000	-	-
<i>POTBGIDL</i>	VK ⁻¹	-3.638x10 ⁻⁴	-	-
<i>PLTBGIDL</i>	VK ⁻¹	0.000	-	-
<i>PWTBGIDL</i>	VK ⁻¹	0.000	-	-
<i>PLWTBGIDL</i>	VK ⁻¹	0.000	-	-
<i>DTA</i>	K	0.000	-	-
<i>LMIN</i>	m	0	no	no
<i>LMAX</i>	m	1	no	no
<i>WMIN</i>	m	0	no	no
<i>WMAX</i>	m	1	no	no

The additional values and clipping values of the additional parameters for the (**n-channel**) model including self-heating (see section 1.6 on page 125) are listed in the table below.

Parameter	Units	Default	Clip low	Clip high
<i>RTH</i>	°C/W	300.0	0.000	-
<i>CTH</i>	J/°C	3.0×10 ⁻⁹	0.000	-

Parameter	Units	Default	Clip low	Clip high
<i>ATH</i>	-	0.0	-	-

The *L*, *W* and *MULT* parameters are listed in the table below.

Parameter	Units	Default	Clip low	Clip high
<i>L</i>	m	2.000×10^{-6}	-	-
<i>W</i>	m	1.000×10^{-5}	-	-
<i>MULT</i>	-	1.000	0.000	-
<i>PRINT-SCALED</i>	-	0	-	-

Remark: The parameters *L*, *W*, and *DTA* are used to calculate the electrical parameters of the actual transistor, as specified in the section on parameter preprocessing.

The default values and clipping values for the parameters of the binning geometrical scaling rules of MOS model, level 1101 (p-channel) are listed below.

Parameter	Units	Default	Clip low	Clip high
<i>LEVEL</i>	-	11011	-	-
<i>PARAMCHK</i>	-	0	-	-
<i>LVAR</i>	m	0.000	-	-
<i>LAP</i>	m	4.0×10^{-8}	-	-
<i>WVAR</i>	m	0.000	-	-
<i>WOT</i>	m	0.000	-	-
<i>TR</i>	°C	21.0	-273.0	-
<i>VFB</i>	V	-1.050	-	-
<i>POKO</i>	$V^{1/2}$	0.500	-	-
<i>PLKO</i>	$V^{1/2}$	0.000	-	-
<i>PWKO</i>	$V^{1/2}$	0.000	-	-
<i>PLWKO</i>	$V^{1/2}$	0.000	-	-
<i>KPINV</i>	$V^{-1/2}$	0.000	-	-
<i>POPHIB</i>	V	0.950	-	-
<i>PLPHIB</i>	V	0.000	-	-
<i>PWPHIB</i>	V	0.000	-	-
<i>PLWPHIB</i>	V	0.000	-	-
<i>POBET</i>	AV^{-2}	3.814×10^{-4}	-	-
<i>PLBET</i>	AV^{-2}	0.000	-	-
<i>PWBET</i>	AV^{-2}	0.000	-	-
<i>PLWBET</i>	AV^{-2}	0.000	-	-
<i>POTHSER</i>	V^{-1}	7.300×10^{-1}	-	-
<i>PLTHESR</i>	V^{-1}	0.000	-	-

Parameter	Units	Default	Clip low	Clip high
<i>PWTHESR</i>	V ⁻¹	0.000	-	-
<i>PLWTHESR</i>	V ⁻¹	0.000	-	-
<i>POTHEPH</i>	V ⁻¹	1.000 × 10 ⁻³	-	-
<i>PLTHEPH</i>	V ⁻¹	0.000	-	-
<i>PWTHEPH</i>	V ⁻¹	0.000	-	-
<i>PLWTHEPH</i>	V ⁻¹	0.000	-	-
<i>POETAMOB</i>	-	3.000	-	-
<i>PLETAMOB</i>	-	0.000	-	-
<i>PWETAMOB</i>	-	0.000	-	-
<i>PLWETAMOB</i>	-	0.000	-	-
<i>POTHER</i>	V ⁻¹	7.900 × 10 ⁻²	-	-
<i>PLTHER</i>	V ⁻¹	0.000	-	-
<i>PWTHER</i>	V ⁻¹	0.000	-	-
<i>PLWTHER</i>	V ⁻¹	0.000	-	-
<i>THER1</i>	V	0.000	-	-
<i>THER2</i>	V	1.000	-	-
<i>POTHE SAT</i>	V ⁻¹	1.728 × 10 ⁻¹	-	-
<i>PLTHE SAT</i>	V ⁻¹	0.000	-	-
<i>PWTHE SAT</i>	V ⁻¹	0.000	-	-
<i>PLWTHE SAT</i>	V ⁻¹	0.000	-	-
<i>POTHE TH</i>	V ⁻³	0.000	-	-
<i>PLTHE TH</i>	V ⁻³	0.000	-	-
<i>PWTHE TH</i>	V ⁻³	0.000	-	-
<i>PLWTHE TH</i>	V ⁻³	0.000	-	-

Parameter	Units	Default	Clip low	Clip high
<i>POSDIBL</i>	V ^{-1/2}	3.551 × 10 ⁻⁵	-	-
<i>PLSDIBL</i>	V ^{-1/2}	0.000	-	-
<i>PWSDIBL</i>	V ^{-1/2}	0.000	-	-
<i>PLWSDIBL</i>	V ^{-1/2}	0.000	-	-
<i>POMO</i>	-	0.000	-	-
<i>PLMO</i>	-	0.000	-	-
<i>PWMO</i>	-	0.000	-	-
<i>PLWMO</i>	-	0.000	-	-
<i>POSSF</i>	V ^{-1/2}	1.000 × 10 ⁻²	-	-
<i>PLSSF</i>	V ^{-1/2}	0.000	-	-
<i>PWSSF</i>	V ^{-1/2}	0.000	-	-
<i>PLWSSF</i>	V ^{-1/2}	0.000	-	-
<i>POALP</i>	-	2.500 × 10 ⁻²	-	-
<i>PLALP</i>	-	0.000	-	-
<i>PWALP</i>	-	0.000	-	-
<i>PLWALP</i>	-	0.000	-	-
<i>VP</i>	V	5.000 × 10 ⁻²	-	-
<i>POMEXP</i>	-	0.200	-	-
<i>PLMEXP</i>	-	0.000	-	-
<i>PWMEXP</i>	-	0.000	-	-
<i>PLWMEXP</i>	-	0.000	-	-
<i>POA1</i>	-	6.858	-	-
<i>PLA1</i>	-	0.000	-	-
<i>PWA1</i>	-	0.000	-	-
<i>PLWA1</i>	-	0.000	-	-

Parameter	Units	Default	Clip low	Clip high
<i>POA2</i>	V	5.732×10^1	-	-
<i>PLA2</i>	V	0.000	-	-
<i>PWA2</i>	V	0.000	-	-
<i>PLWA2</i>	V	0.000	-	-
<i>POA3</i>	-	4.254×10^{-1}	-	-
<i>PLA3</i>	-	0.000	-	-
<i>PWA3</i>	-	0.000	-	-
<i>PLWA3</i>	-	0.000	-	-
<i>POIGINV</i>	AV^{-2}	0.000	-	-
<i>PLIGINV</i>	-	0.000	-	-
<i>PWIGINV</i>	-	0.000	-	-
<i>PLWIGINV</i>	-	0.000	-	-
<i>POBINV</i>	V	87.50	-	-
<i>PLBINV</i>	V	0.000	-	-
<i>PWBINV</i>	V	0.000	-	-
<i>PLWBINV</i>	V	0.000	-	-
<i>POIGACC</i>	AV^{-2}	0.000	-	-
<i>PLIGACC</i>	AV^{-2}	0.000	-	-
<i>PWIGACC</i>	AV^{-2}	0.000	-	-
<i>PLWIGACC</i>	AV^{-2}	0.000	-	-
<i>POBACC</i>	V	48.00	-	-
<i>PLBACC</i>	V	0.000	-	-
<i>PWBACC</i>	V	0.000	-	-
<i>PLWBACC</i>	V	0.000	-	-
<i>VFBOV</i>	V	0.000	-	-

Parameter	Units	Default	Clip low	Clip high
<i>KOV</i>	V ^{1/2}	2.500	1e-12	-
<i>POIGOV</i>	AV ⁻²	0.000	-	-
<i>PLIGOV</i>	AV ⁻²	0.000	-	-
<i>PWIGOV</i>	AV ⁻²	0.000	-	-
<i>PLWIGOV</i>	AV ⁻²	0.000	-	-
<i>POAGIDL</i>	AV ⁻³	0.000	-	-
<i>PLAGIDL</i>	AV ⁻³	0.000	-	-
<i>PWAGIDL</i>	AV ⁻³	0.000	-	-
<i>PLWAGIDL</i>	AV ⁻³	0.000	-	-
<i>POBGIDL</i>	V	4.100 x10 ⁺¹	-	-
<i>PLBGIDL</i>	V	0.000	-	-
<i>PWBGIDL</i>	V	0.000	-	-
<i>PLWBGIDL</i>	V	0.000	-	-
<i>POCGIDL</i>	-	0.000	-	-
<i>PLCGIDL</i>	-	0.000	-	-
<i>PWCGIDL</i>	-	0.000	-	-
<i>PLWCCGIDL</i>	-	0.000	-	-
<i>TOX</i>	m	3.200 ×10 ⁻⁹	1e-12	-
<i>POCOX</i>	F	2.717 ×10 ⁻¹⁴	-	-
<i>PLCOX</i>	F	0.000	-	-
<i>PWCOX</i>	F	0.000	-	-
<i>PLWCOX</i>	F	0.000	-	-
<i>POCGDO</i>	F	6.358 ×10 ⁻¹⁵	-	-
<i>PLCGDO</i>	F	0.000	-	-
<i>PWCGDO</i>	F	0.000	-	-

Parameter	Units	Default	Clip low	Clip high
<i>PLWCGDO</i>	F	0.000	-	-
<i>POCGSO</i>	F	6.358×10^{-15}	-	-
<i>PLCGSO</i>	F	0.000	-	-
<i>PWCGSO</i>	F	0.000	-	-
<i>PLWCGSO</i>	F	0.000	-	-
<i>GATENOISE</i>	-	0.000	0.000	1.000
<i>NT</i>	J	1.656×10^{-20}	0	-
<i>PONFA</i>	$V^{-1}m^{-4}$	1.900×10^{22}	-	-
<i>PLNFA</i>	$V^{-1}m^{-4}$	0.000	-	-
<i>PWNFA</i>	$V^{-1}m^{-4}$	0.000	-	-
<i>PLWNFA</i>	$V^{-1}m^{-4}$	0.000	-	-
<i>PONFB</i>	$V^{-1}m^{-2}$	5.043×10^6	-	-
<i>PLNFB</i>	$V^{-1}m^{-2}$	0.000	-	-
<i>PWNFB</i>	$V^{-1}m^{-2}$	0.000	-	-
<i>PLWNFB</i>	$V^{-1}m^{-2}$	0.000	-	-
<i>PONFC</i>	V^{-1}	3.627×10^{-10}	-	-
<i>PLNFC</i>	V^{-1}	0.000	-	-
<i>PWNFC</i>	V^{-1}	0.000	-	-
<i>PLWNFC</i>	V^{-1}	0.000	-	-
<i>POTVFB</i>	VK^{-1}	0.5×10^{-3}	-	-
<i>PLTVFB</i>	VK^{-1}	0.000	-	-
<i>PWTVFB</i>	VK^{-1}	0.000	-	-
<i>PLWTVFB</i>	VK^{-1}	0.000	-	-
<i>POTPHIB</i>	VK^{-1}	-8.5×10^{-4}	-	-

Parameter	Units	Default	Clip low	Clip high
<i>PLTPHIB</i>	VK ⁻¹	0.000	-	-
<i>PWTPHIB</i>	VK ⁻¹	0.000	-	-
<i>PLWTPHIB</i>	VK ⁻¹	0.000	-	-
<i>POTETABET</i>	-	0.500	-	-
<i>PLTETABET</i>	-	0.000	-	-
<i>PWTETABET</i>	-	0.000	-	-
<i>PLWTETABET</i>	-	0.000	-	-
<i>POTETASR</i>	-	0.500	-	-
<i>PLTETASR</i>	-	0.000	-	-
<i>PWTETASR</i>	-	0.000	-	-
<i>PLWTETASR</i>	-	0.000	-	-
<i>POTETAPH</i>	-	3.750	-	-
<i>PLTETAPH</i>	-	0.000	-	-
<i>PWTETAPH</i>	-	0.000	-	-
<i>PLWTETAPH</i>	-	0.000	-	-
<i>POTETAMOB</i>	K ⁻¹	0.000	-	-
<i>PLTETAMOB</i>	K ⁻¹	0.000	-	-
<i>PWTETAMOB</i>	K ⁻¹	0.000	-	-
<i>PLWTETAMOB</i>	K ⁻¹	0.000	-	-
<i>NU</i>	-	2.000	1	100
<i>POTNUEXP</i>	-	3.230	-	-
<i>PLTNUEXP</i>	-	0.000	-	-
<i>PWTNUEXP</i>	-	0.000	-	-
<i>PLWTNUEXP</i>	-	0.000	-	-
<i>POTETAR</i>	-	0.400	-	-
<i>PLTETAR</i>	-	0.000	-	-

Parameter	Units	Default	Clip low	Clip high
<i>PWTETAR</i>	-	0.000	-	-
<i>PLWTETAR</i>	-	0.000	-	-
<i>POTETASAT</i>	-	0.860	-	-
<i>PLTETASAT</i>	-	0.000	-	-
<i>PWTETASAT</i>	-	0.000	-	-
<i>PLWTETASAT</i>	-	0.000	-	-
<i>POTA1</i>	K ⁻¹	0.000	-	-
<i>PLTA1</i>	K ⁻¹	0.000	-	-
<i>PWTA1</i>	K ⁻¹	0.000	-	-
<i>PLWTA1</i>	K ⁻¹	0.000	-	-
<i>POTBGIDL</i>	VK ⁻¹	-3.638x10 ⁻⁴	-	-
<i>PLTBGIDL</i>	VK ⁻¹	0.000	-	-
<i>PWTBGIDL</i>	VK ⁻¹	0.000	-	-
<i>PLWTBGIDL</i>	VK ⁻¹	0.000	-	-
<i>DTA</i>	K	0.000	-	-
<i>LMIN</i>	m	0	no	no
<i>LMAX</i>	m	1	no	no
<i>WMIN</i>	m	0	no	no
<i>WMAX</i>	m	1	no	no

The additional values and clipping values of the additional parameters for the (**p-channel**) model including self-heating (see section 1.6 on page 125) are listed in the table below.

Parameter	Units	Default	Clip low	Clip high
<i>RTH</i>	°C/W	300.0	0.000	-
<i>CTH</i>	J/°C	3.0×10 ⁻⁹	0.000	-
<i>ATH</i>	-	0.0	-	-

The L , W and $MULT$ parameters are listed in the table below.

Parameter	Units	Default	Clip low	Clip high
L	m	2.000×10^{-6}	-	-
W	m	1.000×10^{-5}	-	-
$MULT$	-	1.000	0.000	-
$PRINT-$ $SCALED$	-	0	-	-

Remark: The parameters L , W , and DTA are used to calculate the electrical parameters of the actual transistor, as specified in the section on parameter preprocessing.

1.3.4 Parameters and clipping: electrical model

These parameter correspond to the electrical model (MNE, MPE, MOS1101e).

Symbol	Progr. Name	Units	Description
-	LEVEL	-	Must be 1101
-	PARAMCHK	-	Level of clip warning info
T_R	TR	°C	Reference temperature
V_{FB}	VFB	V	Flat-band voltage for the actual transistor at the reference temperature
$S_{T;V_{FB}}$	STVFB	VK ⁻¹	Coefficient of the temperature dependence of V_{FB}
k_0	K0	V ^{1/2}	Body-effect factor for the actual transistor
$1/kp$	KPINV	V ^{-1/2}	Inverse of body-effect of the poly-silicon gate for the actual transistor
ϕ_B	PHIB	V	Surface potential at the onset of strong inversion for the actual transistor at the reference temperature
$S_{T;\phi_B}$	STPHIB	VK ⁻¹	Coefficient of the temperature dependence of ϕ_B
β	BET	AV ⁻²	Gain factor for the actual transistor at the reference temperature
η_β	ETABET	-	Exponent of the temperature dependence of the gain factor
θ_{sr}	THESR	V ⁻¹	Coefficient of the mobility reduction due to surface roughness scattering for the actual transistor at the reference temperature
η_{sr}	ETASR	-	Exponent of the temperature dependence of θ_{sr}
θ_{ph}	THEPH	V ⁻¹	Coefficient of the mobility reduction due to phonon scattering for the actual transistor at the reference temperature

Symbol	Progr. Name	Units	Description
η_{ph}	ETAPH	-	Exponent of the temperature dependence of θ_{ph}
η_{mob}	ETAMOB	-	Effective field parameter for dependence on depletion/ inversion charge for the actual transistor at the reference temperature
$S_{T;\eta_{mob}}$	STETAMOB	K ⁻¹	Coefficient of the temperature dependence of η_{mob}
ν	NU	-	Exponent of field dependence of mobility model at the reference temperature
ν_{exp}	NUEXP	-	Exponent of the temperature dependence of ν
θ_R	THER	V ⁻¹	Coefficient of the series resistance for the actual transistor at the reference temperature: $\theta_R = 2 \cdot \beta \cdot R_S$
η_r	ETAR	-	Exponent of the temperature dependence of θ_R
θ_{R1}	THER1	V	Numerator of the gate voltage dependent part of series resistance for the actual transistor
θ_{R2}	THER2	V	Denominator of the gate voltage dependent part of series resistance for the actual transistor
θ_{sat}	THESAT	V ⁻¹	Velocity saturation parameter due to optical/acoustic phonon scattering for the actual transistor at the reference temperature
η_{sat}	ETASAT	-	Exponent of the temperature dependence of θ_{sat}
θ_{Th}	THETH	V ⁻³	Coefficient of self-heating for the actual transistor at the reference temperature
σ_{dibl}	SDIBL	V ^{-1/2}	Drain-induced barrier-lowering parameter for the actual transistor
m_0	MO	-	Parameter for (short-channel) subthreshold slope for the actual transistor

Symbol	Progr. Name	Units	Description
σ_{sf}	SSF	$V^{-1/2}$	Static-feedback parameter for the actual transistor
α	ALP	-	Factor of the channel-length modulation for the actual transistor
V_P	VP	V	Characteristic voltage of the channel-length modulation
m	MEXP	-	Smoothing factor for the actual transistor
a_1	A1	-	Factor of the weak-avalanche current for the actual transistor at the reference temperature
$S_{T;a_1}$	STA1	K^{-1}	Coefficient of the temperature dependence of a_1
a_2	A2	V	Exponent of the weak-avalanche current for the actual transistor
a_3	A3	-	Factor of the drain-source voltage above which weak-avalanche occurs for the actual transistor
I_{GINV}	IGINV	AV^{-2}	Gain factor for intrinsic gate tunnelling current in inversion for the actual transistor
B_{INV}	BINV	V	Probability factor for intrinsic gate tunnelling current in inversion
I_{GACC}	IGACC	AV^{-2}	Gain factor for intrinsic gate tunnelling current in accumulation for the actual transistor
B_{ACC}	BACC	V	Probability factor for intrinsic gate tunnelling current in accumulation
V_{FBov}	VFBOV	V	Flat-band voltage for the source/drain overlap extensions
k_{ov}	KOV	$V^{1/2}$	Body-effect factor for the sourcedrain overlap extensions
I_{GOV}	IGOV	AV^{-2}	Gain factor for source/drain overlap gate tunnelling current for the actual transistor
A_{GIDL}	AGIDL	AV^{-3}	Gain factor for gate-induced drain leakage current for the actual transistor

Symbol	Progr. Name	Units	Description
B_{GIDL}	BGIDL	V	Probability factor for gate-induced leakage current at the reference temperature
$S_{T:B_{GIDL}}$	STBGIDL	VK^{-1}	Coefficient of the temperature dependence of B_{GIDL}
C_{GIDL}	CGIDL	-	Factor for the lateral field dependence of the gate-induced drain leakage current
C_{ox}	COX	F	Oxide capacitance for the intrinsic channel for the actual transistor
C_{GDO}	CGDO	F	Oxide capacitance for the gate-drain overlap for the actual transistor
C_{GSO}	CGSO	F	Oxide capacitance for the gate-source overlap for the actual transistor
-	GATENOISE		Flag for in/exclusion of induced gate thermal noise
N_T	NT	J	Coefficient of the thermal noise at the reference temperature
N_{FA}	NFA	$V^{-1}m^{-4}$	First coefficient of the flicker noise for the actual transistor
N_{FB}	NFB	$V^{-1}m^{-2}$	Second coefficient of the flicker noise for the actual transistor
N_{FC}	NFC	V^{-1}	Third coefficient of the flicker noise for the actual transistor
t_{ox}	TOX	m	Thickness of the gate-oxide layer
ΔT_A	DTA	K	Temperature offset of the device with respect to ambient circuit temperature T_A

The additional parameters for the model including self-heating (see section 1.6 on page 125) are listed in the table below.

Symbol	Progr. Name	Units	Description
R_{TH}	RTH	$^{\circ}C/W$	Thermal resistance
C_{TH}	CTH	$J/^{\circ}C$	Thermal capacitance

Symbol	Progr. Name	Units	Description
A_{TH}	ATH	-	Temperature coefficient of the thermal resistance

The *MULT* parameter is listed in the table below.

Symbol	Progr. Name	Units	Description
N_{MULT}	MULT	-	Number of devices in parallel
-	PRINTSCALED	-	Flag to add scaled parameters to the OP output

3 Note

The parameter t_{ox} is used for calculation of the effective oxide thickness (due to quantum-mechanical effects) and the 1/f noise, not for the calculation of β !!!

Default and clipping values (electrical model)

The default values and clipping values as used for the parameters of the electrical MOS model, level 1101 (n-channel) are listed below.

Parameter	Units	Default	Clip low	Clip high
<i>LEVEL</i>	-	1101	-	-
<i>PARAMCHK</i>	-	0	-	-
<i>TR</i>	°C	21.0	-273.0	-
<i>VFB</i>	V	-1.0500	-	-
<i>STVFB</i>	VK ⁻¹	0.5 × 10 ⁻³	-	-
<i>KO</i>	V ^{1/2}	0.5000	1.0 × 10 ⁻¹²	-
<i>KPINV</i>	V ^{-1/2}	0.000	0.000	-
<i>PHIB</i>	V	0.9500	1.0 × 10 ⁻¹²	-
<i>STPHIB</i>	VK ⁻¹	-8.5 × 10 ⁻⁴	-	-
<i>BET</i>	AV ⁻²	1.9215 × 10 ⁻³	0.0	-
<i>ETABET</i>	-	1.300	-	-
<i>THESR</i>	V ⁻¹	0.3562	1.0 × 10 ⁻¹²	-
<i>ETASR</i>	-	0.650	-	-
<i>THEPH</i>	V ⁻¹	1.29 × 10 ⁻²	1.0 × 10 ⁻¹²	-
<i>ETAPH</i>	-	1.350	-	-
<i>ETAMOB</i>	-	1.4000	1e-12	-
<i>STETAMOB</i>	K ⁻¹	0.000	-	-
<i>NU</i>	-	2.0000	1.000	100
<i>NUEXP</i>	-	5.250	-	-
<i>THER</i>	V ⁻¹	8.12 × 10 ⁻²	0.000	-
<i>ETAR</i>	-	0.950	-	-
<i>THER1</i>	V	0.0000	0.000	-

Parameter	Units	Default	Clip low	Clip high
<i>THER2</i>	V	1.0000	0.000	-
<i>THESAT</i>	V ⁻¹	0.2513	0.000	-
<i>ETASAT</i>	-	1.040	-	-
<i>THETH</i>	V ⁻³	1.0 × 10 ⁻⁵	0.000	-
<i>SDIBL</i>	V ^{-1/2}	8.53 × 10 ⁻⁴	1.0 × 10 ⁻¹²	-
<i>MO</i>	V	0.0000	0.000	0.500
<i>SSF</i>	V ^{-1/2}	0.0120	1.0 × 10 ⁻¹²	-
<i>ALP</i>	-	0.0250	0.000	-
<i>VP</i>	V	0.0500	1.0 × 10 ⁻¹²	-
<i>MEXP</i>	-	5.0000	1.000	-
<i>A1</i>	-	6.0221	0.000	-
<i>STA1</i>	K ⁻¹	0.000	-	-
<i>A2</i>	V	38.017	1.0 × 10 ⁻¹²	-
<i>A3</i>	-	0.6407	0.000	-
<i>IGINV</i>	AV ⁻²	0.0000	0.000	-
<i>BINV</i>	V	48.000	0.000	-
<i>IGACC</i>	AV ⁻²	0.0000	0.000	-
<i>BACC</i>	V	48.000	0.000	-
<i>VFBOV</i>	V	0.0000	-	-
<i>KOV</i>	V ^{1/2}	2.5000	1.0 × 10 ⁻¹²	-
<i>IGOV</i>	AV ⁻²	0.0000	0.000	-
<i>AGIDL</i>	AV ⁻³	0.0000	0.000	-
<i>BGIDL</i>	V	41.000	0.000	-
<i>STBGIDL</i>	VK ⁻¹	-3.638 × 10 ⁻⁴	-	-
<i>CGIDL</i>	-	0.000	0.000	-

Parameter	Units	Default	Clip low	Clip high
<i>COX</i>	F	2.98×10^{-14}	0.000	-
<i>CGDO</i>	F	6.392×10^{-15}	0.000	-
<i>CGSO</i>	F	6.392×10^{-15}	0.000	-
<i>GATENOISE</i>	-	0.0000	0.000	1.000
<i>NT</i>	J	1.656×10^{-20}	0.000	-
<i>NFA</i>	$V^{-1}m^{-4}$	8.323×10^{22}	0.000	-
<i>NFB</i>	$V^{-1}m^{-2}$	2.514×10^7	-	-
<i>NFC</i>	V^{-1}	0.0000	-	-
<i>TOX</i>	m	3.2×10^{-9}	1.0×10^{-12}	-
<i>DTA</i>	K	0.000	-	-

The default values and clipping values of the additional parameters for the (**n-channel**) model including self-heating (see section 1.6 on page 125) are listed in the table below.

Parameter	Units	Default	Clip low	Clip high
<i>RTH</i>	$^{\circ}C/W$	300.0	0.000	-
<i>CTH</i>	$J/^{\circ}C$	3.0×10^{-9}	0.000	-
<i>ATH</i>	-	0.0	-	-

The *MULT* parameter is listed in the table below.

Parameter	Units	Default	Clip low	Clip high
<i>MULT</i>	-	1.000	0.000	-
<i>PRINT-SCALED</i>	-	0	-	-

The default values and clipping values as used for the parameters of the electrical MOS model, level 1101(p-channel) are listed below.

Parameter	Units	Default	Clip low	Clip high
<i>LEVEL</i>	-	1101	-	-
<i>PARAMCHK</i>	-	0	-	-
<i>TR</i>	°C	21.0	-273.0	-
<i>VFB</i>	V	-1.0500	-	-
<i>STVFB</i>	VK ⁻¹	0.5×10^{-3}	-	-
<i>KO</i>	V ^{1/2}	0.5000	1.0×10^{-12}	-
<i>KPINV</i>	V ^{-1/2}	0.000	0.000	-
<i>PHIB</i>	V	0.9500	1.0×10^{-12}	-
<i>STPHIB</i>	VK ⁻¹	-8.5×10^{-4}	-	-
<i>BET</i>	AV ⁻²	3.8140×10^{-4}	0.0	-
<i>ETABET</i>	-	0.500	-	-
<i>THESR</i>	V ⁻¹	0.7300	1.0×10^{-12}	-
<i>ETASR</i>	-	0.500	-	-
<i>THEPH</i>	V ⁻¹	0.0010	1.0×10^{-12}	-
<i>ETAPH</i>	-	3.750	-	-
<i>ETAMOB</i>	-	3.0000	1e-12	-
<i>STETAMOB</i>	K ⁻¹	0.000	-	-
<i>NU</i>	-	2.0000	1.000	100
<i>NUEXP</i>	-	3.230	-	-
<i>THER</i>	V ⁻¹	7.90×10^{-2}	0.000	-
<i>ETAR</i>	-	0.400	-	-
<i>THER1</i>	V	0.0000	0.000	-
<i>THER2</i>	V	1.0000	0.000	-

Parameter	Units	Default	Clip low	Clip high
<i>THESAT</i>	V ⁻¹	0.1728	0.000	-
<i>ETASAT</i>	-	0.860	-	-
<i>THETH</i>	V ⁻³	0.000	0.000	-
<i>SDIBL</i>	V ^{-1/2}	3.551 × 10 ⁻⁵	1.0 × 10 ⁻¹²	-
<i>MO</i>	V	0.0000	0.000	0.500
<i>SSF</i>	V ^{-1/2}	0.0100	1.0 × 10 ⁻¹²	-
<i>ALP</i>	-	0.0250	0.000	-
<i>VP</i>	V	0.0500	1.0 × 10 ⁻¹²	-
<i>MEXP</i>	-	5.0000	1.000	-
<i>A1</i>	-	6.8583	0.000	-
<i>STAI</i>	K ⁻¹	0.000	-	-
<i>A2</i>	V	57.324	1.0 × 10 ⁻¹²	-
<i>A3</i>	-	0.4254	0.000	-
<i>IGINV</i>	AV ⁻²	0.0000	0.000	-
<i>BINV</i>	V	87.500	0.000	-
<i>IGACC</i>	AV ⁻²	0.0000	0.000	-
<i>BACC</i>	V	48.000	0.000	-
<i>VFBOV</i>	V	0.0000	-	-
<i>KOV</i>	V ^{1/2}	2.5000	1.0 × 10 ⁻¹²	-
<i>IGOV</i>	AV ⁻²	0.0000	0.000	-
<i>AGIDL</i>	AV ⁻³	0.0000	0.000	-
<i>BGIDL</i>	V	41.000	0.000	-
<i>STBGIDL</i>	VK ⁻¹	-3.638 × 10 ⁻⁴	-	-
<i>CGIDL</i>	-	0.000	0.000	-
<i>COX</i>	F	2.717 × 10 ⁻¹⁴	0.000	-

Parameter	Units	Default	Clip low	Clip high
<i>CGDO</i>	F	6.358×10^{-15}	0.000	-
<i>CGSO</i>	F	6.358×10^{-15}	0.000	-
<i>GATENOISE</i>	-	0.0000	0.000	1.000
<i>NT</i>	J	1.656×10^{-20}	0.000	-
<i>NFA</i>	$V^{-1}m^{-4}$	1.900×10^{22}	0.000	-
<i>NFB</i>	$V^{-1}m^{-2}$	5.043×10^6	-	-
<i>NFC</i>	V^{-1}	3.627×10^{-10}	-	-
<i>TOX</i>	m	3.2×10^{-9}	1.0×10^{-12}	-
<i>DTA</i>	K	0.000	-	-

The default values and clipping values of the additional parameters for the (**p-channel**) model including self-heating (see section 1.6 on page 125) are listed in the table below.

Parameter	Units	Default	Clip low	Clip high
<i>RTH</i>	$^{\circ}C/W$	300.0	0.000	-
<i>CTH</i>	$J/^{\circ}C$	3.0×10^{-9}	0.000	-
<i>ATH</i>	-	0.0	-	-

The *MULT* parameter is listed in the table below.

Parameter	Units	Default	Clip low	Clip high
<i>MULT</i>	-	1.000	0.000	-
<i>PRINT-SCALED</i>	-	0	-	-

1.3.5 Model constants

The following is a list of constants hardcoded in the model.

Constant	Progr. Name	Units	Description
T_0	TO	K	Offset for conversion from Celsius to Kelvin temperature scale (273.15)
k_B	KB	JK ⁻¹	Boltzmann constant ($1.3806226 \cdot 10^{-23}$)
q	Q	C	Elementary unit charge ($1.6021918 \cdot 10^{-19}$)
ϵ_{ox}	EPSOX	Fm ⁻¹	Absolute permittivity of the oxide layer ($3.453143800 \cdot 10^{-11}$)
QM_N	QMN	Vm ^{4/3} C ^{-2/3}	Constant of quantum-mechanical behavior of electrons ($5.951993 \cdot 10^{+00}$)
QM_p	QMP	Vm ^{4/3} C ^{-2/3}	Constant of quantum-mechanical behavior of holes ($7.448711 \cdot 10^{+00}$)
χ_{BN}	CHIBN	V	Tunnelling barrier height for electrons for Si/SiO2-structure ($3.1 \cdot 10^{+00}$)
χ_{Bp}	CHIBP	V	Tunnelling barrier height for holes for Si/SiO2-structure ($4.5 \cdot 10^{+00}$)

1.4 Parameter scaling

1.4.1 Geometry scaling and temperature scaling

Calculation of Transistor Geometry

$$L_E = L - \Delta L = L + \Delta L_{PS} - 2 \cdot \Delta L_{\text{overlap}} \quad (1.1)$$

$$W_E = W - \Delta W = W + \Delta W_{OD} - 2 \cdot \Delta W_{\text{narrow}} \quad (1.2)$$

WARNING : L_E and W_E after calculation can not be less than 1.0×10^{-9} !

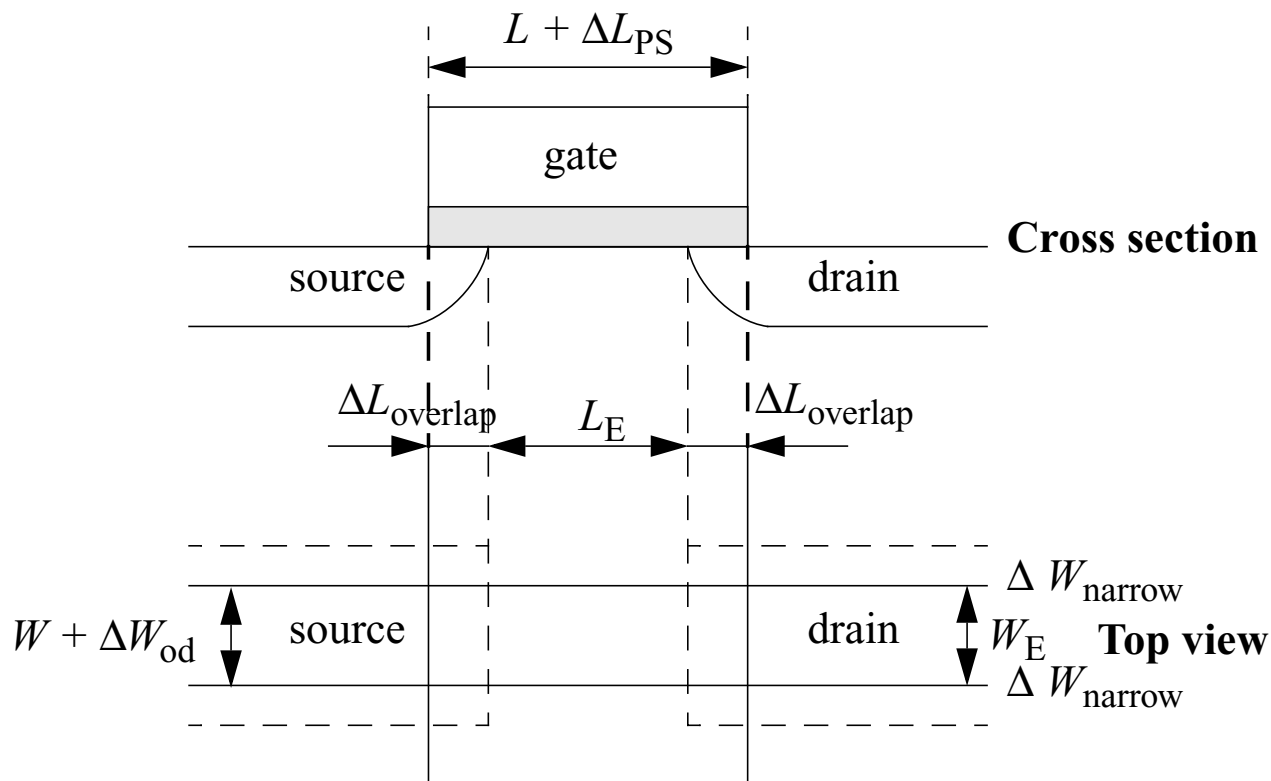


Figure 5: Specification of the dimensions of a MOS transistor

Calculation of Geometry-Dependent Parameters

In MOS Model 11, Level 1101, parameter binning has been facilitated by adding a second, separate set of geometry scaling rules. Consequently, besides the physical geometrical scaling rules there is also a set of binning geometrical scaling rules. The physical geometry scaling rules of Level 1101 have been developed to give a good description over the whole geometry range of CMOS technologies. For processes under development, however, it is sometimes useful to have more flexible scaling relations. In this case one could opt for a binning strategy, where the accuracy with geometry is mostly determined by the number of bins used. The physical scaling rules of Level 1101 are not straightforwardly applicable to binning strategies, since they may result in discontinuities in parameter values at the bin boundaries. Consequently, special binning geometrical scaling relations have been developed, which guarantee continuity in the model parameters at the bin boundaries.

It should be noted that using the source code of the Modelkit on the Philips' website (which can be found at http://www.semiconductors.philips.com/Philips_Models)

1. The physical geometry scaling rules can be selected by using Level 11010, while
2. The binning geometry scaling rules can be selected by using Level 11011.

1.4.2 Geometrical scaling with Physical Scaling Rules

$$L_{EN} = 10^{-6} \quad (1.3)$$

$$W_{EN} = 10^{-6} \quad (1.4)$$

Calculation of Threshold-Voltage Parameters

$$klen = 1 + \frac{L_{EN}}{L_E} \cdot S_{L;k_0} + \left(\frac{L_{EN}}{L_E}\right)^2 \cdot S_{L2;k_0} + \left(\frac{L_{EN}}{L_E}\right)^{SL3KOEXP} \cdot S_{L3;k_0}$$

$$kwid = 1 + \frac{W_{EN}}{W_E} \cdot S_{W;k_0}$$

$$k_0 = k_{0R} \cdot klen \cdot kwid$$

$$\phi_B = \phi_{BR} \cdot \left[1 + \frac{L_{EN}}{L_E} \cdot S_{L;\phi_B} + \left(\frac{L_{EN}}{L_E}\right)^2 \cdot S_{L2;\phi_B} \right] \cdot \left[1 + \frac{W_{EN}}{W_E} \cdot S_{W;\phi_B} \right]$$

Calculation of Mobility/Series-Resistance Parameters

$$G_{P,E} = 1 + f_{\beta,1} \cdot \frac{L_{P,1}}{L_E} \cdot \left\{ 1 - \exp\left(-\frac{L_E}{L_{P,1}}\right) \right\} + \quad (1.5)$$

$$f_{\beta,2} \cdot \frac{L_{P,2}}{L_E} \cdot \left\{ 1 - \exp\left(-\frac{L_E}{L_{P,2}}\right) \right\}$$

$$\beta = \frac{\beta_{sq}}{G_{P,E}} \cdot \frac{W_E}{L_E} \quad (1.6)$$

$$\theta_{sr} = \theta_{srR} \cdot \left[1 + \frac{W_{EN}}{W_E} \cdot S_{W;\theta_{sr}} \right] \quad (1.7)$$

$$\theta_{ph} = \theta_{phR} \cdot \left[1 + \frac{W_{EN}}{W_E} \cdot S_{W;\theta_{ph}} \right] \quad (1.8)$$

$$\eta_{mob} = \eta_{mobR} \cdot \left[1 + \frac{W_{EN}}{W_E} \cdot S_{W;\eta_{mob}} \right] \quad (1.9)$$

$$\theta_R = \theta_{RR} \cdot \left[1 + \frac{W_{EN}}{W_E} \cdot S_{W;\theta_R} \right] \cdot \frac{L_{EN}}{L_E} \cdot \frac{1}{G_{P,E}} \quad (1.10)$$

$$\theta_{sat} = \theta_{satR} \cdot \left[1 + \frac{W_{EN}}{W_E} \cdot S_{W;\theta_{sat}} \right] \cdot \left[1 + S_{L;\theta_{sat}} \cdot \left\{ \left(\frac{L_{EN}}{L_E} \right)^{\theta_{satEXP}} - 1 \right\} \right] \quad (1.11)$$

Calculation of Conductance Parameters

$$\theta_{Th} = \theta_{ThR} \cdot \left[1 + \frac{W_{EN}}{W_E} \cdot S_{W;\theta_{Th}} \right] \cdot \left[\frac{L_{EN}}{L_E} \right]^{\theta_{ThEXP}} \quad (1.12)$$

$$\sigma_{sf} = \sigma_{sfR} \cdot \left[1 + \frac{W_{EN}}{W_E} \cdot S_{W;\sigma_{sf}} \right] \cdot \left[1 + \frac{L_{EN}}{L_E} \cdot S_{L;\sigma_{sf}} \right] \quad (1.13)$$

$$\alpha = \alpha_R \cdot \left[1 + \frac{W_{EN}}{W_E} \cdot S_{W;\alpha} \right] \cdot \left[1 + S_{L;\alpha} \cdot \left\{ \left(\frac{L_{EN}}{L_E} \right)^{\alpha_{EXP}} - 1 \right\} \right] \quad (1.14)$$

Calculation of Sub-Threshold Parameters

$$\sigma_{dibl} = \sigma_{dibl0} \cdot \left(\frac{L_{EN}}{L_E} \right)^{\sigma_{diblEXP}} \quad (1.15)$$

$$m_0 = m_{00} + m_{0R} \cdot \left(\frac{L_{EN}}{L_E} \right)^{m_{0EXP}} \quad (1.16)$$

Calculation of Smoothing Parameters

$$L_{max} = 10 \cdot 10^{-6} \quad (1.17)$$

$$m = \frac{8 \cdot (L_{max} - L_{min})}{L_{max} - 4 \cdot L_{min} + 3 \cdot \frac{L_{max} \cdot L_{min}}{L_E}} \quad (1.18)$$

Calculation of Weak-Avalanche Parameters

$$a_1 = a_{1R} \cdot \left[1 + \frac{L_{EN}}{L_E} \cdot S_{L;a_1} \right] \cdot \left[1 + \frac{W_{EN}}{W_E} \cdot S_{W;a_1} \right] \quad (1.19)$$

$$a_2 = a_{2R} \cdot \left[1 + \frac{L_{EN}}{L_E} \cdot S_{L;a_2} \right] \cdot \left[1 + \frac{W_{EN}}{W_E} \cdot S_{W;a_2} \right] \quad (1.20)$$

$$a_3 = a_{3R} \cdot \left[1 + \frac{L_{EN}}{L_E} \cdot S_{L;a_3} \right] \cdot \left[1 + \frac{W_{EN}}{W_E} \cdot S_{W;a_3} \right] \quad (1.21)$$

Calculation of Gate Current Parameters

$$I_{GINV} = \frac{W_E \cdot L_E}{W_{EN} \cdot L_{EN}} \cdot I_{GINVR} \quad (1.22)$$

$$I_{GACC} = \frac{W_E \cdot L_E}{W_{EN} \cdot L_{EN}} \cdot I_{GACCR} \quad (1.23)$$

$$I_{GOV} = \frac{W_E}{W_{EN}} \cdot I_{GOVR} \quad (1.24)$$

Calculation of Gate-Induced Drain Leakage Parameters

$$A_{GIDL} = \frac{W_E}{W_{EN}} \cdot A_{GIDLR} \quad (1.25)$$

Calculation of Charge Parameters

$$C_{ox} = \epsilon_{ox} \cdot \frac{W_E \cdot L_E}{t_{ox}} \quad (1.26)$$

$$C_{GD0} = \frac{W_E}{W_{EN}} \cdot C_{ol} \quad (1.27)$$

$$C_{GS0} = \frac{W_E}{W_{EN}} \cdot C_{ol} \quad (1.28)$$

Calculation of Noise Parameters

$$N_{FA} = \frac{W_{EN} \cdot L_{EN}}{W_E \cdot L_E} \cdot N_{FAR} \quad (1.29)$$

$$N_{FB} = \frac{W_{EN} \cdot L_{EN}}{W_E \cdot L_E} \cdot N_{FBR} \quad (1.30)$$

$$N_{FC} = \frac{W_{EN} \cdot L_{EN}}{W_E \cdot L_E} \cdot N_{FCR} \quad (1.31)$$

Calculation of Mobility/Series-Resistance Temperature-Scaling Coefficients

$$\eta_{\beta} = \eta_{\beta R} + S_{L;\eta_{\beta}} \cdot \frac{L_{EN}}{L_E} \quad (1.32)$$

1.4.3 Geometrical scaling with binning scaling rules

Three types of binning geometrical scaling rules can be distinguished:

1. Type I

$$P(W_E, L_E) = P_0 + \frac{L_{EN}}{L_E} \cdot P_L + \frac{W_{EN}}{W_E} \cdot P_W + \frac{L_{EN}}{L_E} \cdot \frac{W_{EN}}{W_E} \cdot P_{LW} \quad (1.33)$$

2. Type II

$$P(W_E, L_E) = P_0 + \frac{L_E}{L_{EN}} \cdot P_L + \frac{W_E}{W_{EN}} \cdot P_W + \frac{L_E}{L_{EN}} \cdot \frac{W_E}{W_{EN}} \cdot P_{LW} \quad (1.34)$$

3. Type III

$$P(W_E, L_E) = P_0 + \frac{L_{EN}}{L_E} \cdot P_L + \frac{W_E}{W_{EN}} \cdot P_W + \frac{W_E}{L_E} \cdot P_{LW} \quad (1.35)$$

In these equations L_{EN} and W_{EN} are constants, equal to 10^{-6} .

Table 2 gives a survey of the parameters scaling.

#	Parameter	physical scaling	binning	#	parameter	physical scaling	binning
0	$LEVEL$	no	no	1	T_R	no	no
2	V_{FB}	no	no	3	$S_{T;V_{FB}}$	no	type I
4	k_0	yes	type I	5	$1/k_P$	no	no
6	ϕ_B	yes	type I	7	$S_{T;\phi_B}$	no	type I
8	β	yes	type III	9	η_β	yes	type I
10	θ_{sr}	yes	type I	11	η_{sr}	no	type I

12	θ_{ph}	yes	type I	13	η_{ph}	no	type I
14	η_{mob}	yes	type I	15	$S_{T;\eta_{mob}}$	no	type I
16	υ	no	no	17	υ_{EXP}	no	
18	θ_R	yes	type I	19	η_R	no	type I
20	θ_{R1}	no	no	21	θ_{R2}	no	no
22	θ_{sat}	yes	type I	23	η_{sat}	no	type I
24	θ_{Th}	yes	type I	25	σ_{dibl}	yes	type I
26	m_0	yes	type I	27	σ_{sf}	yes	type I
28	α	yes	type I	29	V_P	no	no
30	m	yes	type I	31	a_1	yes	type I
32	$S_{T;a_1}$	no	type I	33	a_2	yes	type I
34	a_3	yes	type I	35	I_{GINV}	yes	type II
36	B_{INV}	no	type I	37	I_{GACC}	yes	type II
38	B_{ACC}	no	type I	39	V_{RFBov}	no	no
40	k_{ov}	no	no	41	I_{GOV}	yes	type III
42	A_{GIDL}	yes	type III	43	B_{GIDL}	yes	type I
44	$S_{T;B_{GIDL}}$	yes	type I	45	C_{GIDL}	yes	type I
46	C_{ox}	yes	type II	47	C_{GDO}	yes	type III
48	C_{GSO}	yes	type III	49	$GATENOISE$	no	no

50	N_T	no	no	51	N_{FA}	yes	type I
52	N_{FB}	yes	type I	53	N_{FC}	yes	type I
54	t_{ox}	no	no	55	ΔT_A	no	no
56	N_{MULT}	no	no				

Table 2: Survey of parameters scaling. In the third column is indicated if there is a physical geometrical scaling rule for the parameter; in the fourth column the type of binning geometrical scaling rule for the parameter is indicated.

Calculation of Geometry-Dependent Parameters using the Binning Scaling Rules

Note that for each bin ($W_{min}, W_{max}, L_{min}, L_{max}$) there is a separate parameter set, which is valid for (W, L) values with $W_{min} \leq W \leq W_{max}$ and $L_{min} \leq L \leq L_{max}$.

$$L_{EN} = 10^{-6} \quad (1.36)$$

$$W_{EN} = 10^{-6} \quad (1.37)$$

Calculation of Threshold-Voltage Parameters

$$k_0 = P_{0;k_0} + \frac{L_{EN}}{L_E} \cdot P_{L;k_0} + \frac{W_{EN}}{W_E} \cdot P_{W;k_0} + \frac{L_{EN} \cdot W_{EN}}{L_E \cdot W_E} \cdot P_{LW;k_0} \quad (1.38)$$

$$\phi_B = P_{0;\phi_B} + \frac{L_{EN}}{L_E} \cdot P_{L;\phi_B} + \frac{W_{EN}}{W_E} \cdot P_{W;\phi_B} + \frac{L_{EN} \cdot W_{EN}}{L_E \cdot W_E} \cdot P_{LW;\phi_B} \quad (1.39)$$

Calculation of Mobility/Series-Resistance Parameters

$$\beta = P_{0;\beta} + \frac{L_{EN}}{L_E} \cdot P_{L;\beta} + \frac{W_E}{W_{EN}} \cdot P_{W;\beta} + \frac{W_E}{L_E} \cdot P_{LW;\beta} \quad (1.40)$$

$$\theta_{sr} = P_{0;\theta_{sr}} + \frac{L_{EN}}{L_E} \cdot P_{L;\theta_{sr}} + \frac{W_{EN}}{W_E} \cdot P_{W;\theta_{sr}} + \frac{L_{EN} \cdot W_{EN}}{L_E \cdot W_E} \cdot P_{LW;\theta_{sr}} \quad (1.41)$$

$$\theta_{ph} = P_{0;\theta_{ph}} + \frac{L_{EN}}{L_E} \cdot P_{L;\theta_{ph}} + \frac{W_{EN}}{W_E} \cdot P_{W;\theta_{ph}} + \frac{L_{EN} \cdot W_{EN}}{L_E \cdot W_E} \cdot P_{LW;\theta_{ph}} \quad (1.42)$$

$$\eta_{mob} = P_{0;\eta_{mob}} + \frac{L_{EN}}{L_E} \cdot P_{L;\eta_{mob}} + \frac{W_{EN}}{W_E} \cdot P_{W;\eta_{mob}} + \frac{L_{EN} \cdot W_{EN}}{L_E \cdot W_E} \cdot P_{LW;\eta_{mob}} \quad (1.43)$$

$$\theta_R = P_{0;\theta_R} + \frac{L_{EN}}{L_E} \cdot P_{L;\theta_R} + \frac{W_{EN}}{W_E} \cdot P_{W;\theta_R} + \frac{L_{EN} \cdot W_{EN}}{L_E \cdot W_E} \cdot P_{LW;\theta_R} \quad (1.44)$$

$$\theta_{sat} = P_{0;\theta_{sat}} + \frac{L_{EN}}{L_E} \cdot P_{L;\theta_{sat}} + \frac{W_{EN}}{W_E} \cdot P_{W;\theta_{sat}} + \frac{L_{EN} \cdot W_{EN}}{L_E \cdot W_E} \cdot P_{LW;\theta_{sat}} \quad (1.45)$$

Calculation of Conductance Parameters

$$\theta_{Th} = P_{0;\theta_{Th}} + \frac{L_{EN}}{L_E} \cdot P_{L;\theta_{Th}} + \frac{W_{EN}}{W_E} \cdot P_{W;\theta_{Th}} + \frac{L_{EN} \cdot W_{EN}}{L_E \cdot W_E} \cdot P_{LW;\theta_{Th}} \quad (1.46)$$

$$\sigma_{sf} = P_{0;\sigma_{sf}} + \frac{L_{EN}}{L_E} \cdot P_{L;\sigma_{sf}} + \frac{W_{EN}}{W_E} \cdot P_{W;\sigma_{sf}} + \frac{L_{EN} \cdot W_{EN}}{L_E \cdot W_E} \cdot P_{LW;\sigma_{sf}} \quad (1.47)$$

$$\alpha = P_{0;\alpha} + \frac{L_{EN}}{L_E} \cdot P_{L;\alpha} + \frac{W_{EN}}{W_E} \cdot P_{W;\alpha} + \frac{L_{EN} \cdot W_{EN}}{L_E \cdot W_E} \cdot P_{LW;\alpha} \quad (1.48)$$

Calculation of Sub-Threshold Parameters

$$\sigma_{dibl} = P_{0;\sigma_{dibl}} + \frac{L_{EN}}{L_E} \cdot P_{L;\sigma_{dibl}} + \frac{W_{EN}}{W_E} \cdot P_{W;\sigma_{dibl}} + \frac{L_{EN} \cdot W_{EN}}{L_E \cdot W_E} \cdot P_{LW;\sigma_{dibl}} \quad (1.49)$$

$$m_0 = P_{0;m_0} + \frac{L_{EN}}{L_E} \cdot P_{L;m_0} + \frac{W_{EN}}{W_E} \cdot P_{W;m_0} + \frac{L_{EN} \cdot W_{EN}}{L_E \cdot W_E} \cdot P_{LW;m_0} \quad (1.50)$$

Calculation of Smoothing Parameters

$$\frac{1}{m} = P_{0;m} + \frac{L_{EN}}{L_E} \cdot P_{L;m} + \frac{W_{EN}}{W_E} \cdot P_{W;m} + \frac{L_{EN} \cdot W_{EN}}{L_E \cdot W_E} \cdot P_{LW;m} \quad (1.51)$$

Calculation of Weak-Avalanche Parameters

$$a_1 = P_{0;a_1} + \frac{L_{EN}}{L_E} \cdot P_{L;a_1} + \frac{W_{EN}}{W_E} \cdot P_{W;a_1} + \frac{L_{EN} \cdot W_{EN}}{L_E \cdot W_E} \cdot P_{LW;a_1} \quad (1.52)$$

$$a_2 = P_{0;a_2} + \frac{L_{EN}}{L_E} \cdot P_{L;a_2} + \frac{W_{EN}}{W_E} \cdot P_{W;a_2} + \frac{L_{EN} \cdot W_{EN}}{L_E \cdot W_E} \cdot P_{LW;a_2} \quad (1.53)$$

$$a_3 = P_{0;a_3} + \frac{L_{EN}}{L_E} \cdot P_{L;a_3} + \frac{W_{EN}}{W_E} \cdot P_{W;a_3} + \frac{L_{EN} \cdot W_{EN}}{L_E \cdot W_E} \cdot P_{LW;a_3} \quad (1.54)$$

Calculation of Gate Current Parameters

$$I_{GINV} = P_{0;I_{GINV}} + \frac{L_E}{L_{EN}} \cdot P_{L;I_{GINV}} + \frac{W_E}{W_{EN}} \cdot P_{W;I_{GINV}} + \frac{L_E \cdot W_E}{L_{EN} \cdot W_{EN}} \cdot P_{LW;I_{GINV}} \quad (1.55)$$

$$B_{INV} = P_{0;B_{INV}} + \frac{L_{EN}}{L_E} \cdot P_{L;B_{INV}} + \frac{W_{EN}}{W_E} \cdot P_{W;B_{INV}} + \frac{L_{EN} \cdot W_{EN}}{L_E \cdot W_E} \cdot P_{LW;B_{INV}} \quad (1.56)$$

$$I_{GACC} = P_{0;I_{GACC}} + \frac{L_E}{L_{EN}} \cdot P_{L;I_{GACC}} + \frac{W_E}{W_{EN}} \cdot P_{W;I_{GACC}} + \frac{L_E \cdot W_E}{L_{EN} \cdot W_{EN}} \cdot P_{LW;I_{GACC}} \quad (1.57)$$

$$B_{acc} = P_{0;B_{acc}} + \frac{L_{EN}}{L_E} \cdot P_{L;B_{acc}} + \frac{W_{EN}}{W_E} \cdot P_{W;B_{acc}} + \frac{L_{EN} \cdot W_{EN}}{L_E \cdot W_E} \cdot P_{LW;B_{acc}} \quad (1.58)$$

$$I_{GOV} = P_{0;I_{GOV}} + \frac{L_{EN}}{L_E} \cdot P_{L;I_{GOV}} + \frac{W_E}{W_{EN}} \cdot P_{W;I_{GOV}} + \frac{W_E}{L_E} \cdot P_{LW;I_{GOV}} \quad (1.59)$$

Calculation of Gate-Induced Drain Leakage Parameters

$$A_{GIDL} = P_{0;A_{GIDL}} + \frac{L_{EN}}{L_E} \cdot P_{L;A_{GIDL}} + \frac{W_E}{W_{EN}} \cdot P_{W;A_{GIDL}} + \frac{W_E}{L_E} \cdot P_{LW;A_{GIDL}} \quad (1.60)$$

$$B_{GIDL} = P_{0;B_{GIDL}} + \frac{L_{EN}}{L_E} \cdot P_{L;B_{GIDL}} + \frac{W_{EN}}{W_E} \cdot P_{W;B_{GIDL}} + \frac{L_{EN} \cdot W_{EN}}{L_E \cdot W_E} \cdot P_{LW;B_{GIDL}} \quad (1.61)$$

$$C_{GIDL} = P_{0;C_{GIDL}} + \frac{L_{EN}}{L_E} \cdot P_{L;C_{GIDL}} + \frac{W_{EN}}{W_E} \cdot P_{W;C_{GIDL}} + \frac{L_{EN} \cdot W_{EN}}{L_E \cdot W_E} \cdot P_{LW;C_{GIDL}} \quad (1.62)$$

Calculation of Charge Parameters

$$C_{ox} = P_{0;C_{ox}} + \frac{L_E}{L_{EN}} \cdot P_{L;C_{ox}} + \frac{W_E}{W_{EN}} \cdot P_{W;C_{ox}} + \frac{L_E \cdot W_E}{L_{EN} \cdot W_{EN}} \cdot P_{LW;C_{ox}} \quad (1.63)$$

$$C_{GD0} = P_{0;C_{GD0}} + \frac{L_{EN}}{L_E} \cdot P_{L;C_{GD0}} + \frac{W_E}{W_{EN}} \cdot P_{W;C_{GD0}} + \frac{W_E}{L_E} \cdot P_{LW;C_{GD0}} \quad (1.64)$$

$$C_{GS0} = P_{0;C_{GS0}} + \frac{L_{EN}}{L_E} \cdot P_{L;C_{GS0}} + \frac{W_E}{W_{EN}} \cdot P_{W;C_{GS0}} + \frac{W_E}{L_E} \cdot P_{LW;C_{GS0}} \quad (1.65)$$

Calculation of Noise Parameters

$$N_{FA} = P_{0;N_{FA}} + \frac{L_{EN}}{L_E} \cdot P_{L;N_{FA}} + \frac{W_{EN}}{W_E} \cdot P_{W;N_{FA}} + \frac{L_{EN} \cdot W_{EN}}{L_E \cdot W_E} \cdot P_{LW;N_{FA}} \quad (1.66)$$

$$N_{FB} = P_{0;N_{FB}} + \frac{L_{EN}}{L_E} \cdot P_{L;N_{FB}} + \frac{W_{EN}}{W_E} \cdot P_{W;N_{FB}} + \frac{L_{EN} \cdot W_{EN}}{L_E \cdot W_E} \cdot P_{LW;N_{FB}} \quad (1.67)$$

$$N_{FC} = P_{0;N_{FC}} + \frac{L_{EN}}{L_E} \cdot P_{L;N_{FC}} + \frac{W_{EN}}{W_E} \cdot P_{W;N_{FC}} + \frac{L_{EN} \cdot W_{EN}}{L_E \cdot W_E} \cdot P_{LW;N_{FC}} \quad (1.68)$$

Calculation of Treshold-voltage Temperature-Scaling Coefficients

$$S_{T;V_{FB}} = P_{0;T;V_{FB}} + \frac{L_{EN}}{L_E} \cdot P_{L;T;V_{FB}} + \frac{W_{EN}}{W_E} \cdot P_{W;T;V_{FB}} + \frac{L_{EN} \cdot W_{EN}}{L_E \cdot W_E} \cdot P_{LW;T;V_{FB}} \quad (1.69)$$

$$S_{T;\phi_B} = P_{0;T;\phi_B} + \frac{L_{EN}}{L_E} \cdot P_{L;T;\phi_B} + \frac{W_{EN}}{W_E} \cdot P_{W;T;\phi_B} + \frac{L_{EN} \cdot W_{EN}}{L_E \cdot W_E} \cdot P_{LW;T;\phi_B} \quad (1.70)$$

Calculation of Mobility/Series-Resistance Temperature-Scaling Coefficients

$$\eta_{\beta} = P_{0;T;\eta_{\beta}} + \frac{L_{EN}}{L_E} \cdot P_{L;T;\eta_{\beta}} + \frac{W_{EN}}{W_E} \cdot P_{W;T;\eta_{\beta}} + \frac{L_{EN} \cdot W_{EN}}{L_E \cdot W_E} \cdot P_{LW;T;\eta_{\beta}} \quad (1.71)$$

$$\eta_{sr} = P_{0;T;\eta_{sr}} + \frac{L_{EN}}{L_E} \cdot P_{L;T;\eta_{sr}} + \frac{W_{EN}}{W_E} \cdot P_{W;T;\eta_{sr}} + \frac{L_{EN} \cdot W_{EN}}{L_E \cdot W_E} \cdot P_{LW;T;\eta_{sr}} \quad (1.72)$$

$$\eta_{ph} = P_{0;T;\eta_{ph}} + \frac{L_{EN}}{L_E} \cdot P_{L;T;\eta_{ph}} + \frac{W_{EN}}{W_E} \cdot P_{W;T;\eta_{ph}} + \frac{L_{EN} \cdot W_{EN}}{L_E \cdot W_E} \cdot P_{LW;T;\eta_{ph}} \quad (1.73)$$

$$S_{T;\eta_{mob}} = P_{0;T;\eta_{mob}} + \frac{L_{EN}}{L_E} \cdot P_{L;T;\eta_{mob}} + \frac{W_{EN}}{W_E} \cdot P_{W;T;\eta_{mob}} + \frac{L_{EN} \cdot W_{EN}}{L_E \cdot W_E} \cdot P_{LW;T;\eta_{mob}}$$

(1.74)

$$v_{exp} = P_{0;T;v_{exp}} + \frac{L_{EN}}{L_E} \cdot P_{L;T;v_{exp}} + \frac{W_{EN}}{W_E} \cdot P_{W;T;v_{exp}} + \frac{L_{EN} \cdot W_{EN}}{L_E \cdot W_E} \cdot P_{LW;T;v_{exp}}$$

(1.75)

$$\eta_R = P_{0;T;\eta_R} + \frac{L_{EN}}{L_E} \cdot P_{L;T;\eta_R} + \frac{W_{EN}}{W_E} \cdot P_{W;T;\eta_R} + \frac{L_{EN} \cdot W_{EN}}{L_E \cdot W_E} \cdot P_{LW;T;\eta_R}$$

(1.76)

$$\eta_{sat} = P_{0;T;\eta_{sat}} + \frac{L_{EN}}{L_E} \cdot P_{L;T;\eta_{sat}} + \frac{W_{EN}}{W_E} \cdot P_{W;T;\eta_{sat}} + \frac{L_{EN} \cdot W_{EN}}{L_E \cdot W_E} \cdot P_{LW;T;\eta_{sat}}$$

(1.77)

Calculation of Weak-Avalanche Temperature-Scaling Coefficients

$$S_{T;a_1} = P_{0;T;a_1} + \frac{L_{EN}}{L_E} \cdot P_{L;T;a_1} + \frac{W_{EN}}{W_E} \cdot P_{W;T;a_1} + \frac{L_{EN} \cdot W_{EN}}{L_E \cdot W_E} \cdot P_{LW;T;a_1}$$

(1.78)

Calculation of Gate-Induced Drain Leakage Temperature-Scaling Coefficients

$$S_{T;B_{GIDL}} = P_{0;T;B_{GIDL}} + \frac{L_{EN}}{L_E} \cdot P_{L;T;B_{GIDL}} + \frac{W_{EN}}{W_E} \cdot P_{W;T;B_{GIDL}} + \frac{L_{EN} \cdot W_{EN}}{L_E \cdot W_E} \cdot P_{LW;T;B_{GIDL}}$$

(1.79)

1.4.4 Temperature scaling

Calculation of Transistor Temperature

3 Note

Note the addition of the voltage V_{dT} of the thermal node in order to include self-heating. See section 1.6.

$$T_{KR} = T_0 + T_R \quad (1.80)$$

$$T_{amb} = T_0 + T_A + \Delta T_A \quad (1.81)$$

$$T_{KD} = T_0 + T_A + \Delta T_A + V_{dT} \quad (1.82)$$

Calculation of Threshold-Voltage Parameters

$$\phi_T = \frac{k_B \cdot T_{KD}}{q} \quad (1.83)$$

$$V_{FB_T} = V_{FB} + (T_{KD} - T_{KR}) \cdot S_{T;V_{FB}} \quad (1.84)$$

$$\phi_{B_T} = \phi_B + (T_{KD} - T_{KR}) \cdot S_{T;\phi_B} \quad (1.85)$$

Calculation of Mobility/Series-Resistance Parameters

$$\beta_T = \beta \cdot \left(\frac{T_{KR}}{T_{KD}} \right)^{\eta_\beta} \quad (1.86)$$

$$\theta_{sr_T} = \theta_{sr} \cdot \left(\frac{T_{KR}}{T_{KD}} \right)^{\eta_{sr}} \quad (1.87)$$

$$\theta_{ph_T} = \theta_{ph} \cdot \left(\frac{T_{KD}}{T_{KR}} \right)^{\eta_{ph}} \quad (1.88)$$

$$\eta_{mob_T} = \eta_{mob} \cdot [1 + (T_{KD} - T_{KR}) \cdot S_{T;\eta_{mob}}] \quad (1.89)$$

$$v_T = 1 + (v - 1) \cdot (T_{KR}/T_{KD})^{v_{exp}} \quad (1.90)$$

$$\theta_{R_T} = \theta_R \cdot \left(\frac{T_{KR}}{T_{KD}} \right)^{\eta_R} \quad (1.91)$$

$$\theta_{sat_T} = \theta_{sat} \cdot \left(\frac{T_{KR}}{T_{KD}} \right)^{\eta_{sat}} \quad (1.92)$$

Calculation of Conductance Parameters

$$\theta_{Th_T} = \theta_{Th} \cdot \left(\frac{T_{KR}}{T_{KD}} \right)^{\eta_{\beta}} \quad (1.93)$$

Calculation of Weak-Avalanche Parameters

$$a_{1_T} = a_1 \cdot [1 + (T_{KD} - T_{KR}) \cdot S_{T;a_1}] \quad (1.94)$$

Calculation of Gate-Induced Drain Leakage Parameters

$$B_{GIDL_T} = B_{GIDL} \cdot [1 + (T_{KD} - T_{KR}) \cdot S_{T;B_{GIDL}}] \quad (1.95)$$

Calculation of Noise Parameters

$$N_{T_T} = \frac{T_{KD}}{T_{KR}} \cdot N_T \quad (1.96)$$

Calculation of Thermal Resistance

$$R_{Th_T} = R_{Th} \cdot \left(\frac{T_{amb}}{T_{KR}} \right)^{A_{Th}} \quad (1.97)$$

1.4.5 MULT scaling

The N_{MULT} factor determines the number of equivalent parallel devices of a specified model. The N_{MULT} factor has to be applied on the electrical parameters. Hence after the temperature scaling and other parameter processing. Some electrical parameters cannot be specified by the user as parameters but must always be computed from geometrical parameters. They are called electrical quantities here. The parameters: β , I_{GINV} , I_{GACC} , I_{GOV} , C_{OX} , C_{GDO} , C_{GSO} , N_F , N_{FA} , N_{FB} and N_{FC} are affected by the N_{MULT} factor:

$$\beta = \beta \cdot N_{MULT}$$

$$I_{GINV} = I_{GINV} \cdot N_{MULT}$$

$$I_{GACC} = I_{GACC} \cdot N_{MULT}$$

$$I_{GOV} = I_{GOV} \cdot N_{MULT}$$

$$A_{GIDL} = A_{GIDL} \cdot N_{MULT}$$

$$C_{OX} = C_{OX} \cdot N_{MULT}$$

$$C_{GDO} = C_{GDO} \cdot N_{MULT}$$

$$C_{GSO} = C_{GSO} \cdot N_{MULT}$$

$$N_{FA} = \frac{N_{FA}}{N_{MULT}}$$

$$N_{FB} = \frac{N_{FB}}{N_{MULT}}$$

$$N_{FC} = \frac{N_{FC}}{N_{MULT}}$$

Convention:

No distinction is made between the symbol before and after the N_{MULT} scaling, e.g: the symbol β represents the actual parameter after the N_{MULT} processing and temperature scaling. This parameter may be used to put several MOSTs in parallel.

1.5 Model Equations

The definition of the hyp function, which provides for a smooth C_∞ -continuous clipping, is found in Appendix A *Hyp functions*.

In this section, a function is denoted by $F\{\text{variable}, \dots\}$, where F denotes the function name and the function variables are enclosed by braces $\{\}$.

Internal Parameters

$$\varepsilon_1 = 2 \cdot 10^{-2} \quad (1.98)$$

$$\varepsilon_2 = 1 \cdot 10^{-2} \quad (1.99)$$

$$\varepsilon_3 = 4 \cdot 10^{-2} \quad (1.100)$$

$$\varepsilon_4 = 1 \cdot 10^{-1} \quad (1.101)$$

$$\varepsilon_5 = 1 \cdot 10^{-4} \quad (1.102)$$

$$P_D = 1 + (k_0/k_p)^2 \quad (1.103)$$

$$V_{limit} = 4 \cdot \phi_T \quad (1.104)$$

$$\theta_{R_{eff}} = \frac{1}{2} \cdot \theta_{R_T} \cdot \left(1 + \frac{\theta_{R1}}{1/2 + \theta_{R2}} \right) \quad (1.105)$$

$$Acc = \left. \frac{\partial \psi_s}{\partial V_{GB}} \right|_{V_{GB} = V_{FB_T}} = \frac{1}{1 + k_0 / (\sqrt{2} \cdot \phi_T)} \quad (1.106)$$

$$N_{\phi_T} = (2.6)^2 / k_0 \quad (1.107)$$

$$Acc_{ov} = \left. \frac{\partial \psi_{sov}}{\partial V_{GB}} \right|_{V_{GB} = V_{FB_{ov}}} = \frac{1}{1 + k_{ov} / (\sqrt{2} \cdot \phi_T)} \quad (1.108)$$

$$QM_{\psi} = \begin{cases} QM_N \cdot (\epsilon_{ox} / t_{ox})^{2/3} & \text{for NMOS} \\ QM_P \cdot (\epsilon_{ox} / t_{ox})^{2/3} & \text{for PMOS} \end{cases} \quad (1.109)$$

$$QM_{tox} = \frac{2}{5} \cdot QM_{\psi} \quad (1.110)$$

$$\chi_{B_{inv}} = \begin{cases} \chi_{B_N} & \text{for NMOS} \\ \chi_{B_P} & \text{for PMOS} \end{cases} \quad (1.111)$$

$$\chi_{B_{acc}} = \chi_{B_N} \quad (1.112)$$

Extended Current Equations

$$V_{GB_{eff}} = \text{hyp}_1(V_{GS} + V_{SB} - V_{FB_T}; \epsilon_1) \quad (1.113)$$

$$V_{SB_t} = \text{hyp}_1(V_{SB} + 0.9 \cdot \phi_{B_T}; \epsilon_2) + 0.1 \cdot \phi_{B_T} \quad (1.114)$$

$$\Psi_{sat_0} = \left(\frac{\sqrt{P_D \cdot V_{GB_{eff}} + k_0^2/4 - k_0/2}}{P_D} \right)^2 \quad (1.115)$$

Drain induced barrier lowering and Static Feedback

$$D_{dibl} = \sigma_{dibl} \cdot \sqrt{V_{SB_t}} \quad (1.116)$$

$$D_{sf} = \sigma_{sf} \cdot \sqrt{\text{hyp}_1(\Psi_{sat_0} - V_{SB_t}; \epsilon_3)} \quad (1.117)$$

$$D = D_{dibl} + \text{hyp}_1(D_{sf} - D_{dibl}; \sigma_{sf} \cdot \epsilon_4) \quad (1.118)$$

$$V_{DS_{eff}} = \frac{V_{DS}^4}{(V_{limit}^2 + V_{DS}^2)^{3/2}} \quad (1.119)$$

$$\Delta V_G = D \cdot V_{DS_{eff}} \quad (1.120)$$

Redefinition of $V_{GB_{eff}}$, equation (1.113)

$$V_{GB_{eff}} = \text{hyp}_1(V_{GS} + V_{SB} + \Delta V_G - V_{FB_T}; \epsilon_1) \quad (1.121)$$

$$\Delta_{acc} = \phi_T \cdot \left[\exp\left(-\frac{Acc \cdot [V_{GB_{eff}} - \epsilon_1]}{\phi_T}\right) - 1 \right] \quad (1.122)$$

$$\Psi_{sat_1} = \left(\frac{\sqrt{P_D \cdot (V_{GB_{eff}} + \Delta_{acc}) + k_0^2/4 - k_0/2}}{P_D} \right)^2 - \Delta_{acc} \quad (1.123)$$

Drain Saturation Voltage:

$$V_{DSAT_{long}} = \Psi_{sat_1} - V_{SB_t} \quad (1.124)$$

$$T_{sat} = \begin{cases} \theta_{sat_T} & \text{for NMOS} \\ \frac{\theta_{sat_T}}{(1 + \theta_{sat_T}^2 \cdot V_{DSAT_{long}}^2)^{1/4}} & \text{for PMOS} \end{cases} \quad (1.125)$$

$$\Delta_{SAT} = \frac{T_{sat} - \theta_{R_{eff}}}{\sqrt{\frac{2}{V_{DSAT_{long}}^2 + \epsilon_4} + T_{sat}^2 + \theta_{R_{eff}}}} \quad (1.126)$$

$$V_{DSAT_{short}} = V_{DSAT_{long}} \cdot \left(1 - \frac{9}{10} \cdot \frac{\Delta_{SAT}}{1 + \sqrt{1 - \Delta_{SAT}^2}} \right) \quad (1.127)$$

$$V_{DSAT} = V_{limit} + \text{hyp}_1(V_{DSAT_{short}} - V_{limit}; \epsilon_3) \quad (1.128)$$

$$V_{DS_x} = \frac{V_{DS} \cdot V_{DSAT}}{[V_{DS}^{2m} + V_{DSAT}^{2m}]^{1/(2 \cdot m)}} \quad (1.129)$$

$$V_{DB_t} = \text{hyp}_1(V_{DS_x} + V_{SB} + 0.9 \cdot \phi_{B_T}; \epsilon_2) + 0.1 \cdot \phi_{B_T} \quad (1.130)$$

Surface Potential:

$$f_1\{\Psi\} = \Psi_{sat_1} - \text{hyp}_1\{\Psi_{sat_1} - \Psi; \epsilon_1\} \quad (1.131)$$

$$f_2\{\Psi\} = f_1\{\Psi\} + \frac{\Psi_{sat_1} - f_1\{\Psi\}}{\sqrt{1 + \frac{[\Psi_{sat_1} - f_1\{\Psi\}]^2}{N_{\phi_T} \cdot \phi_T^2}}} \quad (1.132)$$

$$f_3\{\Psi\} = \frac{2 \cdot [V_{GB_{eff}} - f_2\{\Psi\}]}{1 + \sqrt{1 + 4/k_p^2 \cdot [V_{GB_{eff}} - f_2\{\Psi\}]}} \quad (1.133)$$

$$\Psi_{S_{inv}}\{\Psi\} = f_1\{\Psi\} + \phi_T \cdot [1 + m_0] \cdot \ln \left[\frac{\left[\frac{f_3\{\Psi\}}{k_0} \right]^2 - f_1\{\Psi\} - \Delta_{acc} + \phi_T}{\phi_T} \right] \quad (1.134)$$

$$\Psi_{S_0}^* = \Psi_{S_{inv}} \cdot \{V_{SB_t}\} \quad (1.135)$$

$$\Psi_{S_L}^* = \Psi_{S_{inv}} \cdot \{V_{DB_t}\} \quad (1.136)$$

Surface Potential in Accumulation:

$$f_1 = Acc \cdot [V_{GS} + V_{SB} + \Delta V_G - V_{FB_T} - V_{GB_{eff}}] \quad (1.137)$$

$$f_2 = \frac{f_1}{\sqrt{1 + \frac{f_1^2}{N_{\phi_T} \cdot \phi_T^2}}} \quad (1.138)$$

$$\Psi_{s_{acc}} = -\phi_T \cdot \ln \left[\frac{\left[\frac{f_1/(Acc) - f_2}{k_0} \right]^2 - f_2 + \phi_T}{\phi_T} \right] \quad (1.139)$$

Auxiliary Variables:

$$\Delta\Psi = \Psi_{s_L}^* - \Psi_{s_0}^* \quad (1.140)$$

$$\bar{\Psi}_{inv} = \frac{\Psi_{s_L}^* + \Psi_{s_0}^*}{2} \quad (1.141)$$

$$V_{G_T}\{\Psi_{s_{inv}}\} = \frac{2 \cdot [V_{GB_{eff}} - \Psi_{s_{inv}}]}{1 + \sqrt{1 + 4/k_p^2 \cdot [V_{GB_{eff}} - \Psi_{s_{inv}}]}} - k_0 \cdot \sqrt{\text{hyp}_1\{\Psi_{s_{inv}} + \Delta_{acc}; \epsilon_2\}} \quad (1.142)$$

$$V_{G_{T_0}} = \text{hyp}_1\left\{V_{G_T}\left\{\Psi_{s_0}^*\right\}; \epsilon_5\right\} \quad (1.143)$$

$$V_{G_{T_L}} = \text{hyp}_1\left\{V_{G_T}\left\{\Psi_{s_L}^*\right\}; \epsilon_5\right\} \quad (1.144)$$

$$\bar{V}_{G_T} = V_{G_T}\{\bar{\Psi}_{inv}\} \quad (1.145)$$

$$V_{ox} = \frac{2 \cdot [V_{GS} + V_{SB} + \Delta V_G - V_{FB_T} - \bar{\Psi}_{inv} - \Psi_{acc}]}{1 + \sqrt{1 + 4/k_p^2 \cdot [V_{GB_{eff}} - \bar{\Psi}_{inv}]}} \quad (1.146)$$

$$\partial V_{ox} = \frac{2}{1 + \sqrt{1 + 4/k_p^2 \cdot [V_{GB_{eff}} - \bar{\Psi}_{inv}]}} \quad (1.147)$$

$$V_{eff} = \bar{V}_{G_T} + \eta_{mob} \cdot (V_{ox} - \bar{V}_{G_T}) \quad (1.148)$$

$$\xi_{ox} = -\phi_T \cdot \frac{\partial V_{ox}}{\partial \bar{\Psi}_{inv}} = \phi_T \cdot \frac{1}{\sqrt{1 + 4/k_p^2 \cdot [V_{GB_{eff}} - \bar{\Psi}_{inv}]}} \quad (1.149)$$

$$\xi = \phi_T \cdot \left[\frac{1}{\sqrt{1 + 4/k_p^2 \cdot [V_{GB_{eff}} - \bar{\Psi}_{inv}]}} + \frac{k_0}{2 \cdot \sqrt{\text{hyp}_1\{\bar{\Psi}_{inv} + \Delta_{acc}; \epsilon_5\}}} \right] \quad (1.150)$$

$$\bar{V}_{G_T}^* = \frac{V_{GT_0} + V_{GT_L}}{2} + \xi \quad (1.151)$$

Second-Order Effects

Mobility Degradation:

$$V_{eff_1} = \text{hyp}_1(V_{eff}; \epsilon_2) \quad (1.152)$$

$$G_{mob} = \frac{\mu_0}{\mu} = \begin{cases} 1 + [(\theta_{ph_T} \cdot V_{eff_1})^{v_T/3} + (\theta_{sr_T} \cdot V_{eff_1})^{2v_T}]^{1/v_T} & \text{for NMOS} \\ [1 + (\theta_{ph_T} \cdot V_{eff_1})^{v_T/3} + (\theta_{sr_T} \cdot V_{eff_1})^{v_T}]^{1/v_T} & \text{for PMOS} \end{cases} \quad (1.153)$$

Velocity Saturation:

$$x = \begin{cases} \frac{2 \cdot \theta_{sat_T} \cdot \Delta\psi}{\sqrt{G_{mob}}} & \text{for NMOS} \\ \frac{2 \cdot \theta_{sat_T} \cdot \Delta\psi}{\sqrt{G_{mob}} \cdot (1 + \theta_{sat_T}^2 \cdot \Delta\psi^2)^{1/4}} & \text{for PMOS} \end{cases} \quad (1.154)$$

$$G_{vsat} = \begin{cases} \frac{G_{mob}}{2} \cdot \left[\sqrt{1+x^2} + 1 - \frac{x^2}{6} \right] & x < 1 \cdot 10^{-4} \\ \frac{G_{mob}}{2} \cdot \left[\sqrt{1+x^2} + \frac{\ln(x + \sqrt{1+x^2})}{x} \right] & x \geq 1 \cdot 10^{-4} \end{cases} \quad (1.155)$$

Channel Length Modulation:

$$G_{\Delta L} = \text{hyp}_1 \left(1 - \alpha \cdot \ln \left[\frac{V_{DS} - V_{DS_x} + \sqrt{(V_{DS} - V_{DS_x})^2 + V_p^2}}{V_p} \right]; \epsilon_5 \right) \quad (1.156)$$

Series Resistance and Self-Heating:

$$G_R = \theta_{R_T} \cdot \left(1 + \frac{\theta_{R1}}{\theta_{R2} + \bar{V}_{G_T}} \right) \cdot \bar{V}_{G_T} \quad (1.157)$$

$$G_{Th} = \theta_{Th_T} \cdot V_{DS} \cdot \Delta\Psi \cdot \bar{V}_{G_T} \quad (1.158)$$

$$G_{tot} = G_{Th} + \frac{[G_{\Delta L} \cdot G_{vsat} + G_R]}{2} \cdot \left[1 + \sqrt{\text{hyp}_1 \left(1 - \frac{4 \cdot G_R / G_{vsat}}{[G_{\Delta L} \cdot G_{vsat} + G_R]^2} \cdot [G_{vsat}^2 - G_{mob}^2]; \epsilon_5 \right)} \right] \quad (1.159)$$

Inversion-Layer Charge

$$(Q_{inv} = -\epsilon_{ox} / t_{ox} \cdot V_{inv}) :$$

$$\Psi_{S_{inv}}^* \{ \Psi_{S_{inv}} \} = \text{hyp}_1(\Psi_{S_{inv}} + \Delta_{acc} ; \epsilon_5) \quad (1.160)$$

$$V_{inv} \{ \Psi_{S_{inv}}, \Psi \} = \frac{k_0 \cdot \phi_T \cdot \exp \left[\frac{\Psi_{S_{inv}} - \Psi}{(1 + m_0) \cdot \phi_T} \right]}{\sqrt{\Psi_{S_{inv}}^* \{ \Psi_{S_{inv}} \} + \phi_T \cdot \exp \left[\frac{\Psi_{S_{inv}} - \Psi}{(1 + m_0) \cdot \phi_T} \right]} + \sqrt{\Psi_{S_{inv}}^* \{ \Psi_{S_{inv}} \}}} \quad (1.161)$$

$$V_{inv_0} = V_{inv} \left\{ \Psi_{s_0}^*, V_{SB_t} \right\} \quad (1.162)$$

$$V_{inv_L} = V_{inv} \left\{ \Psi_{s_L}^*, V_{DB_t} \right\} \quad (1.163)$$

Drain Current

$$x_0 = \frac{2}{\phi_T} \cdot (\Psi_{sat_1} + \phi_T - V_{SB_t}) \quad (1.164)$$

$$x_L = \frac{2}{\phi_T} \cdot (\Psi_{sat_1} + \phi_T - V_{DB_t}) \quad (1.165)$$

$$G = \frac{\exp(x_0) + \exp(x_L)}{\exp(x_0) + \exp(x_L) + 1} \quad (1.166)$$

$$I_{drift} = \begin{cases} \beta_T \cdot \bar{V}_{G_T} \cdot \Delta\Psi & x_0 > 80 \text{ or } x_L > 80 \\ \beta_T \cdot \bar{V}_{G_T} \cdot \Delta\Psi \cdot G & x_0 \leq 80 \text{ and } x_L \leq 80 \end{cases} \quad (1.167)$$

$$I_{diff} = \beta_T \cdot \phi_T \cdot (V_{inv_0} - V_{inv_L}) \quad (1.168)$$

$$I_{DS} = \frac{I_{drift} + I_{diff}}{G_{tot}} \quad (1.169)$$

Weak-Avalanche

$$I_{avl} = \begin{cases} 0 & \text{for: } V_{DS} - a_3 \cdot V_{DSAT} \leq -a_2/A \\ a_{1T} \cdot I_{DS} \cdot \exp\left(-\frac{a_2}{V_{DS} - a_3 \cdot V_{DSAT}}\right) & \text{for: } V_{DS} - a_3 \cdot V_{DSAT} > -a_2/A \end{cases} \quad (1.170)$$

Gate Current Equations

The tunnelling probability is given by:

$$P_{tun}\{V_{ox}; \chi_B; B\} = \begin{cases} \exp\left(-\frac{B}{\chi_B} \cdot \frac{\left[\left(\frac{V_{ox}}{\chi_B}\right)^2 - 3 \cdot \frac{V_{ox}}{\chi_B} + 3\right]}{1 + \left(1 - \frac{V_{ox}}{\chi_B}\right)^{3/2}}\right) & V_{ox} < \chi_B \\ \exp(-B/V_{ox}) & V_{ox} \geq \chi_B \end{cases} \quad (1.171)$$

Source/Drain Gate Overlap Current:

First calculate the oxide voltage V_{ov} at both Source and Drain overlap:

$$V_{GX_{eff}}\{V_{GX}\} = V_{GX} - V_{FBov} - \text{hyp}_1(V_{GX} - V_{FBov}; \epsilon_1) \quad (1.172)$$

$$\Delta_{ov}\{V_{GX}\} = \phi_T \cdot \left[\exp\left(\frac{Acc_{ov} \cdot [V_{GX_{eff}}\{V_{GX}\} + \epsilon_1]}{\phi_T}\right) - 1 \right] \quad (1.173)$$

$$\Psi_{sat_{ov}}\{V_{GX}\} = -\left[\sqrt{\frac{k_{ov}^2}{4} - V_{GX_{eff}}\{V_{GX}\} + \Delta_{ov}\{V_{GX}\} - \frac{k_{ov}}{2}} \right]^2 + \Delta_{ov}\{V_{GX}\} \quad (1.174)$$

$$f_1\{V_{GX}\} = Acc_{ov} \cdot [V_{GX} - V_{FBov} - V_{GX_{eff}}\{V_{GX}\}] \quad (1.175)$$

$$f_2\{V_{GX}\} = \frac{f_1\{V_{GX}\}}{\sqrt{1 + \frac{[f_1\{V_{GX}\}]^2}{N_{\phi_T} \cdot \phi_T^2}}} \quad (1.176)$$

$$f_3\{V_{GX}\} = \frac{2 \cdot \left[\frac{f_1\{V_{GX}\}}{Acc_{ov}} - f_2\{V_{GX}\} \right]}{1 + \sqrt{1 + 4/k_p^2 \cdot \left[\frac{f_1\{V_{GX}\}}{Acc_{ov}} - f_2\{V_{GX}\} \right]}} \quad (1.177)$$

$$\Psi_{s_{ov}}^*\{V_{GX}\} = \phi_T \cdot \ln \left(\frac{\left(\frac{f_3\{V_{GX}\}}{k_{ov}} \right)^2 + f_2\{V_{GX}\} + \phi_T}{\phi_T} \right) \quad (1.178)$$

$$V_{ov}\{V_{GX}\} = \frac{2 \cdot [V_{GX} - V_{FBov} - \Psi_{s_{ov}}^*\{V_{GX}\} - \Psi_{sat_{ov}}\{V_{GX}\}]}{1 + \sqrt{1 + 4/k_p^2 \cdot [(f_1\{V_{GX}\})/Acc_{ov} - \Psi_{s_{ov}}^*\{V_{GX}\}]}} \quad (1.179)$$

$$V_{ov_0} = V_{ov}\{V_{GS}\} \quad (1.180)$$

$$V_{ov_L} = V_{ov} \{V_{GS} - V_{DS}\} \quad (1.181)$$

Next calculate the gate tunnelling current in both Source and Drain overlap:

$$P_{ov} \{V_{ov}\} = P_{tun} \{V_{ov}; \chi_{B_{inv}}; B_{inv}\} \quad (1.182)$$

$$I_{Gov} \{V_{GX}, V_{ov}\} = I_{GOV} \cdot V_{GX} \cdot V_{ov} \cdot [P_{ov} \{V_{ov}\} - P_{ov} \{-V_{ov}\}] \quad (1.183)$$

$$I_{Gov_0} = I_{Gov} \{V_{GS}, V_{ov_0}\} \quad (1.184)$$

$$I_{Gov_L} = I_{Gov} \{V_{GS} - V_{DS}, V_{ov_L}\} \quad (1.185)$$

Intrinsic Gate Current

The gate tunnelling current in accumulation:

$$P_{acc} = P_{tun} \{-V_{ox}; \chi_{B_{acc}}; B_{acc}\} \quad (1.186)$$

$$V_{acc} = V_{ox} - \text{hyp}_1(V_{ox}; \epsilon_5) \quad (1.187)$$

$$I_{GB} = -I_{GACC} \cdot (V_{GS} + V_{SB}) \cdot V_{acc} \cdot P_{acc} \quad (1.188)$$

The tunnelling current in inversion, including quantum-mechanical barrier lowering $\Delta\chi_B$:

$$\Delta\chi_B = QM_{\psi} \cdot [(\bar{V}_{G_T}/3 + V_{ox} - \bar{V}_{G_T})^2 + V_{limit}^2]^{1/3} \quad (1.189)$$

$$\chi_{B_{eff}} = 0.7 \cdot \chi_{B_{inv}} + \text{hyp}_1(0.3 \cdot \chi_{B_{inv}} - \Delta\chi_B; \epsilon_5) \quad (1.190)$$

$$B_{eff} = B_{inv} \cdot (\chi_{B_{eff}} / \chi_{B_{inv}})^{3/2} \quad (1.191)$$

$$P_{inv} = P_{tun}(V_{ox}; \chi_{B_{eff}}; B_{eff}) \quad (1.192)$$

$$B_{inv}^* = \frac{3}{8} \cdot \chi_{B_{eff}}^{-2} \cdot B_{eff} \cdot \partial V_{ox} \quad (1.193)$$

$$\xi^* = \frac{\xi}{\phi_T \cdot \bar{V}_{G_T}^*} \quad (1.194)$$

$$\partial V_{ox}^* = \frac{\partial V_{ox}}{\sqrt{V_{ox}^2 + V_{limit}^2}} \quad (1.195)$$

$$P_{GC} = 1 + \frac{[(B_{inv}^*)^2 + 4 \cdot B_{inv}^* \cdot \xi^* + 2 \cdot B_{inv}^* \cdot \partial V_{ox}^* + 2 \cdot \xi^{*2} + 4 \cdot \partial V_{ox}^* \cdot \xi^*] \cdot \Delta \psi^2}{24}$$

(1.196)

$$\bar{I}_{GC} = I_{GINV} \cdot G_{\Delta L} \cdot \left(V_{GS} - \frac{1}{2} \cdot V_{DS_x} \right) \cdot P_{inv} \quad (1.197)$$

$$\bar{V}_{inv} = \frac{V_{inv_0} + V_{inv_L}}{2} \quad (1.198)$$

The total intrinsic gate current I_{GC} :

$$I_{GC} = \bar{I}_{GC} \cdot \bar{V}_{inv} \cdot P_{GC} \quad (1.199)$$

$$P_{GS} = [B_{inv}^* + \partial V_{ox}^*] \cdot \frac{\Delta\Psi}{12} + [(B_{inv}^*)^2 \cdot (B_{inv}^* + 5 \cdot \xi^* + 3 \cdot \partial V_{ox}^*) + 2 \cdot \xi^{*2} \cdot (B_{inv}^* - \xi^* + \partial V_{ox}^*) + 10 \cdot B_{inv}^* \cdot \xi^* \cdot \partial V_{ox}^*] \cdot \frac{\Delta\Psi^3}{480} \quad (1.200)$$

$$I_{GS} = \frac{1}{2} \cdot I_{GC} + \left(P_{GS} \cdot \bar{V}_{inv} + \frac{V_{inv_0} - V_{inv_L}}{12} \right) \cdot \bar{I}_{GC} + I_{Gov_0} \quad (1.201)$$

$$I_{GD} = I_{GC} - I_{GS} + I_{Gov_0} + I_{Gov_L} \quad (1.202)$$

Gate-Induced Drain/Source Leakage Current:

$$V_{tov}\{V_{ov};V\} = \sqrt{(V_{ov} - hyp_1\{V_{ov};\epsilon_5\})^2 + C_{GIDL}^2 \cdot V^2} \quad (1.203)$$

$$I_{gixl}\{V_{ov};V\} = \begin{cases} A_{GIDL} \cdot V \cdot V_{tov}\{V_{ov};V\}^2 \cdot e^{-\frac{B_{GIDL_T}}{V_{tov}\{V_{ov};V\}}} & \text{for: } V_{tov}\{V_{ov};V\} > -\frac{B_{GIDL_T}}{A} \\ 0 & \text{for: } V_{tov}\{V_{ov};V\} \leq -\frac{B_{GIDL_T}}{A} \end{cases} \quad (1.204)$$

$$I_{gisl} = I_{gixl}\{V_{ov_0};V_{SB}\} \quad (1.205)$$

$$I_{gidl} = I_{gixl}\{V_{ov_L};V_{DS} + V_{SB}\} \quad (1.206)$$

1.5.1 Extended equations

Extended Charge Equations

Bias-Dependent Overlap Capacitance:

$$Q_{ov_0} = C_{GSO} \cdot V_{ov_0} \quad (1.207)$$

$$Q_{ov_L} = C_{GDO} \cdot V_{ov_L} \quad (1.208)$$

Intrinsic Charges:

$$C_{ox_{eff}} = \frac{C_{ox}}{1 + QM_{t_{ox}} \cdot \left[\left(\frac{V_{eff}}{\eta_{mob}} \right)^2 + (20 \cdot \phi_T)^2 \right]^{-1/6}} \quad (1.209)$$

$$\Delta V_{G_T} = \frac{V_{GT_0} - V_{GT_L}}{2 \cdot \left(1 + \theta_{R_T} \cdot \frac{\bar{V}_{G_T}^*}{G_{tot}} \right)} \quad (1.210)$$

$$F_j = \frac{\Delta V_{G_T}}{\bar{V}_{G_T}^*} \quad (1.211)$$

$$Q_S = -\frac{C_{ox_{eff}}}{2} \cdot \left[\bar{V}_{G_T}^* + \frac{\Delta V_{G_T}}{3} \cdot \left(F_j - \frac{F_j^2}{5} + 1 \right) - \xi \right] \quad (1.212)$$

$$Q_D = -\frac{C_{ox_{eff}}}{2} \cdot \left[\bar{V}_{G_T}^* + \frac{\Delta V_{G_T}}{3} \cdot \left(F_j + \frac{F_j^2}{5} - 1 \right) - \xi \right] \quad (1.213)$$

$$Q_G = C_{ox_{eff}} \cdot \left[V_{ox} + \frac{\Delta V_{G_T}}{3} \cdot F_j \cdot \frac{\xi_{ox}}{\xi} \right] \quad (1.214)$$

$$Q_B = -[Q_S + Q_D + Q_G] \quad (1.215)$$

Extended Noise Equations

In these equations f represents the operation frequency of the transistor.

$$g_m = \frac{\partial I_{DS}}{\partial V_{GS}} \quad (1.216)$$

$$T_{sat} = \begin{cases} \theta_{sat_T}^2 & \text{for NMOS} \\ \frac{\theta_{sat_T}^2}{\sqrt{1 + \theta_{sat_T}^2 \cdot \Delta\psi^2}} & \text{for PMOS} \end{cases} \quad (1.217)$$

$$R_{ideal} = \frac{\beta_T \cdot G_{vsat}^2}{G_{tot}} \cdot \left[\frac{V_{inv_0} + V_{inv_L}}{2} + \frac{(V_{inv_0} - V_{inv_L})^2}{12 \cdot \left(\frac{V_{inv_0} + V_{inv_L}}{2} + \xi \right)} \right] \quad (1.218)$$

$$S_{th} = \begin{cases} 0 & R_{ideal} \leq T_{sat} \cdot I_{DS} \cdot \Delta\psi \\ \frac{N_{T_T}}{G_{mob}^2} \cdot (R_{ideal} - T_{sat} \cdot I_{DS} \cdot \Delta\psi) & R_{ideal} > T_{sat} \cdot I_{DS} \cdot \Delta\psi \end{cases} \quad (1.219)$$

$$N_0 = \frac{\epsilon_{ox}}{qt_{ox}} \cdot V_{inv_0} \quad (1.220)$$

$$N_L = \frac{\epsilon_{ox}}{qt_{ox}} \cdot V_{invL} \quad (1.221)$$

$$N^* = \frac{\epsilon_{ox}}{qt_{ox}} \cdot \xi \quad (1.222)$$

$$S_{fl} = \frac{q \cdot \phi_T^2 \cdot t_{ox} \cdot \beta_T \cdot I_{DS}}{f \cdot \epsilon_{ox} \cdot G_{vsat} \cdot N^*} \cdot [(N_{FA} - N^* \cdot N_{FB} + N^{*2} \cdot N_{FC}) \cdot \ln \frac{N_0 + N^*}{N_L + N^*} + (N_{FB} - N^* \cdot N_{FC}) \cdot (N_0 - N_L) + \frac{N_{FC}}{2} \cdot (N_0^2 - N_L^2)] + \frac{\phi_T \cdot I_{DS}^2}{f} \cdot (1 - G_{\Delta L}) \cdot \left[\frac{N_{FA} + N_{FB} \cdot N_L + N_{FC} \cdot N_L^2}{N_L + N^{*2}} \right] \quad (1.223)$$

$$S_{ig} = \begin{cases} \frac{\frac{1}{3} \cdot N_{TT} \cdot (2 \cdot \pi \cdot f \cdot C_{ox})^2 / g_m}{1 + 0.075 \cdot (2 \cdot \pi \cdot f \cdot C_{ox} / g_m)^2} & \text{GATENOISE} = 0 \\ 0 & \text{GATENOISE} = 1 \end{cases} \quad (1.224)$$

$$\rho_{igth} = 0.4j \quad (1.225)$$

$$S_{igth} = \rho_{igth} \cdot \sqrt{S_{ig} \cdot S_{th}} \quad (1.226)$$

1.6 Self-heating

1.6.1 Equivalent circuit

Self-heating is part of the model. It is defined in the usual way by adding a self-heating network (see Figure 6) containing a current source describing the dissipated power and both a thermal resistance R_{TH} and a thermal capacitance C_{TH} .

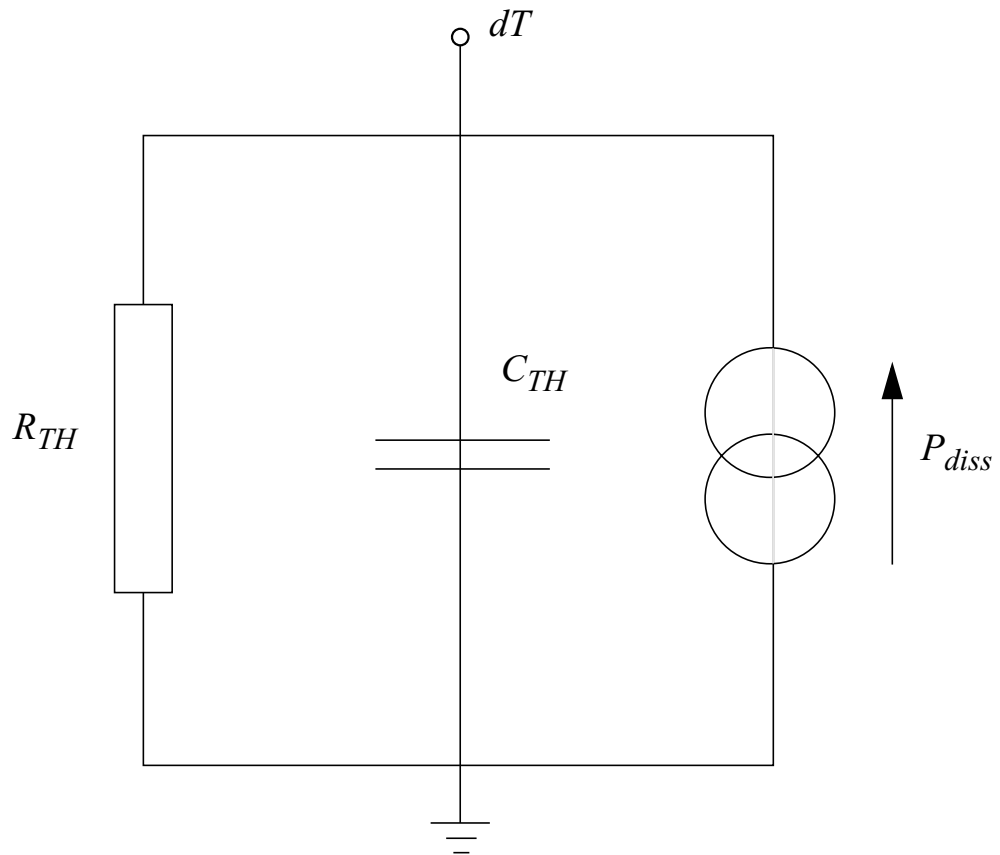


Figure 6: The self-heating network, where the node voltage V_{dT} is used in the temperature scaling relations. Note that for increased flexibility the node dT is available to the user.

The resistance and capacitance are both connected between ground and the temperature node dT . The value of the voltage V_{dT} at the temperature node gives the increase in local temperature, which is included in the calculation of the temperature scaling relations (12.2) and (12.197), see sections 12.4.2 and 12.5.1..

For example, if the value of V_{dT} is 0.5V, the increase in temperature is 0.5 degrees Celsius.

1.6.2 Model equations

The total dissipated power is a sum of the dissipated power of each branch of the equivalent circuit and is given by:

$$\begin{aligned}
 P_{diss} &= I_D^e \cdot V_D^e + I_G^e \cdot V_G^e + I_S^e \cdot V_S^e + I_B^e \cdot V_B^e \\
 &= I_{DS}'' \cdot V_{DS}'' + I_{DB}'' \cdot (V_{DS}'' - V_{SB}'') + I_{SB}'' \cdot V_{SB}'' + I_{GS}'' \cdot V_{GS}'' \\
 &\quad + I_{GD}'' \cdot (V_{GS}'' - V_{DS}'') + I_{GB}'' \cdot (V_{GS}'' - V_{SB}'')
 \end{aligned}$$

where all variables are given in Figure 7 on the previous pages. Note that only the steady-state currents contribute to the dissipated power.

The total dissipation applies for the electrical model (mnet¹, mpet¹, mos1101et²), geometrical binning model (mnt¹, mpt¹, mos11011t²), and geometrical physical model (mnt¹, mpt¹, mos11010t²).

1.6.3 Usage

Below a *Pstar* example is given to illustrate how self-heating works.

q Example

Title: example self-heating 1101;

```

circuit;
mnet_1(Vd, Vg, Vs, 0, dt) level=1101, Rth=1e4,Cth=1e-9;
R_1 ( Vdd, Vd) 100;
R_2 ( Vgg, Vg) 1k;
R_3 ( Vs, 0) 100;
e_SRC_2 (Vgg ,net101) 5;
e_SRC_1 ( Vdd, 0) 1;
e_SRC_3 ( net101, 0) 0;
end;

```

1.*Pstar* model name.
2.*Spectre/ADS* model name.

```
dc;  
print: vn(dt), op(pdiss.mnet_1);  
end; run;
```

```
result:  
DC Analysis.  
VN(dt)          =9.513E+00  
Pdiss.MNT_1     =951.275E-6
```

The voltage on node *dt* is 9.513E+00 V, which means that the local temperature is increased by 9.513E+00 °C.

1.7 DC operating point output

The DC operating point output facility gives information on the state of a device at its operation point. Besides terminal currents and voltages, the magnitudes of linearized internal elements are given. In some cases, meaningful quantities can be derived which are then also given (e.g. f_T). The objective of the DC operating-facility is twofold:

- Calculate small-signal equivalent circuit element values.
- Open a window on the internal bias conditions of the device and its basic capabilities.

Below, the printed items are described. $C_{x(y)}$ indicates the derivate of the charge Q at terminal x to the voltage at terminal y , when all other terminals remain constant.

Symbol	Program Name	Units	Description
I_{DS}	IDS	A	Drain current, excl. avalanche and tunnel currents.
I_{avl}	I AVL	A	Substrate current due to weak-avalanche
I_{GS}	IGS	A	Gate-to-source current due to direct tunnelling
I_{GD}	IGD	A	Gate-to-drain current due to direct tunnelling
I_{GB}	IGB	A	Gate-to-bulk current due to direct tunnelling
V_{DS}	VDS	V	Drain-Source voltage
V_{GS}	VGS	V	Gate-Source voltage
V_{SB}	VS B	V	Source-Bulk voltage
V_{TO}	VTO	V	Zero-bias threshold voltage: $V_{TO} = V_{FB} + P_D \cdot (\phi_B + 2 \cdot \phi_T) + k_0 \cdot \sqrt{\phi_B + 2 \cdot \phi_T}$
V_{TS}	VTS	V	Threshold voltage including back-bias effects: $V_{TS} = V_{FB} + P_D \cdot (V_{SB_i} + 2 \cdot \phi_T) - (V_{SB_i} - \phi_B) + k_0 \cdot \sqrt{V_{SB_i} + 2 \cdot \phi_T}$

Symbol	Program Name	Units	Description
V_{TH}	VTH	V	Threshold voltage including back-bias and drain-bias effects: $V_{TH} = V_{FB} + P_D \cdot (V_{SB_t} + 2 \cdot \phi_T) - (V_{SB_t} - \phi_B) + k_0 \cdot \sqrt{V_{SB_t} + 2 \cdot \phi_T} - \Delta V_G$
V_{GT}	VGT	V	Effective gate drive including back-bias and drain voltage effects: $V_{GT} = V_{inv_0}$
V_{DSAT}	VDSS	V	Drain saturation voltage at actual bias
$V_{DS_{eff}}$	VSAT	V	Saturation limit: $V_{DS_{eff}} = V_{DS} - V_{DSAT}$
g_m	GM	A/V	Transconductance (assumed $V_{DS} > 0$): $g_m = \partial I_{DS} / \partial V_{GS}$
g_{mb}	GMB	A/V	Substrate-transconductance (assumed $V_{DS} > 0$): $g_{mb} = \partial I_{DS} / \partial V_{BS}$
g_{ds}	GDS	A/V	Output conductance: $g_{ds} = \partial I_{DS} / \partial V_{DS}$
$C_{D(D)}$	CDD	F	$C_{D(D)} = \partial Q_D / \partial V_{DS}$
$C_{D(G)}$	CDG	F	$C_{D(G)} = -\partial Q_D / \partial V_{GS}$
$C_{D(S)}$	CDS	F	$C_{D(S)} = C_{D(D)} - C_{D(G)} - C_{D(B)}$
$C_{D(B)}$	CDB	F	$C_{D(B)} = \partial Q_D / \partial V_{SB}$
$C_{G(D)}$	CGD	F	$C_{G(D)} = -\partial Q_G / \partial V_{DS}$
$C_{G(G)}$	CGG	F	$C_{G(G)} = \partial Q_G / \partial V_{GS}$
$C_{G(S)}$	CGS	F	$C_{G(S)} = C_{G(G)} - C_{G(D)} - C_{G(B)}$
$C_{G(B)}$	CGB	F	$C_{G(B)} = \partial Q_G / \partial V_{SB}$
$C_{S(D)}$	CSD	F	$C_{S(D)} = -\partial Q_S / \partial V_{DS}$
$C_{S(G)}$	CSG	F	$C_{S(G)} = -\partial Q_S / \partial V_{GS}$

Symbol	Program Name	Units	Description
$C_{S(S)}$	CSS	F	$C_{S(S)} = C_{S(G)} + C_{S(D)} + C_{S(B)}$
$C_{S(B)}$	CSB	F	$C_{S(B)} = \partial Q_S / \partial V_{SB}$
$C_{B(D)}$	CBD	F	$C_{B(D)} = -\partial Q_B / \partial V_{DS}$
$C_{B(G)}$	CBG	F	$C_{B(G)} = -\partial Q_B / \partial V_{GS}$
$C_{B(S)}$	CBS	F	$C_{B(S)} = C_{B(B)} - C_{B(D)} - C_{B(G)}$
$C_{B(B)}$	CBB	F	$C_{B(B)} = -\partial Q_B / \partial V_{SB}$
$C_{GD_{ov}}$	CGDOL	F	Gate-drain overlap capacitance of the actual transistor: $C_{GD_{ov}} = \partial Q_{OV_L} / \partial V_{DS}$
$C_{GS_{ov}}$	CGSOL	F	Gate-source overlap capacitance of the actual transistor: $C_{GS_{ov}} = \partial Q_{OV_0} / \partial V_{GS}$
W_E	WE	m	Effective channel width for geometrical models
L_E	LE	m	Effective channel length for geometrical models
u	U	-	Transistor gain: $u = g_m / g_{ds}$
R_{out}	ROUT	Ω	Small-signal output resistance: $R_{out} = 1 / g_{ds}$
V_{Early}	VEARLY	V	Equivalent Early voltage: $V_{Early} = I_{DS} / g_{ds}$
k_{eff}	KEFF	\sqrt{V}	Body effect parameter: $k_{eff} = k_0$
β_{eff}	BEFF	A/V^2	Gain factor: $2 \cdot I_{DS} / V_{inv_0}^2$
f_T	FUG	Hz	Unity gain frequency at actual bias: $f_T = \frac{g_m}{2\pi(C_{G(G)} + C_{GS_{ov}} + C_{GD_{ov}})}$
$\sqrt{S_{V_{Gth}}}$	SQRTSFW	V / \sqrt{Hz}	Input-referred RMS white noise voltage density: $\sqrt{S_{V_{Gth}}} = \sqrt{S_{th}} / g_m$

Symbol	Program Name	Units	Description
$\sqrt{S_{V_{gfl}}}$	SQRTSFF	V/\sqrt{Hz}	Input-referred RMS white noise voltage density at 1 kHz: $\sqrt{S_{V_{gfl}}} = \sqrt{S_{fl}(1kHz)}/g_m$
f_{knee}	FKNEE	Hz	Cross-over frequency above which white noise is dominant: $f_{knee} = 1Hz \cdot S_{fl}(1Hz)/S_{th}$

The additional operating point output for the model including self-heating (see section 1.7) is listed in the table below:

Symbol	Program Name	Units	Description
T_{KD}	TK	K	Actual temperature including self-heating
P_{diss}	PDISS	W	Power dissipation

When the parameter PRINTSCALED is set to 1, the device parameter set after geometrical and temperature scaling is added to the OP output:

Quantity	Description
<i>VFB</i>	Flat-band voltage for the actual transistor
<i>KO</i>	Body-effect factor
<i>KPINV</i>	Inverse of body-effect factor of the poly-silicon gate
<i>PHIB</i>	Surface potential at the onset of strong inversion
<i>BET</i>	Gain factor
<i>THESR</i>	Mobility degradation parameter due to surface roughness scattering
<i>THEPH</i>	Mobility degradation parameter due to phonon scattering
<i>ETAMOB</i>	Effective field parameter for dependence on depletion charge
<i>NU</i>	Exponent of field dependence of mobility model
<i>THER</i>	Coefficient of series resistance
<i>THER1</i>	Numerator of gate voltage dependent part of series resistance
<i>THER2</i>	Denominator of gate voltage dependent part of series resistance
<i>THESAT</i>	Velocity saturation parameter due to optical/acoustic phonon scattering
<i>THETH</i>	Coefficient of self-heating

Quantity	Description
<i>SDIBL</i>	Drain-induced barrier lowering parameter
<i>MO</i>	Parameter for (short-channel) subthreshold slope
<i>SSF</i>	Static-feedback parameter
<i>ALP</i>	Factor of channel length modulation
<i>VP</i>	Characteristic voltage of channel-length modulation
<i>MEXP</i>	Smoothing factor
<i>PHIT</i>	Thermal voltage at the actual temperature
<i>A1</i>	Factor of the weak-avalanche current
<i>A2</i>	Exponent of the weak-avalanche current
<i>A3</i>	Factor of the drain-source voltage above which weak-avalanche occurs
<i>IGINV</i>	Gain factor for intrinsic gate tunnelling current in inversion
<i>BINV</i>	Probability factor for intrinsic gate tunnelling current in inversion
<i>IGACC</i>	Gain factor for intrinsic gate tunnelling current in accumulation
<i>BACC</i>	Probability factor for intrinsic gate tunnelling current in accumulation
<i>VFBOV</i>	Flat-band voltage for the Source/Drain overlap extensions
<i>KOV</i>	Body-effect factor for the Source/Drain overlap extensions
<i>IGOV</i>	Gain factor for Source/Drain overlap tunnelling current
<i>AGIDL</i>	Gain factor for gate-induced leakage current
<i>BGIDL</i>	Probability factor for gate-induced drain leakage current at reference temperature
<i>CGIDL</i>	Factor for the lateral field dependence of the gate-induced leakage current
<i>COX</i>	Oxide capacitance for the intrinsic channel
<i>CGDO</i>	Oxide capacitance for the gate-drain overlap
<i>CGSO</i>	Oxide capacitance for the gate-source overlap
<i>GATENOISE</i>	Flag for in/exclusion of induced gate thermal noise
<i>NT</i>	Thermal noise coefficient
<i>NFA</i>	First coefficient of the flicker noise
<i>NFB</i>	Second coefficient of the flicker noise
<i>NFC</i>	Third coefficient of the flicker noise
<i>TOX</i>	Thickness of gate oxide layer

Remarks:

- When $V_{ds} < 0$, g_m and g_{mb} are calculated with drain and source terminals interchanged. The terminal voltages and I_{DS} keep their sign.
- The signs of V_{TO} and V_{TS} follow the conventions of the model parameter set. The parameter set is always assumed to correspond to an n-channel device.
- W and L are not available for the electrical MOS models.
- $MULT$ is a scaling parameter that multiplies all currents and charges by the value of $MULT$. This is equivalent to putting $MULT$ (a number) MOS transistors in parallel. And as a consequence $MULT$ effects the operating point output.

A non-existent conductance, G_{min} , is connected between the nodes D and S . This conductance G_{min} does not influence the DC-operating point.

1.8 Embedding

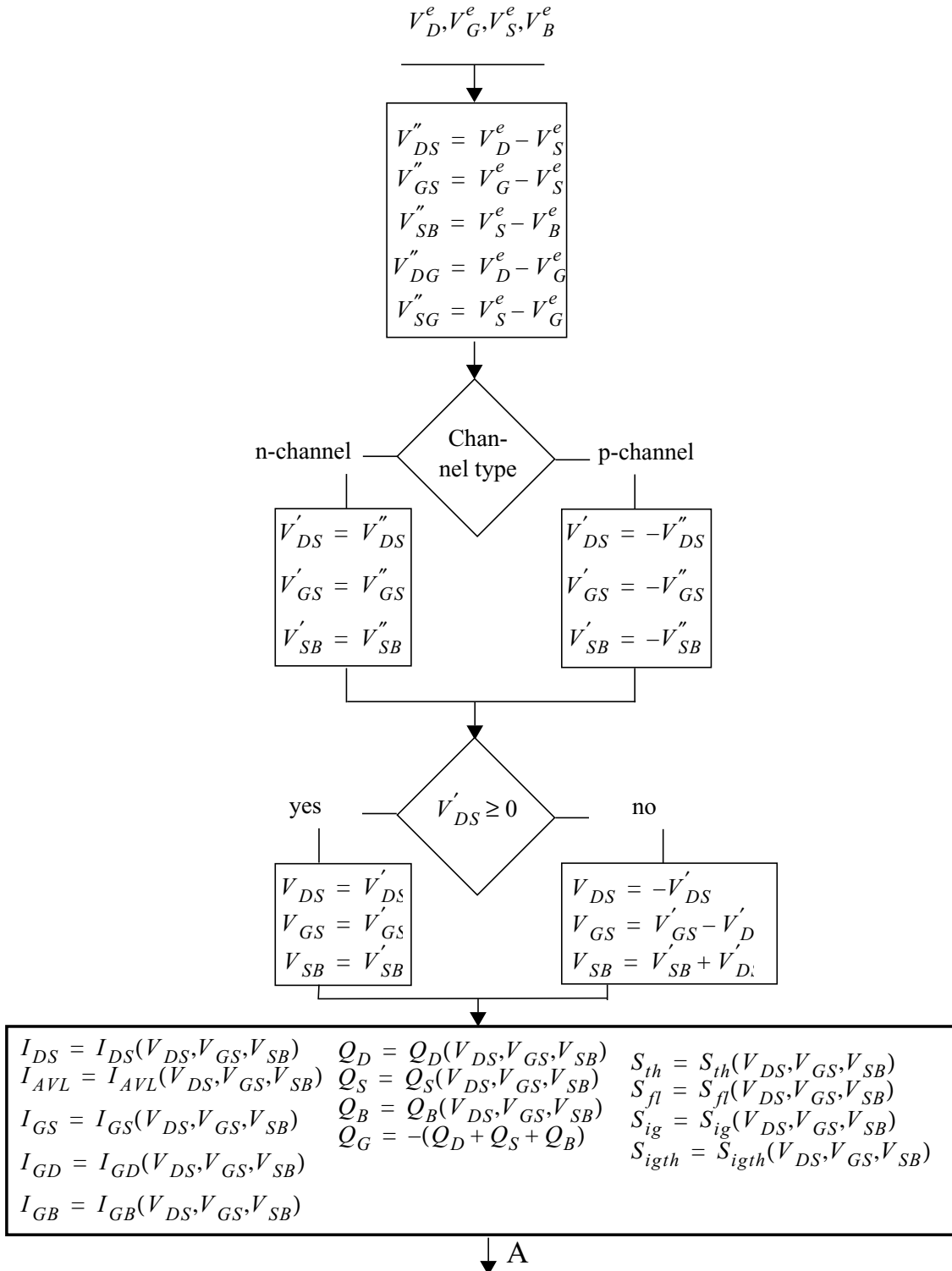
1.8.1 Model embedding in a circuit simulator

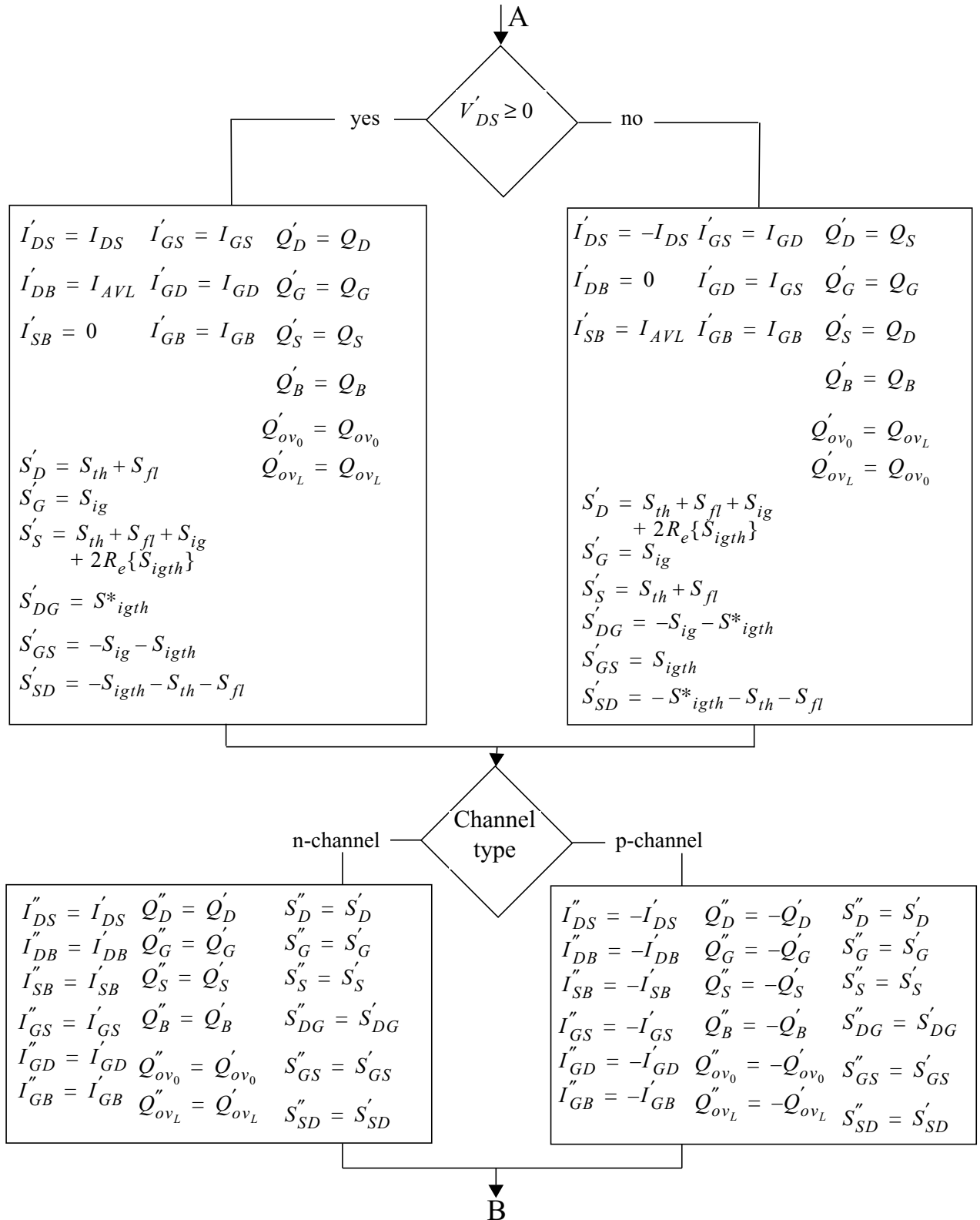
In CMOS technologies both n- and p-channel MOS transistors are supported. It is convenient to use one model for both type of transistors instead of two separate models. This is accomplished by mapping a p-channel device with its bias conditions and parameter set onto an equivalent n-channel device with appropriately changed bias conditions (i.e. currents, voltages and charges) and parameters. In this way both type of transistors can be treated as an n-channel transistor. Nevertheless, the electrical behaviour of electrons and holes is not exactly the same (e.g. the mobility and tunnelling behaviour), and consequently slightly different equations have to be used in case of n- or p-type transistors, see section 1.4.4 on page 102.

As said earlier, any circuit simulator internally identifies the terminals of a MOS transistor by a number. However, designers are used to the standard terminology of source, drain, gate and bulk. Therefore, in the context of a circuit simulator it is traditionally possible to address, say, the drain of MOST number 17, even if in reality the corresponding source is at a higher potential (n channel case). More strongly, most circuit simulators provide for model evaluation a so called V_{DS} , V_{GS} , and V_{SB} based on an a priori assignment of source, drain and bulk that is independent of the actual bias conditions. Since MOS Model 1101 assumes saturation occurs at the drain side of the MOSFET, the basic model cannot cope with bias conditions that correspond to $V_{DS} < 0$. Again a transformation of the bias conditions is necessary. In this case, the transformation corresponds to internally reassigning source and drain, applying the standard electrical model, and then reassigning the currents and charges to the original terminals. In MOS Model 1101 care has been taken to preserve symmetry with respect to drain and source at $V_{DS} = 0$. In other words no non-singularities will occur in the higher-order derivatives at $V_{DS} = 0$.

In detail, in order to embed MOS Model 1101 correctly into a circuit simulator, the following procedure, illustrated in Figure 7 should be followed. We have assumed that indeed the simulator provides the nodal potentials V_D^e , V_G^e , V_S^e and V_B^e based on an a priori assignment of drain, gate, source and bulk.

- Step 1** Calculate the voltages V''_{DS} , V''_{GS} and V''_{SB} , and the additional voltages V''_{DG} and V''_{SG} . The latter are used for calculating the charges associated with overlap capacitances.
- Step 2** Based on n- or p-channel devices, calculate the modified voltages V'_{DS} , V'_{GS} and V'_{SB} . From here onwards only n-channel behaviour needs to be considered.
- Step 3** Based on a positive or negative V'_{DS} , calculate the internal nodal voltages. At this level, the voltages - and the parameters, see below - comply to all the requirements for input quantities of MOS Model 1101.
- Step 4** Evaluate all the internal output quantities - channel current, weak avalanche current, gate current, nodal charges, and noise-power spectral densities - using the standard MOS Model 1101 equations and the internal voltages.
- Step 5** Correct the internal output quantities for a possible source-drain interchange. In fact, this directly establishes the external noise power spectral densities.
- Step 6** Correct for a possible p-channel transformation.
- Step 7** Change from branch current to nodal currents, establishing the external current output quantities. Calculate the overlap charges that are related to the physical regions and add them to the nodal charges, thus forming the external charge output quantities.





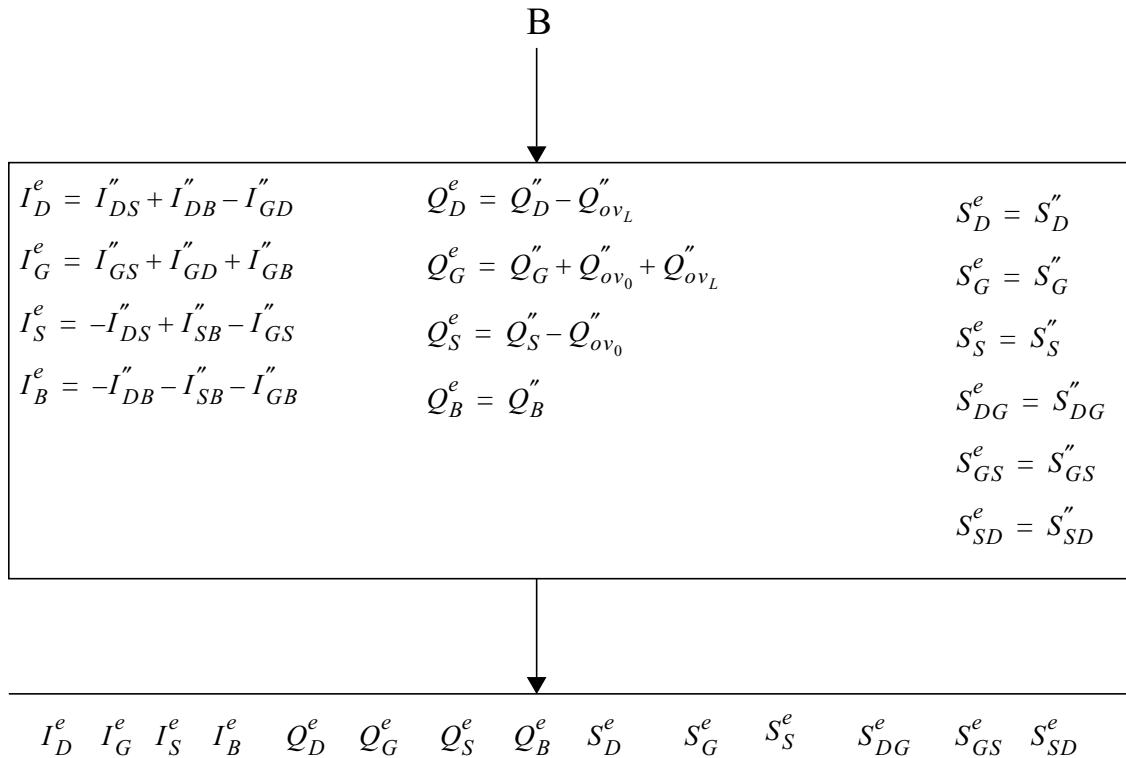


Figure 7: Transformation scheme

It is customary to have separate user models in the circuit simulators for n- and p-channel transistors. In that manner it is easy to use a different set of reference and scaling parameters for the two channel types. As a consequence, the changes in the parameter values necessary for a p-channel type transistor are normally already included in the parameter sets on file. The changes should not be included in the simulator.

1.8.2 Implementation issues

To implement the model in a circuit simulator, care must be taken of the numerical stability of the simulation program. A small non-physical conductance, G_{min} , is connected between the nodes D and S . The value of the conductance is 10^{-15} [1/Ω].

1.9 Simulator specific items

1.9.1 Pstar syntax

n channel electrical model: mne_n (d,g,s,b) level=1101, <parameters>
 p channel electrical model: mpe_n (d,g,s,b) level=1101, <parameters>
 n channel electrical self-heating model:
 mnet_n (d,g,s,b,dt) level=1101, <parameters>
 p channel electrical self-heating model:
 mpet_n (d,g,s,b,dt) level=1101, <parameters>
 n channel physical geometrical model:
 mn_n (d,g,s,b) level=11010 <parameters>
 p channel physical geometrical model:
 mp_n (d,g,s,b) level=11010 <parameters>
 n channel physical geometrical self-heating model:
 mnt_n (d,g,s,b,dt) level=11010 <parameters>
 p channel physical geometrical self-heating model:
 mpt_n (d,g,s,b,dt) level=11010 <parameters>
 n channel binning geometrical model:
 mn_n (d,g,s,b)level=11011 <parameters>
 p channel binning geometrical model:
 mp_n (d,g,s,b)level=11011 <parameters>
 n channel binning geometrical self-heating model:
 mnt_n (d,g,s,b,dt)level=11011 <parameters>
 p channel binning geometrical self-heating model:
 mpt_n (d,g,s,b,dt)level=11011 <parameters>

n : occurrence indicator
 <parameters> : list of model parameters
 d,g,s,b and dt are drain, gate, source, bulk and self-heating terminals respectively.

1.9.2 Spectre syntax

n channel electrical model: model modelname mos1101e type=n <modpar>
 componentname d g s b modelname <inpar>
 p channel electrical model: model modelname mos1101e type=p <modpar>
 componentname d g s b modelname <inpar>
 n channel electrical self-heating model:
 model modelname mos1101et type=n <modpar>
 componentname d g s b dt modelname <inpar>

p channel electrical self-heating model:
 model modelname mos1101et type=p <modpar>
 componentname d g s b dt modelname <inpar>

n channel physical geometrical model:
 model modelname mos11010 type=n <modpar>
 componentname d g s b modelname <inpar>

p channel physical geometrical model:
 model modelname mos11010 type=p <modpar>
 componentname d g s b modelname <inpar>

n channel physical geometrical self-heating model:
 model modelname mos11010t type=n <modpar>
 componentname d g s b dt modelname <inpar>

p channel physical geometrical self-heating model:
 model modelname mos11010t type=p <modpar>
 componentname d g s b dt modelname <inpar>

n channel binning geometrical model:
 model modelname mos11011 type=n <modpar>
 componentname d g s b modelname <inpar>

p channel binning geometrical model:
 model modelname mos11011 type=p <modpar>
 componentname d g s b modelname <inpar>

n channel binning geometrical self-heating model:
 model modelname mos11011t type=n <modpar>
 componentname d g s b dt modelname <inpar>

p channel binning geometrical self-heating model:
 model modelname mos11011t type=p <modpar>
 componentname d g s b dt modelname <inpar>

modelname	:	name of model, user defined
componentname	:	occurrence indicator
<modpar>	:	list of model parameters
<inpar>	:	list of instance parameters

d,g,s,b and dt are drain, gate, source, bulk and self-heating terminals respectively.

3 Note

Warning! In Spectre, use only the parameter statements type=n or type=p. Using any other string and/or numbers will result in unpredictable and possibly erroneous results.

1.9.4 The ON/OFF condition for Pstar

The solution for a circuit involves a process of successive calculations. The calculations are started from a set of 'initial guesses' for the electrical quantities of the nonlinear elements. A simplified DCAPPROX mechanism for devices using ON/OFF keywords is mentioned in [1]. By default the devices start in the default state.

n-channel				p-channel			
	Default	ON	OFF		Default	ON	OFF
V_{DS}	1.25	1.25	2.5	V_{DS}	-1.25	-1.25	-2.5
V_{GS}	1.25	1.25	0.0	V_{GS}	-1.25	-1.25	0.0
V_{SB}	0.0	0.0	0.0	V_{SB}	0.0	0.0	0.0

1.9.5 The ON/OFF condition for Spectre

n-channel							
	OFF	Triode	Saturation	Subthreshold	Reverse	Forward	Breakdown
V_{DS}	0.0	0.75	1.25	2.00	0.0	0.0	0.0
V_{GS}	0.0	2.0	1.25	0.25	0.0	0.0	0.0
V_{SB}	0.0	0.0	0.0	0.0	0.0	0.0	0.0

p-channel							
	OFF	Triode	Saturation	Subthreshold	Reverse	Forward	Breakdown
V_{DS}	0.0	-0.75	-1.25	-2.00	0.0	0.0	0.0
V_{GS}	0.0	-2.0	-1.25	-0.25	0.0	0.0	0.0
V_{SB}	0.0	0.0	0.0	0.0	0.0	0.0	0.0

1.9.6 The ON/OFF condition for ADS

n-channel	
	Default
V_{DS}	0.0
V_{GS}	0.0
V_{SB}	0.0

p-channel	
	Default
V_{DS}	0.0
V_{GS}	0.0
V_{SB}	0.0

1.10 Parameter Extraction

The parameter extraction strategy for MOS Model 11 using an **optimization method** consists of four main steps:

1. measurements
2. extraction of miniset parameters at room temperature
3. extraction of temperature scaling parameters
4. extraction of geometry scaling parameters.

The above steps will be briefly described in the following sections.

1.10.1 Measurements

The parameter extraction routine consists of four different dc-measurements and two (optional) capacitance measurements¹:

- **Measurement I:** $I_D/g_m/I_G-V_{GS}$ - characteristics in linear region:

n-channel : $V_{GS} = 0 \dots V_{sup}$ (with steps of maximum 50 mV).
 $V_{DS} = 50 \text{ mV}$
 $V_{BS} = 0 \dots -V_{sup}$

p-channel : $V_{GS} = 0 \dots -V_{sup}$ (with steps of maximum 50 mV).
 $V_{DS} = -50 \text{ mV}$
 $V_{BS} = 0 \dots V_{sup}$

- **Measurement II:** Subthreshold I_D-V_{GS} - characteristics:

n-channel : $V_{GS} = V_T - 0.6 \text{ V} \dots V_T + 0.3 \text{ V}$
 $V_{DS} = 3 \text{ values starting from } 100 \text{ mV to } V_{sup}$
 $V_{BS} = 0 \dots -V_{sup}$

p-channel : $V_{GS} = V_T + 0.6 \text{ V} \dots V_T - 0.3 \text{ V}$
 $V_{DS} = 3 \text{ values starting from } -100 \text{ mV to } -V_{sup}$
 $V_{BS} = 0 \dots V_{sup}$

¹The bias conditions to be used for the measurements are dependent on the supply voltage of the process. Of course it is advisable to restrict the range of voltages to this supply voltage V_{sup} . Otherwise physical effects, atypical for normal transistor operation and therefore less well described by MOS Model 11, may dominate the characteristics.

- **Measurement III:** $I_D/g_{DS}/I_G-V_{DS}$ - characteristics:
 - n-channel : $V_{DS} = 0 \dots V_{sup}$ (with steps of maximum 50 mV).
 $V_{GS} = 4$ values starting from $V_T + 0.1$ V , not above V_{sup}
 $V_{BS} = 3$ values starting from 0 V to $-V_{sup}$
 - p-channel : $V_{DS} = 0 \dots -V_{sup}$ (with steps of maximum 50 mV).
 $V_{GS} = 4$ values starting from $V_T + 0.1$ V , not below $-V_{sup}$
 $V_{BS} = 3$ values starting from 0 V to V_{sup}

- **Measurement IV:** $I_D/I_S/I_G/I_B-V_{GS}$ - characteristics in all operation regions:
 - n-channel : $V_{GS} = -V_{sup} \dots V_{sup}$ (with steps of maximum 50 mV).
 $V_{DS} = 4$ values starting from 0 V to V_{sup}
 $V_{BS} = 0$ V
 - p-channel : $V_{GS} = -V_{sup} \dots -V_{sup}$ (with steps of maximum 50 mV).
 $V_{DS} = 4$ values starting from 0 V to $-V_{sup}$
 $V_{BS} = 0$ V

- **Measurement V:** $C_{gg}-V_{GS}$ - characteristics (optional):
 - n/p-channel : $V_{GS} = -V_{sup} \dots V_{sup}$ (with steps of maximum 50 mV).
 $V_{DS} = 0$ V
 $V_{BS} = 0$ V

- **Measurement VI:** $C_{cg}-V_{GS}$ - characteristics:
 - n/p-channel : $V_{GS} = -V_{sup} \dots V_{sup}$
 $V_{DS} = 0$ V
 $V_{BS} = 0$ V

The values of transconductance g_m and output conductance g_{DS} are extracted from the I - V-curves by calculating in a numerical way the derivative of I_D to V_{GS} and V_{DS} , respectively. In the subthreshold measurements, Measurement II, use is made of threshold voltage V_T , which has to be determined for all the bulk-source bias values V_{BS} . The determination of V_T is rather arbitrary, and it can be either determined using the lineas extrapolation method or the constant current criterion. The channel-to-gate capacitance C_{cg} is the summation of the

drain-to-gate capacitance C_{dg} and the source-to-gate capacitance C_{sg} (i.e. source and drain are short-circuited), it is needed to extract overlap capacitance parameters.

For the miniset extraction measurements I through IV have to be performed at room temperature for every device. In addition measurements V and VI need to be performed for a long/broad and a short/broad (i.e. $L = L_{\min}$) transistor (at room temperature). Furthermore, for the extraction of temperature scaling parameters measurements I, III and IV have to be performed at different temperatures (at least two, typically -40°C and 125°C) for at least a long/broad and a short/broad transistor.

1.10.2 Extraction of Miniset Parameters at Room Temperature

The extraction of miniset parameters is performed for every device. In order to ensure that the temperature scaling relations do not affect the behaviour at room temperature, the reference temperature T_R is chosen equal to room temperature. In general the simultaneous determination of all miniset parameters is not advisable, because the value of some parameters can be wrong due to correlation and suboptimization. Therefore it is more practical to split the parameters into several groups, where each parameter group can be determined using specific measurements.

Although the poly-depletion effect affects the dc-behaviour of a MOSFET, the poly-depletion parameter KPINV can only be determined accurately from C - V -measurements. If the (physical) oxide thickness t_{ox} and the polysilicon impurity concentration N_p are known, the parameter KPINV ($= 1/(k_p)$) can be calculated from¹:

$$k_p = \frac{t_{ox} \cdot \sqrt{2 \cdot q \cdot \epsilon_{si} \cdot N_p}}{\epsilon_{ox}} \quad (1.227)$$

If the polysilicon impurity concentration N_p is not known, as a good first-order estimate one can use $N_p = 1 \cdot 10^{26} \text{ m}^{-3}$ for n^+ -polysilicon gates and $N_p = 5 \cdot 10^{25} \text{ m}^{-3}$ for p^+ -polysilicon gates. In the latter case a measured C_{GG} - V_{GS} -characteristic for a long-channel transistor is essential for an accurate determination of KPINV.

1. For metal gates the poly-depletion effect does not occur and in this case KPINV = 0.

Table 3: Starting miniset parameter values for parameter extraction at room temperature T_R of a typical MOSFET with channel length L (m), channel width W (m), oxide thickness t_{ox} (m), polysilicon impurity concentration N_P (m^{-3}) and minimum technology feature size L_{min} . If the polysilicon concentration N_P is not known, one can use $N_p = 1 \cdot 10^{26} m^{-3}$ or $5 \cdot 10^{25} m^{-3}$ for n^+ - resp. p^+ -polysilicon gates. Parameters C_{ox} , C_{GSO} and C_{GDO} are only important for the charge model, and do not affect the dc-model; they have to be extracted from C-V-characteristics. In order to determine the parameter geometry-scaling, the last column indicates for which conditions the parameters have to be extracted: L=long-channel device (fixed for short-channel devices), S=short-channel devices, A=all devices and F=fixed parameter.

Parameter	Program Name	Parameter Value		Extracted for
		NMOS	PMOS	
V_{FB}	VFB	-1.1	-0.95	L
k_0	KO	0.25	0.25	A
$1/k_p$	KPINV	$6.0 \cdot 10^3 / (t_{OX} \cdot \sqrt{N_p})$	$6.0 \cdot 10^3 / (t_{OX} \cdot \sqrt{N_p})$	L
ϕ_B	PHIB	0.95	0.95	A
β	BET	$1.7 \cdot 10^{-12} / t_{OX} \cdot W/L$	$4.5 \cdot 10^{-13} / t_{OX} \cdot W/L$	A
θ_{sr}	THESR	$1.5 \cdot 10^{-9} / t_{OX}$	$2.3 \cdot 10^{-9} / t_{OX}$	L
θ_{ph}	THEPH	$1.3 \cdot 10^{-10} / t_{OX}$	$2.2 \cdot 10^{-10} / t_{OX}$	L
η_{mob}	ETAMOB	1.3	3.0	L
ν	NU	2.0	2.0	A
θ_R	THER	$1.3 \cdot 10^{-7} / L$	$8.0 \cdot 10^{-8} / L$	S
θ_{R1}	THER1	0	0	-
θ_{R2}	THER2	1	1	-
θ_{sat}	THESAT	$4.5 \cdot 10^{-7} / L$	$2.0 \cdot 10^{-7} / L$	A
θ_{Th}	THETH	$1.0 \cdot 10^{-6}$	$1.0 \cdot 10^{-6}$	A
σ_{dib1}	SDIBL	$5.0 \cdot 10^{-2} \cdot (L_{min}/L)^2$	$5.0 \cdot 10^{-2} \cdot (L_{min}/L)^2$	S

Table 3: Starting miniset parameter values for parameter extraction at room temperature T_R of a typical MOSFET with channel length L (m), channel width W (m), oxide thickness t_{ox} (m), polysilicon impurity concentration N_P (m^{-3}) and minimum technology feature size L_{min} . If the polysilicon concentration N_P is not known, one can use $N_p = 1 \cdot 10^{26} m^{-3}$ or $5 \cdot 10^{25} m^{-3}$ for n^+ - resp. p^+ -polysilicon gates. Parameters C_{ox} , C_{GSO} and C_{GDO} are only important for the charge model, and do not affect the dc-model; they have to be extracted from C-V-characteristics. In order to determine the parameter geometry-scaling, the last column indicates for which conditions the parameters have to be extracted: L=long-channel device (fixed for short-channel devices), S=short-channel devices, A=all devices and F=fixed parameter.

Parameter	Program Name	Parameter Value		Extracted for
		NMOS	PMOS	
m_0	MO	$1.0 \cdot 10^{-3}$	$1.0 \cdot 10^{-3}$	A
σ_{sf}	SSF	$6.0 \cdot 10^{-2} \cdot L_{min}/L$	$6.0 \cdot 10^{-2} \cdot L_{min}/L$	A
α	ALP	$6.0 \cdot 10^{-2} \cdot L_{min}/L$	$6.0 \cdot 10^{-2} \cdot L_{min}/L$	A
V_p	VP	$5.0 \cdot 10^{-2}$	$1.0 \cdot 10^{-1}$	F
m	MEXP	use Eq. (12.132)	use Eq. (12.132)	-
a_1	A1	25	100	A
a_2	A2	25	37	A
a_3	A3	1	1	A
I_{GINV}	IGINV	$3.0 \cdot 10^{-5} \cdot W \cdot L/t_{ox}^2$	$4.0 \cdot 10^{-5} \cdot W \cdot L/t_{ox}^2$	A
B_{INV}	BINV	$2.9 \cdot 10^{+10} \cdot t_{ox}$	$4.3 \cdot 10^{+10} \cdot t_{ox}$	L
I_{GACC}	IGACC	$3.0 \cdot 10^{-5} \cdot W \cdot L/t_{ox}^2$	$2.0 \cdot 10^{-5} \cdot W \cdot L/t_{ox}^2$	A
B_{ACC}	BACC	B_{INV}	$2.9 \cdot 10^{+10} \cdot t_{ox}$	L
V_{FBov}	VFBOV	0.1	0.1	L
k_{ov}	KOV	$9.3 \cdot 10^{+8} \cdot t_{ox}$	$3.8 \cdot 10^{+8} \cdot t_{ox}$	L
I_{GOV}	IGOV	$5.0 \cdot 10^{-13} \cdot W/t_{ox}^2$	$5.0 \cdot 10^{-12} \cdot W/t_{ox}^2$	A
A_{GIDL}	AGIDL	$1.6 \cdot 10^{-13} \cdot W/t_{ox}^2$	$1.2 \cdot 10^{-17} \cdot W/t_{ox}^2$	A

Table 3: Starting miniset parameter values for parameter extraction at room temperature T_R of a typical MOSFET with channel length L (m), channel width W (m), oxide thickness t_{ox} (m), polysilicon impurity concentration N_P (m^{-3}) and minimum technology feature size L_{min} . If the polysilicon concentration N_P is not known, one can use $N_P = 1 \cdot 10^{26} m^{-3}$ or $5 \cdot 10^{25} m^{-3}$ for n^+ - resp. p^+ -polysilicon gates. Parameters C_{ox} , C_{GSO} and C_{GDO} are only important for the charge model, and do not affect the dc-model; they have to be extracted from C-V-characteristics. In order to determine the parameter geometry-scaling, the last column indicates for which conditions the parameters have to be extracted: L=long-channel device (fixed for short-channel devices), S=short-channel devices, A=all devices and F=fixed parameter.

Parameter	Program Name	Parameter Value		Extracted for
		NMOS	PMOS	
B_{GIDL}	BGIDL	$1.6 \cdot 10^{+8} \cdot t_{ox}$	$1.0 \cdot 10^{+10} \cdot t_{ox}$	L
C_{GIDL}	CGIDL	0	0	L
C_{ox}	COX	$\epsilon_{ox}/t_{ox} \cdot W \cdot L$	$\epsilon_{ox}/t_{ox} \cdot W \cdot L$	-
C_{GDO}	CGDO	$3.0 \cdot 10^{-10} \cdot W$	$3.0 \cdot 10^{-10} \cdot W$	-
C_{GSO}	CGSO	$3.0 \cdot 10^{-10} \cdot W$	$3.0 \cdot 10^{-10} \cdot W$	-

Before the optimization is started a parameter set has to be determined which contains a first estimation of the parameters to be extracted and the parameters which remain constant. The value of smoothing factor m is calculated from the device length L and from the minimum feature size of the technology L_{min} using eq. (1.132). The parameter set used as a first-order estimation of the parameters to be extracted is given in Table 4. With this parameter set a first optimization following the scheme below, is performed. After this the new parameter set serves as an estimation for the second optimization, which is performed following the same scheme. This method yields a proper set of parameters after the second optimization. Experi-

ments with transistors of different processes show that the parameter set does not change very much after a third optimization.

Table 4: DC-parameter extraction procedure for a long-channel n-MOSFET, where Steps 2 and 12 are optional. For p-type transistors all voltages and currents have to be multiplied by -1. The optimization is either performed on the absolute or relative deviation between model and measurements. Parameter I_{tst} is 2.5 μA for NMOS and 0.8 μA for PMOS. For n-MOSFETs $B_{acc} = B_{inv}$, and as a result B_{acc} does not have to be extracted. For p-MOSFETs this is not the case, see Table. 10.

Step	Optimised Parameters	Measurement	Fitted On	Absolute/Relative	Specific Conditions
1	$\phi_B, k_0, \beta, \theta_{sr}$	I	I_D	Absolute	-
2	V_{FB}, k_0, k_p, C_{ox}	V	C_{gg}	Relative	-
3	ϕ_B, k_0, m_0	II	I_D	Relative	-
4	$\beta, \theta_{sr}, \theta_{ph}$	I	I_D/g_m	Relative	$V_{SB} = 0V$ $V_{GS} > V_T + 0.3V$
5	η_{mob}	I	I_D	Absolute	$I_D > W/L \cdot I_{tst}$
6	θ_{sat}	III	I_D	Absolute	-
7	$\sigma_{sf}, \alpha, \theta_{Th}$	III	g_{DS}	Relative	-
8	θ_{sat}	III	I_D	Absolute	-
9	I_{GINV}, B_{INV}	I	I_G	Absolute	-
19	$I_{GOV} (B_{ACC}), I_{GACC}, k_{ov}$	IV	I_G	Relative	$V_{GS} < 0V$
11	a_1, a_2, a_3	IV	I_B	Absolute	$V_{GS} \geq 0V$
12	$A_{GIDL}, B_{GIDL}, C_{GIDL}$	IV	I_B	Absolute	$V_{GS} < 0V$
13	V_{FB}, k_p, C_{ox}	V	C_{gg}	Relative	-
14	Repeat steps 3, 4, 5, 6, 7, 8, 9, 10, 11 and 12				

For an accurate extraction of parameter values, the parameter set for a long-channel transistor has to be determined first. In the long-channel case the poly-depletion parameter $1/k_p$, the flat-band voltage VFB, the carrier mobility (i.e. θ_{sr} , θ_{ph} and η_{mob}) and the gate tunnelling

probability factors (B_{inv} and B_{acc}) can be determined, and they can subsequently be fixed for the short and narrow-channel devices, see Tab. 8. In Table 1 the extraction procedure for long-channel transistors is given. Since the value of body-factor k_0 may change much over geometry and over technology, the first-order estimate in Tab. 7.1 is very crude and a more accurate, preliminary value is obtained using Step 1. In Step 2 (optional) more accurate values of the poly-depletion parameter $1/k_P$ and the flat-band voltage V_{FB} (which determines the onset of accumulation) are extracted. Next the subthreshold parameters ϕ_B , k_0 and m_0 are optimized in Step 3, neglecting short-channel effects such as drain-induced barrier-lowering (DIBL). After that the mobility parameters are optimized using Steps 4 and 5, neglecting the influence of series-resistance. In Step 6 a preliminary value of the velocity saturation parameter is obtained, and subsequently the conductance parameters σ_{sf} , α and θ_{Th} are determined in Step 7. A more accurate value of θ_{sat} can now be obtained using Step 8 (which is Step 6 repeated). The gate current parameters are determined in Steps 9 and 10, followed by the weak-avalanche parameters in Step 11, and finally, the gate-induced leakage current parameters are optimized in step 12.

Table 5: DC-parameter extraction procedure for a short-channel n-MOSFET. For p-type transistors all voltages and currents have to be multiplied by -1. Parameters $1/k_P$, V_{FB} , θ_{sr} , θ_{ph} , η_{mob} , B_{inv} , B_{acc} , k_{ov} , B_{GIDL} and C_{GIDL} are taken from the long-channel case. The optimization is either performed on the absolute or relative deviation between model and measurements.

Step	Optimised Parameters	Measurement	Fitted On	Absolute/Relative	Specific Conditions
1	$\phi_B, k_0, \beta, \theta_R$	I	I_D	Absolute	-
2	$\phi_B, k_0, m_0, \sigma_{dibl}$	II	I_D	Relative	-
3	β, θ_R	I	I_D/g_m	Relative	$V_{SB} = 0V$ $V_{GS} > V_T + 0.3V$
4	θ_{sat}	III	I_D	Absolute	-
5	$\sigma_{sf}, \alpha, \theta_{Th}, \sigma_{dibl}$	III	g_{DS}	Relative	-
6	θ_{sat}	III	I_D	Absolute	-
7	$I_{GINV}, I_{GOV}, I_{GACC}$	IV	I_D	Relative	-
8	a_1, a_2, a_3	IV	I_B	Absolute	$V_{GS} \geq 0V$
9	A_{GIDL}	IV	I_B	Absolute	$V_{GS} < 0V$

Table 5: DC-parameter extraction procedure for a short-channel n-MOSFET. For p-type transistors all voltages and currents have to be multiplied by - 1. Parameters $1/k_p$, V_{FB} , θ_{sr} , θ_{ph} , η_{mob} , B_{inv} , B_{acc} , k_{ov} , B_{GIDL} and C_{GIDL} are taken from the long-channel case. The optimization is either performed on the absolute or relative deviation between model and measurements.

Step	Optimised Parameters	Measurement	Fitted On	Absolute/Relative	Specific Conditions
10	Repeat steps 2, 3, 4, 5, 7, 8 and 9				

For short-channel devices the values of the poly-depletion parameter $1/k_p$, flat-band voltage V_{FB} , the carrier mobility parameters (θ_{sr} , θ_{ph} and η_{mob}) and the gate tunnelling probability factors (B_{inv} and B_{acc}) of the long-channel device are copied, and next the extraction procedure as given in Table 2 is executed. In contrast to the long-channel case, the extraction procedure for short-channel devices also optimizes the parameters for series-resistance¹ and DIBL.

AC-parameters: The AC-parameters C_{ox} , C_{GSO} , C_{GDO} , k_{ov} and V_{FBov} cannot be (accurately) determined from DC-characteristics, and as a consequence they have to be determined from C–V– characteristics². Since normal MOS transistors are symmetrical devices, one can assume that the oxide capacitance of the source and drain extension are identical, which implies that $C_{GSO}=C_{GDO}$. The oxide capacitance of the intrinsic MOSFET C_{ox} can be extracted from Measurement VI. In Table 3 the extraction procedure for the AC-parameters is given.

1.10.3 Extraction of Temperature Scaling Parameters

For a specific device the temperature scaling parameters can be extracted after the miniset at room temperature has been extracted. In order to do so, measurements I, III and IV need to be

1. Note that in Table 10 parameters θ_{R1} and θ_{R2} are not included, which implies that the series-resistance is assumed to be voltage-independent. This holds true for modern CMOS technologies, where no use is made of LDD-structures.

2. Although parameter k_{ov} can be determined from overlap gate current, see Table 9, it is nonetheless more accurately determined from the C_{cg} - V_{GS} characteristics.

performed at various temperature values (at least two values different from room temperature, typically - 40° C and 125° C).

Table 6: AC-parameter extraction procedure for a MOSFET. Here it is assumed that $C_{GSO} = C_{GDO}$. In the first instance flat-band voltage V_{FBov} is not optimised, although it may be optimised during Step 1 in order to obtain more accurate results. The optimization is either performed on the absolute or relative deviation between model and measurements.

Step	Optimised Parameters	Measurement	Fitted On	Absolute/Relative	Specific Conditions
1	k_{ov}, C_{GSO}	VI	C_{cg}	Relative	$V_{GS} < 0V$
2	C_{ox}	V	C_{gg}	Relative	-
3	Repeat steps 1 and 2				

Since the reference temperature T_R has been chosen equal to room temperature, the modelled behaviour at room temperature is not affected by different values of the temperature scaling parameters. As a first-order estimation of the temperature scaling parameter values, the default values as given in Section 1.4.4 are used. Again, the parameter extraction scheme is slightly different for the long-channel and for the short-channel case.

Table 7: Temperature scaling parameter extraction procedure for a long-channel n-MOSFET, where measurements have been performed at various temperature values. For p-type transistors all voltages and currents have to be multiplied by -1. The optimization is either performed on the absolute or relative deviation between model and measurements. Parameter I_{tst} is 2.5 μA for NMOS and 0.8 μA for PMOS.

Step	Optimised Parameters	Measurement	Fitted On	Absolute/Relative	Specific Conditions
1	$S_{T;\phi_B}$	I	I_D	Relative	$I_D < W/L \cdot I_{tst}$
2	$\eta_\beta, \eta_{sr}, \eta_{ph}, v_{exp}, S_{T;\eta_{mob}}$	I	I_D	Relative	$I_D > W/L \cdot I_{tst}$
3	η_{sat}	III	I_D	Absolute	-
4	$S_{T;a_1}$	IV	I_B	Absolute	$V_{GS} \geq 0V$
5	$S_{T;B_{GIDL}}$	IV	I_B	Absolute	$V_{GS} < 0V$

For an accurate extraction, the temperature scaling parameters for a long-channel device have to be determined first. In the long-channel case the carrier mobility parameters (i.e. η_{sr} , η_{ph} , v_{exp} and $S_{T;\eta_{mob}}$) can be determined, and they can subsequently be fixed for the short-channel devices. In Table 4 the extraction procedure for long-channel transistors is given. In Step 1 the subthreshold temperature dependence is optimized, followed by the optimization of mobility reduction parameters in Step 2. Next the temperature dependence of velocity saturation is optimized in Step 3. In Step 4 the temperature dependence of impact ionization is determined, and finally, in step 5 the temperature dependence of the gate-induced drain leakage is optimized.

For short-channel devices the values of the mobility reduction temperature scaling parameters (i.e. η_{sr} , η_{ph} , v_{exp} and $S_{T;\eta_{mob}}$) of the long-channel device are copied, and next the extraction procedure as given in Table 5 is executed. In contrast to the long-channel case, the extraction procedure for short-channel devices optimizes the parameter for series-resistance.

Table 8: Temperature scaling parameter extraction procedure for a short-channel n-MOSFET, where measurements have been performed at various temperature values. For p-type transistors all voltages and currents have to be multiplied by -1. The optimization is either performed on the absolute or relative deviation between model and measurements. Parameter I_{tst} is 2.5 μA for NMOS and 0.8 μA for PMOS.

Step	Optimised Parameters	Measurement	Fitted On	Absolute/Relative	Specific Conditions
1	$S_{T;\phi_B}$	I	I_D	Relative	$I_D < W/L \cdot I_{tst}$
2	η_β, η_R	I	I_D	Relative	$I_D > W/L \cdot I_{tst}$
3	η_{sat}	III	I_D	Absolute	-
4	$S_{T;a_1}$	IV	I_B	Absolute	$V_{GS} \geq 0V$
5	$S_{T;B_{GIDL}}$	IV	I_B	Absolute	$V_{GS} < 0V$

1.10.4 Extraction of Geometry Scaling Parameters

In general, the most important part of the geometry scaling scheme is the determination of ΔL and ΔW , see eqs. (1.112) and (1.113), since it affects the DC-, the AC- as well as the noise model. Traditionally ΔW can be determined from the extrapolated zero-crossing in the gain factor β versus mask width W . In a similar way ΔL can be determined from the inverse gain factor $1/\beta$ versus mask length L . For modern MOS devices with pocket implants, however, it has been found that the above ΔL extraction method is no longer valid [17], [19]. Another, more accurate method is to measure the gate-to-bulk capacitance C_{GB} in accumulation for different channel lengths [18], [19]. In this case the extrapolated zero-crossing in the C_{GB} versus mask length L curve will give ΔL . Unfortunately for CMOS technologies in which gate current is non-negligible, capacitance measurements may be hampered by gate current [20]. In this case either gate current parameter I_{GINV} or I_{GACC} plotted as a function of channel length L may be used to extract ΔL [20].

In MM11, Level 1101, one can use either physical or binning geometry scaling rules. When using the binning rules of Section 1.4.3, the scaling parameters for one bin can be directly calculated from the minisets of the four corner devices of the bin. The binning scheme ensures that the minisets are exactly reproduced in the bin corners, and that no humps occur in parameter values across bin borders. The exact way to calculate binning parameters from minisets is described in *Appendix D Coefficients in the binning rules for geometry scaling*.

When using the physical scaling relations of Section 1.4.2 it is possible to calculate a parameter set for a process, given the parameter set of typical transistors of this process. To accomplish this, transistors of different lengths, widths and at different temperatures have to be measured. Using these measurements the sensitivities of the parameters on length, width and temperature can be found. For the determination of a geometry-scaled parameter set a three-step procedure is recommended:

1. Determine minisets ($\phi_B, k_0, \beta, \dots$) for all measured devices, as explained in Sections 12.8.2 and 12.8.3.
2. The width and length sensitivity coefficients are optimized by fitting the appropriate geometry scaling rules to these miniset parameters.
3. Finally the width and length sensitivity coefficients are optimized by fitting the result of the scaling rules and current equations to the measured currents of all devices simultaneously.

Parameter sets have been determined for several processes using this parameter extraction strategy and taking care of not exceeding the supply voltage. For all processes good results have been obtained.

1.11 References

- [1] **Pstar** User Manual.
- [2] Kwok K. Hung *et al.*, IEEE Trans El. Dev. Vol. 37, No. 3, March 1990
- [3] Kwok K. Hung *et al.*, IEEE Trans El. Dev. Vol. 37, No. 5, May 1990
- [4] A.J. Scholten and D.B.M. Klaassen, *New 1/f noise model in MOS Model 9, level 903*, Nat.Lab Unclassified Report, NL-UR 816/98
- [5] R. van Langevelde, *A Compact MOSFET Model for Distortion Analysis in Analog Circuit Design*, PhD Thesis, TU Eindhoven, Eindhoven 1998.
Available on request. Write to: Ronald.van.Langevelde@philips.com
- [6] R. van Langevelde and F.M. Klaassen, *An Explicit Surface-Potential Based MOSFET Model for Circuit Simulation*, Solid-State Electron., Vol. 44, pp. 409-418, 2000.
- [7] R.M.D.A. Velghe, D.B.M. Klaassen, F.M. Klaassen, *MOS Model 9*, NL-UR 003/94, 1994. internet: <http://www.semiconductors.philips.com/PhilipsModels>.
- [8] R. van Langevelde and F.M. Klaassen, *Influence of Mobility Degradation on Distortion Analysis in MOSFETs*, in Proceedings ESSDERC 1996, Bologna, Italy, pp. 667-670, 1996.
- [9] R. van Langevelde and F.M. Klaassen, *Effect of Gate-Field Dependent Mobility Degradation on Distortion Analysis in MOSFETs*, IEEE Trans. Electron Devices, Vol. ED-44, No. 11, pp. 2044-2052, 1997.
- [10] R. van Langevelde and F.M. Klaassen, *Accurate Drain Conductance Modeling for Distortion Analysis in MOSFETs*, IEDM 1997 Tech. Digest, pp. 313-316, 1997.
- [11] A.R. Boothroyd, S.W. Tarasewicz and C. Slaby, *MISNAN A Physically Based Continuous MOSFET Model for CAD Applications*, IEEE Trans. Computer-Aided Design, Vol. CAD-10, No. 12, pp. 1512-1529, 1991.
- [12] K. Joardar, K.K. Gullapulli, C.C. McAndrew, M.E. Burnham and A. Wild, *An Improved MOSFET Model for Circuit Simulation*, IEEE Trans. Electron Devices, Vol. ED-45, No. 1, pp. 134-148, 1998.

- [13] Z.A. Weinberg, *On Tunneling in Metal-Oxide-Silicon Structures*, J. Appl. Phys., Vol. 53, pp. 5052-56, 1982.
- [14] F. Stern, *Quantum Properties of Surface Space-Charge Layers*, CRC Crit. Rev. Solid State Sci., pp. 499-514, 1974.
- [15] S.-Y. Oh, D.E. Ward and R.W. Dutton, *Transient Analysis of MOS Transistors*, IEEE J. Solid-State Circ., Vol. 15, pp. 636-643, 1980.
- [16] R. Rios and N.D. Arora, *Determination of Ultra-Thin Gate Oxide Thicknesses for CMOS Structures Using Quantum Effects*, IEDM 1994 Tech. Digest, pp. 613-316, 1994.
- [17] A.J. Scholten, L.F. Tiemeijer, P.W.H. de Vreede and D.B.M. Klaassen, *A Large Signal Non-Quasi-Static MOS Model for RF Circuit Simulation*, IEDM 1999 Tech. Digest, pp. 163-166, 1999.
- [18] K.K. Hung, P.K. Ko, C. Hu and Y.C. Cheng, *A Unified Model for the Flicker Noise in Metal-Oxide-Semiconductor Field-Effect Transistors*, IEEE Trans. Electron Devices, Vol. ED-37, No. 3, pp. 654-665, 1990.
- [19] K.K. Hung, P.K. Ko, C. Hu and Y.C. Cheng, *A Physics-Based MOSFET Noise Model for Circuit Simulators*, IEEE Trans. Electron Devices, Vol. ED-37, No. 5, pp. 1323-1333, 1990.
- [20] A.J. Scholten and D.B.M. Klaassen, *New 1/f Noise Model in MOS Model 9, Level 903*, NL-UR 816/98, 1998.
- [21] H.C. de Graaff and F.M. Klaassen, *Compact transistor modelling for circuit design*. Vienna/New York: Springer-Verlag, 1990.
- [22] R. van Langevelde et al., *New Compact Model for Induced Gate Current Noise*, IEDM 2003 Tech. Digest, pp. 867-870, 2003.
- [23] A.J. Scholten et al., *Accurate Thermal Noise Model for Deep-Submicron CMOS*, IEDM 1999 Tech. Digest, pp. 155-158, 1999.
- [24] R. van Langevelde, A.J. Scholten and D.B.M. Klaassen, "Physical Background of MOS Model 11, Level 1101," NL-UR 2003/00239, 2003.
internet: http://www.semiconductors.philips.com/Philips_Models/mos_models
- [25] R. van Langevelde and F.M. Klaassen, "An Explicit Surface-Potential Based MOSFET Model for Circuit Simulation," Solid-State Electron., Vol. 44, pp. 409-418, 2000.

- [26] R. van Langevelde and F.M. Klaassen, "Influence of Mobility Degradation on Distortion Analysis in MOSFETs," in Proceedings ESSDERC, pp. 667-670, 1996.
- [27] R. van Langevelde and F.M. Klaassen, "Effect of Gate-Field Dependent Mobility Degradation on Distortion Analysis in MOSFET's," IEEE Trans. Electron Devices, Vol. ED-44, No. 11, pp. 2044-2052, 1997.
- [28] R. van Langevelde and F.M. Klaassen, "Accurate Drain Conductance Modeling for Distortion Analysis in MOSFETs," IEDM Tech. Digest, pp. 313-316, 1997.
- [29] R. van Langevelde, A.J. Scholten, R.J. Havens, L.F. Tiemeijer and D.B.M. Klaassen, "Advanced Compact MOS Modelling (invited paper)," in Proceedings ESSDERC, pp. 81-88, 2001.
- [30] A.J. Scholten, L.F. Tiemeijer, R. van Langevelde, R.J. Havens, A.T.A. Zegers-van Duijnhoven and V.C. Venezia, "Noise Modeling for RF CMOS Circuit Simulation," IEEE Trans. Electron Devices, Vol. ED-50, No. 3, pp. 618-632, 2003.

A Hyp functions

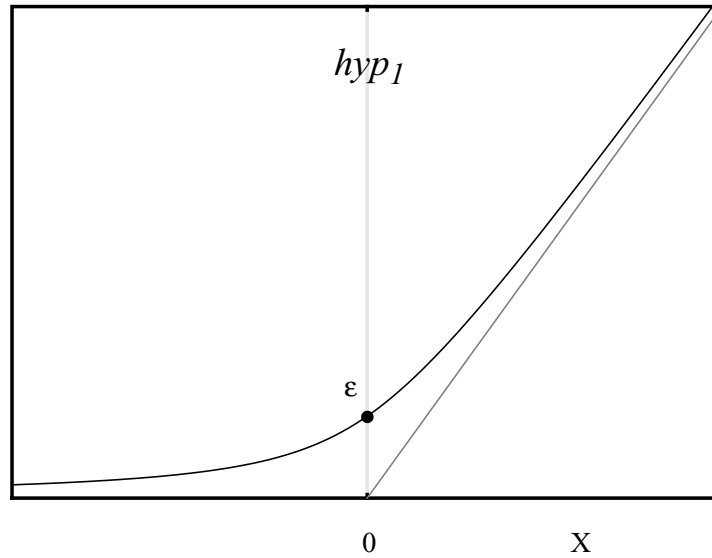


Figure 8: $hyp_1(x;\epsilon) = \frac{1}{2} \cdot (x + \sqrt{x^2 + 4 \cdot \epsilon^2})$

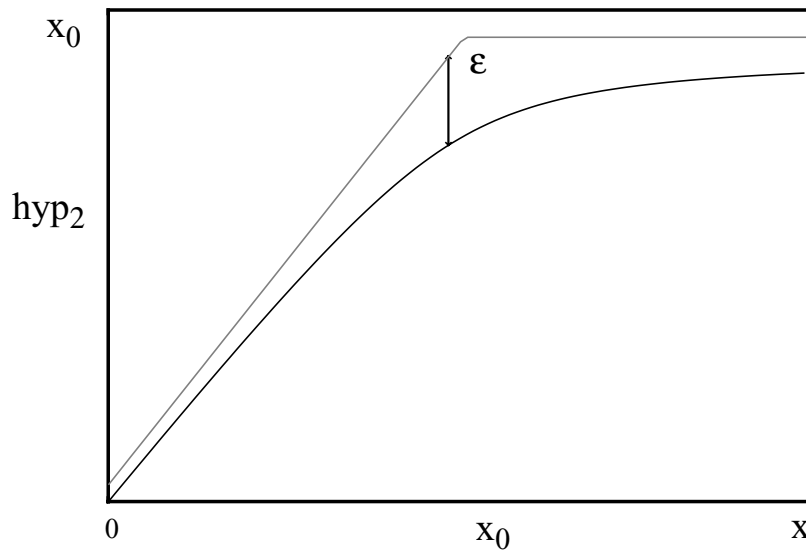


Figure 9: $hyp_2(x;x_0;\epsilon) = x - hyp_1(x - x_0;\epsilon)$

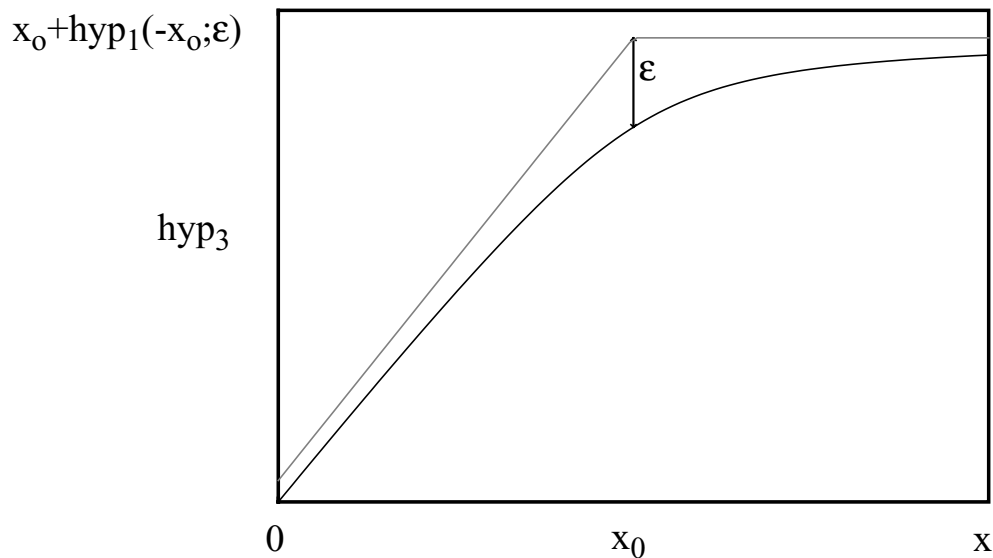


Figure 10: $hyp_3(x; x_0; \epsilon) = hyp_2(x; x_0; \epsilon) - hyp_2(0; x_0; \epsilon)$ for $\epsilon = \epsilon(x_0)$

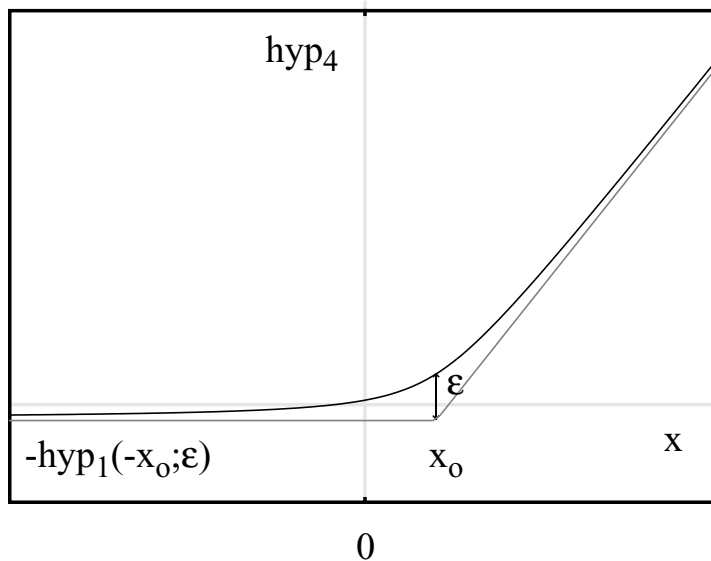


Figure 11: $hyp_4(x; x_0; \epsilon) = hyp_1(x - x_0; \epsilon) - hyp_1(-x_0; \epsilon)$

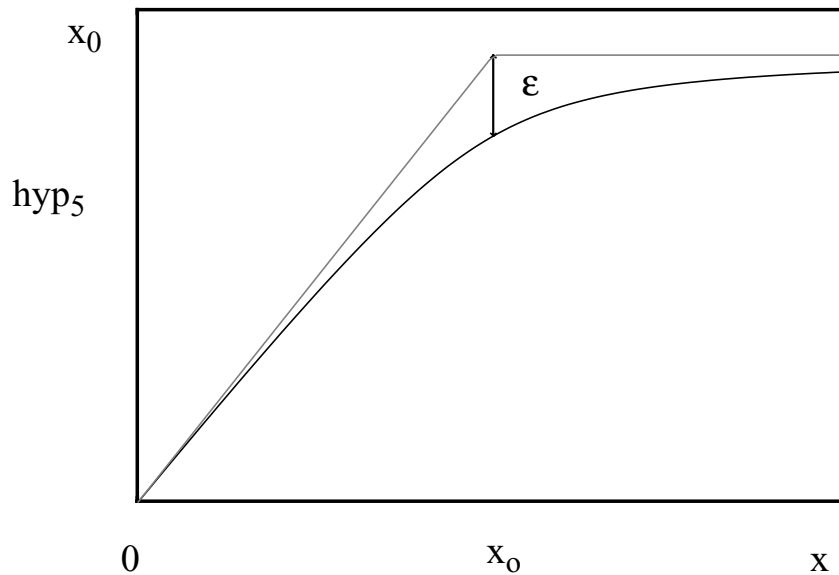


Figure 12: $hyp_5(x; x_0; \varepsilon) = x_0 - hyp_1\left(x_0 - x - \frac{\varepsilon^2}{x_0}, \varepsilon\right)$ for $\varepsilon = \varepsilon(x_0)$

The hypm-function:

$$hypm[x, y; m] = \frac{x \cdot y}{(x^{2 \cdot m} + y^{2 \cdot m})^{1/(2 \cdot m)}} \quad (1.228)$$

B Spectre Specific Information

Imax, Imelt, Jmelt parameters

Introduction

Imax, Imelt and Jmelt are Spectre-specific parameters used to help convergence and to prevent numerical problems. We refer in this text only to the use of Imax model parameter in Spectre with SiMKit devices since the other two parameters, Imelt and Jmelt, are not part of the SiMKit code. For information on Imelt and Jmelt refer to Cadence documentation.

Imax model parameter

Imax is a model parameter present in the following SiMKit models:

- juncap and juncap2
- psp and pspnqs (since they contain juncap models)

In Mextram 504 (bjt504) and Modella (bjt500) SiMKit models, Imax is an internal parameter and its value is set through the adapter via the Spectre-specific parameter Imax.

The default value of the Imax model parameter is 1000A. Imax should be set to a value which is large enough so it does not affect the extraction procedure.

In models that contain junctions, the junction current can be expressed as:

$$I = I_s \exp\left(\frac{V}{N \cdot \phi_{TD}} - 1\right) \quad (1.229)$$

The exponential formula is used until the junction current reaches a maximum (explosion) current Imax.

$$I_{max} = I_s \exp\left(\frac{V_{expl}}{N \cdot \phi_{TD}} - 1\right) \quad (1.230)$$

The corresponding voltage for which this happens is called Vexpl (explosion voltage). The voltage explosion expression can be derived from (1):

$$V_{expl} = N \cdot \phi_{TD} \log\left(\frac{I_{max}}{I_s}\right) + 1 \quad (1.231)$$

For $V > V_{expl}$ the following linear expression is used for the junction current:

$$I = I_{max} + (V - V_{expl}) \frac{I_s}{N \cdot \phi_{TD}} \exp\left(\frac{V_{expl}}{N \cdot \phi_{TD}}\right) \quad (1.232)$$

Region parameter

Region is an Spectre-specific model parameter used as a convergence aid and gives an estimated DC operating region. The possible values of region depend on the model:

- For Bipolar models:
 - subth: Cut-off or sub-threshold mode
 - fwd: Forward
 - rev: Reverse
 - sat: Saturation.
 - off¹
 -
- For MOS models:
 - subth: Cut-off or sub-threshold mode;
 - triode: Triode or linear region;
 - sat: Saturation
 - off¹

For PSP and PSPNQS all regions are allowed, as the PSP(NQS) models both have a MOS part and a juncap (diode). Not all regions are valid for each part, but when e.g. region=forward is set, the initial guesses for the MOS will be set to zero. The same holds for setting a region that is not valid for the JUNCAP.

- For diode models:
 - fwd: Forward
 - rev: Reverse
 - brk: Breakdown
 - off¹

Model parameters for device reference temperature in Spectre

This text describes the use of the tnom, tref and tr model parameters in Spectre with SiMKit devices to set the device reference temperature.

¹.Off is not an electrical region, it just states that the user does not know in what state the device is operating

A Simkit device in Spectre has three model parameter aliases for the model reference temperature, `tnom`, `tref` and `tr`. These three parameters can only be used in a model definition, not as instance parameters.

There is no difference in setting `tnom`, `tref` or `tr`. All three parameters have exactly the same effect. The following three lines are therefore completely equivalent:

```
model nmos11020 mos11020 type=n tnom=30
model nmos11020 mos11020 type=n tref=30
model nmos11020 mos11020 type=n tr=30
```

All three lines set the reference temperature for the `mos11020` device to 30 C.

Specifying combinations of `tnom`, `tref` and `tr` in the model definition has no use, only the value of the last parameter in the model definition will be used. E.g.:

```
model nmos11020 mos11020 type=n tnom=30 tref=34
```

will result in the reference temperature for the `mos11020` device being set to 34 C, `tnom=30` will be overridden by `tref=34` which comes after it.

When there is no reference temperature set in the model definition (so no `tnom`, `tref` or `tr` is set), the reference temperature of the model will be set to the value of `tnom` in the options statement in the Spectre input file. So setting:

```
options1 options tnom=23 gmin=1e-15 reltol=1e-12 \
  vabstol=1e-12 iabstol=1e-16
model nmos11020 mos11020 type=n
```

will set the reference temperature of the `mos11020` device to 23 C.

When no `tnom` is specified in the options statement and no reference temperature is set in the model definition, the default reference temperature is set to 27 C.

So the lines:

```
options1 options gmin=1e-15 reltol=1e-12 vabstol=1e-12 \
  iabstol=1e-16
model nmos11020 mos11020 type=n
```

will set the reference temperature of the `mos11020` device to 27 C.

The default reference temperature set in the SiMKit device itself is in the Spectre simulator never used. It will always be overwritten by either the default "options tnom", an explicitly set option tnom or by a tnom, tref or tr parameter in the model definition.

C OvervoltageSpecification

Overvoltage warnings in SiMKit

Introduction

Overvoltage flagging is signalling that a (terminal) voltage is outside a specified safe range. A warning will be given when the conditions for giving a warning are fulfilled.

Simple checks for overvoltage have been added to the following models: mos903, mos1100, mos1101, mos1102, mos2002, mos2003, mos3100, mos4000, psp102, psp103.

The checks are done on terminal voltages of the models.

There are many ways to define overvoltage. For a general overvoltage flagging solution Verilog-A should be used.

Extra parameters for overvoltage flagging

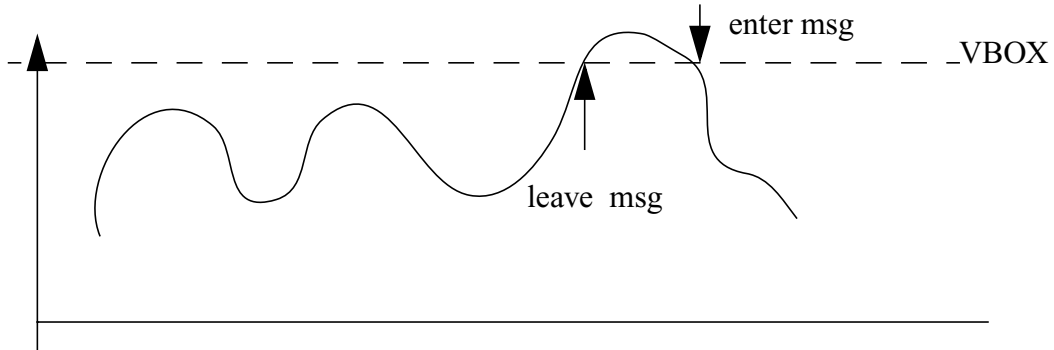
A set of extra parameters has been added to the mos models mos903, mos1100, mos1101, mos1102, mos2002, mos2003, mos3100, mos4000, psp102, psp103.

Table 9:

Name	Unit	Default	Description
VBOX	V	0.0	Oxide breakdown voltage. Checking will be done if $VBOX > 0$
VBDS	V	0.0	Drain-source breakdown voltage Checking will be done if $VBDS > 0$
TMIN	s	0.0	Ovcheck tmin value

For mos models the safe region is:

$$|V_{gs}| < VBOX \text{ and } |V_{gd}| < VBOX \text{ and } |V_{ds}| < VBDS$$



Ovcheck: two terminal dummy model

A (dummy) two-terminal model ovcheck has been implemented that can be used to check if the voltage between the two terminals is within or without a so called safe region.

The model parameters are:

Name	Unit	Default	Description
VLOW	V	0.0	Lower bound of safe region
VHIGH	V	0.0	Upper bound of safe region Checking will be done when $VHIGH > VLOW$
TMIN	s	0.0	Ovcheck tmin value

For the ovcheck model the safe region is:

$$VLOW \leq V_{t1} - V_{t2} \leq VHIGH, \text{ where } t1 \text{ is the first and } t2 \text{ is the second terminal.}$$

Functionality

In Spectre and Pstar

At the end of a DC analysis or in a transient analysis after each time step a check will be done if the device is inside or outside the safe region.

A warning is given whenever the device enters or leaves the safe region.

In Spectre only

To prevent too many warnings in a Spectre transient analysis the model parameter TMIN has been introduced. If the time between leaving and entering the safe region is less than the TMIN value no warning is given.

Because of the TMIN parameter a warning cannot be issued when leaving the safe region. A warning is given when the device enters the safe region again. This warning includes the time and the voltage when the safe region was exited. At the end of the transient warnings are given for devices that are still out of the safe range.

In Pstar TMIN may be specified as a model parameter, but it will be ignored.

D Parameter PARAMCHK

Parameter PARAMCHK

Introduction

All models have the parameter PARAMCHK. It is not related to the model behavior, but has been introduced control the clip warning messages. Various situations may call for various levels of warnings. This is made possible by setting this parameter.

PARAMCHK model parameter

This model parameter has been added to control the amount of clip warnings.

- PARAMCHK < 0 No clip warnings
- PARAMCHK ≥ 0 Clip warnings for instance parameters (default)
- PARAMCHK ≥ 1 Clip warnings for model parameters
- PARAMCHK ≥ 2 Clip warnings for electrical parameters at initialisation
- PARAMCHK ≥ 3 Clip warnings for electrical parameters during evaluation.
This highest level is of interest only for selfheating jobs,
where electrical parameters may change dependent on
temperature.

E Bibliography

- [1] Sze, S.M., *Physics of semiconductor devices*, 2nd edition, John Wiley & Sons, Inc., New York, 1981
- [2] Muller, R.S. and Kamins, T.I., *Device electronics for integrated circuits*, 2nd edition, John Wiley & Sons, Inc., New York, 1986
- [3] Ong D.G., *Modern MOS Technology: Processes, Devices and Design*, McGraw-Hill Book Company, 1984
- [4] Tsividis Y.P., *Operation and modelling of the MOS Transistor*, McGraw-Hill Book Company, 1987
- [5] Paolo Antognetti, Giuseppe Massobrio, *Semiconductor Device Modeling with SPICE*, McGraw-Hill, 1988.
- [6] Dileep A. Divekar, *FET Modeling for Circuit Simulation*, Kluwer Academic Publishers, 1988
- [7] Laurence W. Nagel, *Spice2: A computer program to simulate semiconductor circuits*, University of California, Berkeley, 1975
- [8] *PSpice manual*, MicroSim Corporation, January 1989
- [9] **Pstar** User Manual.
- [10] J.J.A. Hegge, *Model Specification of MOS level 1 Spice model (Metal Oxide Semiconductor Transistor)*, version 2, January 1991.
- [11] Andrei Vladimirescu, Sally Liu, *The simulation of MOS integrated circuits using SPICE2*, Univ. of Cal. Berkeley, 1980
- [12] N. Vossenstijn, G.J. Mulder, *Model specification of a Junction Field Effect Transistor*, CFT-CAD-E, 1990
- [13] Y. Tsividis, G. Masetti, *Problems in precision of the MOS transistor for analog applications*, *IEE trans. CAD*, 1983
- [14] K.A. Sakallah, Yao-Tsung Yen, S. Greenberg, *The Meyer model revisited: explaining and correcting the charge nonconservation problem*, *Proceedings IEEE ICCAD*, 1987
- [15] P.B.L. Meijer, *Meijer model for Meyer model*
- [16] *SPICE version 2G6 source code*, Dep. Elec. Eng. and Comput. Sci., Univ. of California Berkeley, March 15, 1983.

- [17] Klaassen, F.M., *Compact models for circuit simulation*, Springer, Vienna, chapter 7: Models for the enhancement - type MOSFET (1989)
- [18] Klaassen, F.M., *Compact models for circuit simulation*, Springer, Vienna, chapter 6: MOSFET - physics (1989)
- [19] Wright, G.T., *Physical and CAD models for the VLSI mosfet*, IEEE Trans. on Electron Devices, vol ED-34, page 823 (1987)
- [20] Oh, S.Y., Ward D.E. and Dutton R.W., *Transient analysis of MOS transistors*/, IEEE Journal Solid-State Circuits, Vol. SC-15, page 636 (1980)
- [21] Sevat, M.F., *On the channel charge division in MOSFET modeling*, Digest technical papers ICCAD-87, Santa Clara CA, page 208 (1987)
- [22] Ir. C. Kortekaas, *Description and users guide of the MOS interconnect capacitance extractor; MICE 2.0*/, Nat. Lab Technical note 1988
- [23] Ir. C. Kortekaas, *Junction capacitance- and current description for simulator models*/, Nat. Lab. Technical Note 1988
- [24] H. Elzinga, *Extending INTCAP/LOCAL with lateral capacitances between non-overlapping PS-INS, IN-PS and INS-IN layers*, RNR-46/92-IX-044, 17-09-1992
- [25] Bittel und Sturm, *Rauschen*, Springer, page 241, (1971)
- [26] Ir. A. v. Steenwijk, *Private communication*, (1994)
- [27] R.M.D.A. Velghe and D.B.M. Klaassen, *First official parameter set for MOS Model 9.02 for the C150DM2 process*, Nat. Lab. Report 6689
- [28] A.J. Scholten and D.B.M. Klaassen, *Geometrical scaling of θ_1 in MOS Model 9*, Nat. Lab. Report 6992
- [29] A.J. Scholten and D.B.M. Klaassen, *Anomalous geometry dependence of source/drain resistance in narrow-width MOSFETs*, Proc. IEEE 1998 Int. Conference on Microelectronic Test Structures Vol. II, March 1998
- [30] Kwok K. Hung *et al.*, IEEE Trans El. Dev. Vol. 37, No. 3, March 1990
- [31] Kwok K. Hung *et al.*, IEEE Trans El. Dev. Vol. 37, No. 5, May 1990
- [32] A.J. Scholten and D.B.M. Klaassen, *New 1/f noise model in MOS Model 9, level 903*, Nat.Lab Unclassified Report, NL-UR 816/98
- [33] R. van Langevelde, *MOS Model 11, Level 1100* NL-UR 2001/813, 2001.

internet: http://www.semiconductors.philips.com/Philips_Models.

[34] R. van Langevelde, A.J. Scholten and D.B.M. Klaassen, *MOS Model 11, Level 1101* NL-UR 2002/802, 2002.

internet: http://www.semiconductors.philips.com/Philips_Models.

[35] R. van Langevelde, *A Compact MOSFET Model for Distortion Analysis in Analog Circuit Design*, PhD Thesis, TU Eindhoven, Eindhoven 1998.
Available on request. Write to: Ronald.van.Langevelde@philips.com

[36] R. van Langevelde and F.M. Klaassen, *An Explicit Surface-Potential Based MOSFET Model for Circuit Simulation*, Solid-State Electron., Vol. 44, pp. 409-418, 2000.

[37] R.M.D.A. Velghe, D.B.M. Klaassen, F.M. Klaassen, *MOS Model 9*, NL-UR 003/94, 1994. internet: http://www.semiconductors.philips.com/Philips_Models.

[38] R. van Langevelde and F.M. Klaassen, *Influence of Mobility Degradation on Distortion Analysis in MOSFETs*, in Proceedings ESSDERC 1996, Bologna, Italy, pp. 667-670, 1996.

[39] R. van Langevelde and F.M. Klaassen, *Effect of Gate-Field Dependent Mobility Degradation on Distortion Analysis in MOSFETs*, IEEE Trans. Electron Devices, Vol. ED-44, No. 11, pp. 2044-2052, 1997.

[40] R. van Langevelde and F.M. Klaassen, *Accurate Drain Conductance Modeling for Distortion Analysis in MOSFETs*, IEDM 1997 Tech. Digest, pp. 313-316, 1997.

[41] A.R. Boothroyd, S.W. Tarasewicz and C. Slaby, *MISNAN A Physically Based Continuous MOSFET Model for CAD Applications*, IEEE Trans. Computer-Aided Design, Vol. CAD-10, No. 12, pp. 1512-1529, 1991.

[42] K. Joardar, K.K. Gullapulli, C.C. McAndrew, M.E. Burnham and A. Wild, *An Improved MOSFET Model for Circuit Simulation*, IEEE Trans. Electron Devices, Vol. ED-45, No. 1, pp. 134-148, 1998.

[43] Z.A. Weinberg, *On Tunneling in Metal-Oxide-Silicon Structures*, J. Appl. Phys., Vol. 53, pp. 5052-56, 1982.

[44] F. Stern, *Quantum Properties of Surface Space-Charge Layers*, CRC Crit. Rev. Solid State Sci., pp. 499-514, 1974.

[45] S.-Y. Oh, D.E. Ward and R.W. Dutton, *Transient Analysis of MOS Transistors*,

- IEEE J. Solid-State Circ., Vol. 15, pp. 636-643, 1980.
- [46] R. Rios and N.D. Arora, *Determination of Ultra-Thin Gate Oxide Thicknesses for CMOS Structures Using Quantum Effects*, IEDM 1994 Tech. Digest, pp. 613-316, 1994.
- [47] A.J. Scholten, L.F. Tiemeijer, P.W.H. de Vreede and D.B.M. Klaassen, *A Large Signal Non-Quasi-Static MOS Model for RF Circuit Simulation*, IEDM 1999 Tech. Digest, pp. 163-166, 1999.
- [48] K.K. Hung, P.K. Ko, C. Hu and Y.C. Cheng, *A Unified Model for the Flicker Noise in Metal-Oxide-Semiconductor Field-Effect Transistors*, IEEE Trans. Electron Devices, Vol. ED-37, No. 3, pp. 654-665, 1990.
- [49] K.K. Hung, P.K. Ko, C. Hu and Y.C. Cheng, *A Physics-Based MOSFET Noise Model for Circuit Simulators*, IEEE Trans. Electron Devices, Vol. ED-37, No. 5, pp. 1323-1333, 1990.
- [50] A.J. Scholten and D.B.M. Klaassen, *New 1/f Noise Model in MOS Model 9, Level 903, NL-UR 816/98*, 1998.
- [51] H.C. de Graaff and F.M. Klaassen, *Compact transistor modelling for circuit design*. Vienna/New York: Springer-Verlag, 1990.
- [52] R. van Langevelde et al., *New Compact Model for Induced Gate Current Noise*, IEDM 2003 Tech. Digest, pp. 867-870, 2003.
- [53] A.J. Scholten et al., *Accurate Thermal Noise Model for Deep-Submicron CMOS*, IEDM 1999 Tech. Digest, pp. 155-158, 1999.
- [54] M. Minondo, G. Gouget and A. Juge, *New Length Scaling of Current Gain Factor and Characterization Method for Pocket Implanted MOSFETs*, Proc. ICMTS 2001, pp. 263-267, 2001.
- [55] T.S. Hsieh, Y.W. Chang, W.J. Tsai and T.C. Lu, *A New Leff Extraction Approach for Devices with Pocket Implants*, Proc. ICMTS 2001, pp. 15-18, 2001.
- [56] A.J. Scholten, R. Duffy, R. van Langevelde and D.B.M. Klaassen, *Compact Modelling of Pocket-Implanted MOSFETs*, in Proceedings ESSDERC 2001, pp. 311-314, 2001.
- [57] R. van Langevelde et al., *Gate Current: Modeling, ΔL Extraction and Impact on RF Performance*, IEDM 2001 Tech. Digest, pp. 289-292, 2001.
- [58] R. van Langevelde, A.J. Scholten and D.B.M. Klaassen, *MOS Model 11, level*

1101, Nat.Lab Unclassified Report, NL-UR 2002/802

[59] http://www.semiconductors.philips.com/Philips_Models

[60] N. D' Halleweyn, *Modelling and Characterisation of Silicon-On-Insulator Lateral Double Diffused MOSFETs for Analogue Circuit Simulation*, Ph.D. Thesis, University of Southampton, August 2001

[61] R. van Langevelde and F.M. Klaassen, *An Explicit Surface-Potential Based MOSFET Model for Circuit Simulation*, Solid-State Electronics, Vol 44, 2000, pp. 409-418

[62] R. van Langevelde, A.J. Scholten and D.B.M. Klaassen, *MOS Model 11, level 1101*, Philips Research Unclassified Report, NL-UR 2002/802, December 2002 see http://www.semiconductors.philips.com/Philips_Models

[63] A.C.T. Aarts and R. van Langevelde, *A Robust and Physically Based Compact SOI-LDMOS Model*, Proc. of the 32nd European Solid-State Device Research Conference (ESSDERC), University of Bologna, September 2002, pp. 455-458

[64] D.E. Ward and R.W. Dutton, *A Charge-Oriented Model for MOS Transistor Capacitances*, IEEE Journal of Solid-State Electronics, Vol 13, No. 5, October 1978, pp. 703-708

[65] A.C.T. Aarts M.J. Swanenberg and W.J. Kloosterman, *Modelling of High-Voltage SOI-LDMOS Transistors including Self-Heating*, Proc. SISPAD, Springer, 2001, pp. 246-249

[66] V. Palankovski R. Schultheis and S. Selberherr, *Modelling of power heterojunction bipolar transistor on gallium arsenide*, IEEE Trans. Elec. Dev., vol 48, pp. 1264-1269, 2001. Note: the paper uses $\alpha = 1.65$ for Si, but $\alpha = 1.3$ gives a better fit: also, k_{300} for GaAs is closer to 40 than to the published value of 46 (Palankovski, personal communication).

[67] JUNCAP:

http://www.semiconducors.philips.com/Philips_Models/

[68] G.A.M. Hurkx, D.B.M. Klassen and M.P.G. Knuvers, *A new recombination model for device simulation including tunneling*, IEEE Trans. El. Dev., Vol.39, No.2, pp.331-338, February 1992.

[69] W. Jin, C.H. Chan, S.K.H. Fung, and P.K. Ko, *Shot-noise-induced excess low-frequency noise in floating-body partially depleted SOI MOSFET's*, IEEE Trans. El. Dev., Vol. 46, No. 6, pp. 1180– 1185, June 1999.

[70] MOSModel 9:
<http://www.nxp.com/models/>

